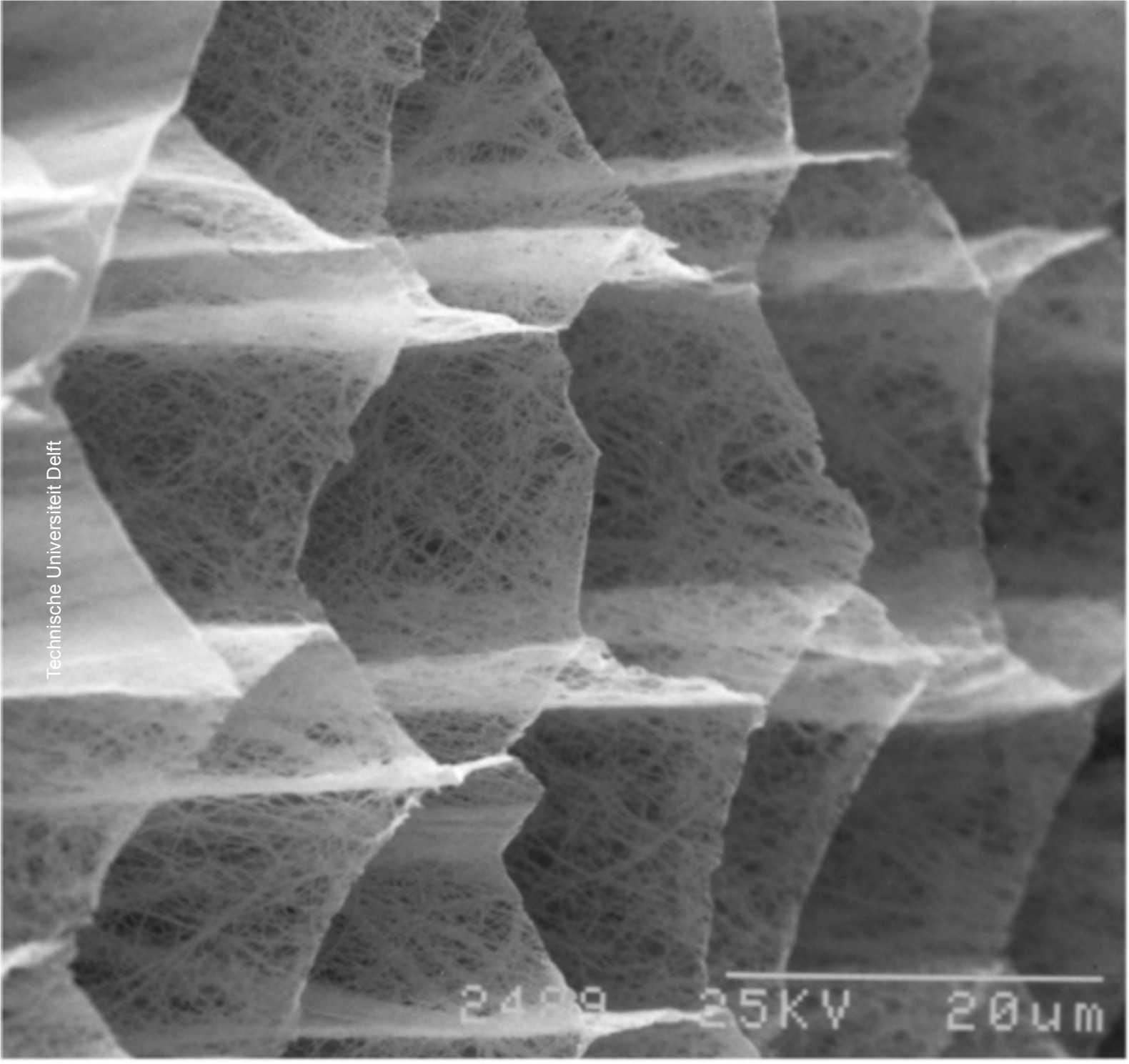

Emerging properties of a micromechanical muscle contraction model

H.G.M. Calkoen

TU Delft

Emerging properties of a micromechanical muscle contraction model

by

H.G.M. Calkoen

to obtain the degree of Master of Science
at the Delft University of Technology,
to be defended on Monday December 19, 2016 at 2:30 PM.

Student number:	4019946	
Thesis committee:	Prof. dr. F.C.T. van der Helm,	TU Delft, chair
	Dr. ir. W. Mugge,	TU Delft
	Dr. ir. J.H. de Groot,	LUMC
	prof. dr. ir. J.L. van Leeuwen,	WUR

An electronic version of this thesis is available at http://repository.tudelft.nl/.

Cover image from:
Purslow, Peter P. "The structure and functional significance of variations in the connective tissue within muscle." *Comparative Biochemistry and Physiology Part A: Molecular & Integrative Physiology 133.4 (2002): 947-966.*

TU Delft

L U M C

Preface

This report is the result of my thesis project that is part of a collaboration between the TU Delft and the Leiden University Medical Center. It all started a little over a year ago with a literature study looking into the myofascia an the role they could play in predicting active muscle stiffness. This denounced the need for a micro-mechanical architectural muscle model. This period was followed by an internship at Wageningen University and Research Center where I started building a first model version and it all ends here in Delft where I spent a couple of months on creating the model and interpreting its results. The main content of this report is the graduation paper. This paper describes the composition of a micro-mechanical model for analyzing the emerging properties of skeletal muscle. The rest of the work consists of appendices where preliminary and explanatory work can be found. The topic requires a certain amount of background knowledge on skeletal muscle morphology and muscle contraction, this is described in the first Appendix. The main findings of the work is that initial orientation angle and collagen stiffness of muscle connective have a considerable influence on model output.

Before wrapping up I would like to acknowledge the valuable contribution of a number of people.
First of all Erwin the Vlugt who introduced me to the topic together with Jurriaan de Groot who has mentored me throughout the project. My mentors during the internship in Wageningen, Johan van Leeuwen and Kees Voesenek, who taught me the basics of building a model. Furthermore I would like to thank Winfred Mugge and Frans van der Helm for stepping in as supervisors for my graduation project and I would like to thank Arend Schwab for helping me out with the model development. Finally I would like to thank my friends and family for supporting me throughout the process of my graduation.

H.G.M. Calkoen
Delft, December 2016

Contents

1

Scientific Paper

Emerging properties of a micromechanical muscle contraction model

H.G.M. Calkoen

Abstract—**The structural response of active skeletal muscle is derived from a combination of sarcomere contraction properties, collagen fibres in the connective tissue, and incompressibility. The role of collagen tissues could be substantial but is still not completely understood. Only few studies have looked into the functionality of collagen reorientation within connective tissues during contraction. The objective of this paper is to propose a discrete static micro-mechanical model to study the sensitivity of kinematic properties of skeletal muscle depending on initial braiding angle of the endomysium lattice and the stiffness of collagen fibers. Two models are developed, first a hexagonally shaped single muscle fibre surrounded by connective tissue, and second, a fascicle model encompassing a single fiber surrounded by neighbouring fibres on all sides with their portion of connective tissue. Connective tissue is modelled in a crossed-helical setup of tension-only elements. Contraction is simulated by pretensioned 'sarcomere' spring elements that follow the muscle force-length relationship. the model calculates displacements, forces, pressures and work developed as a result of contraction. The most important conclusion of the model is that the contribution of braiding angle and collagen stiffness can be considered very important. For a sufficiently small angle, the observed model behaviour can solely be attributed to sarcomere properties. When the orientation angle is increased, the passive properties of the myofascia start playing a larger role. The model response then becomes very much influenced by a pressure term that is induced by stretch in the collagen acting on the incompressible muscle. Although validation methods are limited, the model results are promising and further research is encouraged.**

I. Introduction

Skeletal muscle has a complex hierarchical structure. Muscle fibers are surrounded by connective tissue (endomysium), see Figure 1), and are arranged into fascicles. Fascicles are also surrounded by connective tissue (perimysium). Together with the connective tissue surrounding a whole muscle (epimysium) these tissues are called the myofascia (see Appendix A). These structures play important roles in muscle development, structural support and the endomysium is mentioned to be a key component in muscle flexibility [1]. Furthermore a role is allocated in efficient force transmission [2]–[5]. Myofascia can also dramatically adapt their structure as a result of imposed loads and several pathological conditions [6], [7]. The shapes and geometrical arrangements of muscle fiber, fascicle and connective tissue vary significantly across muscles [4]. Gaining more insight in the myofascia could lead to advancements in all sorts of research directions, from rehabilitation engineering to physical therapy and sports sciences. A specific part of muscle research is dedicated to the strong relation between architecture and functional capabilities. This relation is still not fully understood [8]. Collagen fibers have been demonstrated to change orientation with muscle length changes in endomysium and perimysium of active as well as passive muscle tissue [9], [10], (see Figure 2). The much described theoretical fiber angle of 54.44° [11], where longitudinal and circumferential stresses are balanced given a closed constant volume, shows resemblence with the numerically weighted average orientation angle at resting length for endomysium and perimysium [12] (59° and 55° respectively [9], [10]). Therefore one can suspect that the collagen lattice plays an important role in muscle mechanics, and that the collagen lattice interferes with the mechanics of the contractile filaments. The mechanical role of the myofascia and the crossed-helical orientation is neglected in current muscle modeling. This hampers understanding of changes imposed under training and pathological conditions. Most models incorporating the myofascia focus on myofascial force transmission [13]–[16] and do not take the into account the braiding structure of the myofascia. Furthermore many lump the active contractile properties and the passive connective tissue properties into one continuum for which transverse isotropy is assumed [13], [17], [18]. These models therefore do not consider how variations in muscle microstructure could affect the macroscopic material properties. Micromechanical models, in combination with mechanical experiments of fiber and fiber bundle, are needed to understand how variations in the myofascia result in the emerging macroscopic behavior of muscle [19]. Only two prior studies considered the re-orientation of the collagen fibers [10], [21]. Purslow [10] made a geometric model to describe the angle reorientation at different sarcomere lengths. Gindre [21] presented a structural model for passive loaded skeletal muscle. Neither of these models looked into the possible interplay between active muscle contractile properties and the passive properties of the crossed-helical braiding structure. In current Hill-based models, muscles are represented by volume independent line elements with sarcomere properties. This type of model is insufficient for gaining insight into the relation between architecture and functional capability of skeletal muscle. To model the properties of the myofascia a three-dimensional micro-architectural model is needed and finite element modeling offers possibilities to predict in vivo muscle behaviour that cannot yet be experimentally determined.

The first goal of this paper is the development and introduction of a micro-structural muscle model for fiber and fascicle incorporating collagen braiding re-orientation. The second goal is running model simulations for different theoretical conditions to analyze the sensitivity of kinematic properties

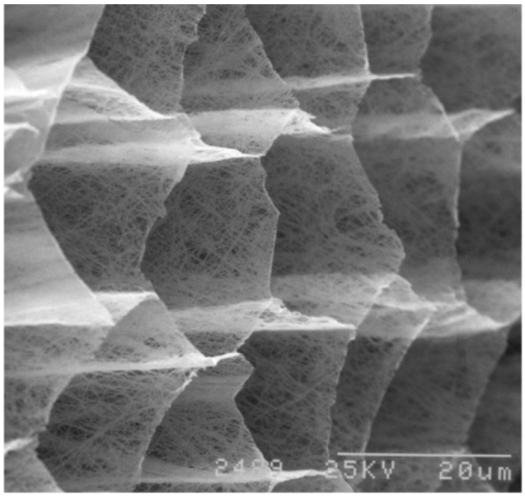

Fig. 1: Microscopic image of the threedimensional endomysium lattice structure from which the muscle fibers are removed. Collagen fibers can be seen laying in the endomysial walls. (from: [20]).

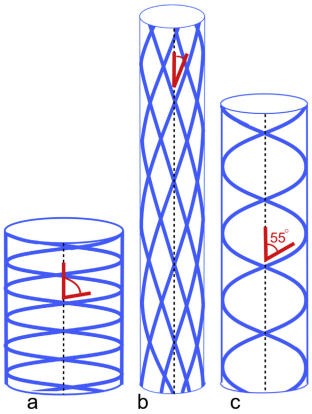

Fig. 2: Schematic image of crossed-helixes showing how a shortened and thickened fiber (a) causes the braiding angle to increase and a lengthened fiber (b) causes a decrease in braiding angle. Original fiber in rest with collagen braiding angles of 54.44° (c) balances both longitudinal and circumferential fiber stresses. The braiding angle is indicated in red. (from: [12]).

of skeletal muscle depending on initial braiding angle of the collagen lattice and the stiffness of the collagen fibers. The focus will be on the initial orientation angle of the structure as well as the difference between fiber and fascicle. Finally within the fascicle model force transmission will examined.

The expected outcome of the model is that for a smaller initial braiding angle (i.e. collagen fibers oriented relative to the longitudinal axis of the muscle fibers) initial strain during muscle fiber contraction will be low compared to a lattice with a higher braiding angle. Therefore the expectancy is that this will lead to a lower stiffness, pressure and internal work compared to a higher initial angle. This will furthermore result in a larger angle rotation, higher resultant force and larger displacement. The latter two being the result of an interaction with the force-length relationship of the contractile elements. The same results are expected from reducing collagen stiffness. For simulations initiated at an angle lower than 54.44° this angle is expected to be a point where a minimum is reached in collagen strain that will increase with further rotation. For a fiber-fascicle comparison the expectancy is that pressures will be higher in a fascicle resulting in higher stiffness. Finally we expect to find force being transmitted within a fascicle.

II. Materials and Methods

This study consists of a model composition, several model simulations and a parameter sensitivity analysis.

A. Model Composition

Two static micro-mechanical models were developed. The first one representing a single muscle fiber and the second one a fascicle. Both models are subject to a volume constraint due to the incompressibility of muscle tissue. Since the fascicle model is an extension of the fiber model, only the fiber model will be described in detail here and some important characteristics of the fascicle model will be described further on in this section. Muscle fibers are modeled as a hexagonal prism shape consisting of n identical hexagonal prism elements stacked on top of one another (see Figure 3) to discretize the system. The hexagonal prism elements form compartments that play an important role in the model because the constant volume constraint is enforced locally in each of the compartments. The fiber is modeled as a hexagonally shaped tube as this is similar to the shape that can be seen in Figure 1, furthermore it allows for extension to a fascicle model because the hexagonal shape allows for sharing of the endomysial walls between different fibers. The endomysium is represented in the model as crossed truss elements with opposing angles on each outer surface of a hexagon segment. Sarcomere elements are placed in between all nodes in longitudinal direction.

1) Boundary conditions: All bottom nodes were fixed during simulations and all top nodes were connected to very weak external spring elements. These elements help stabilize the system while allowing for a contraction movement.

B. Model Assumptions and Simplifications

- The model is static and contains no masses.
- collagen structures are assumed not to interact with one another.
- No minimal or maximal braiding angles are assumed.

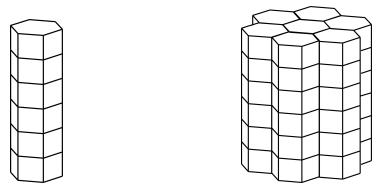

(a) Single Fiber (b) Fascicle

Fig. 3: Single fiber (a) and fascicle model (b) built up out of stacked hexagonal volume elements. Each element is subject to a volume constraint.

- Muscle is an incompressible material and therefore the volume is constrained to remain the same.
- A discrete, rather than a continuous description is used to simplify modeling, the minimum of 25 segments is assumed to be a sufficiently accurate approximation to the continuous structure of a muscle fiber.
- Collagen fiber is linearly elastic.
- Collagen fiber has stiffness in tension but not in compression.
- Preferred orientation angle in endomysium is represented by 2 opposing angle orientations.
- The human force-length relationship from [22] is represented by a Gaussian and does not shift with change in activation.

The way the model is built, the braiding angle is not independent of the discretization, this is assumed to be of little influence on the outcome of the model. Furthermore the collagen fibers are represented as two truss elements with opposing orientation, this is a significant simplification of the of the actual situation where collagen fibers are scattered over multiple angles, however [9] stated that a mean orientation distribution can be determined, therefore this simplification is defensible.

C. Model Implementation

The two models were constructed and implemented in Matlab (The Mathworks, Natick Massachusetts, see Appendix B). For the model simulations all parameters were scaled to a micro scale. For the scenario-analysis three configurations were defined for different initial fiber orientation angles of 34.97°, 54.44° and 70.33°. These values were chosen because with 25, 50 and 100 segments respectively, the configurations result in the same initial fiber length L_{init}. Where 54.44°, the most realistic configuration is chosen as the reference configuration. For all configurations simulations were conducted where collagen modulus E_{col}, external spring stiffness k_{ex} and activation a were varied. Approximately

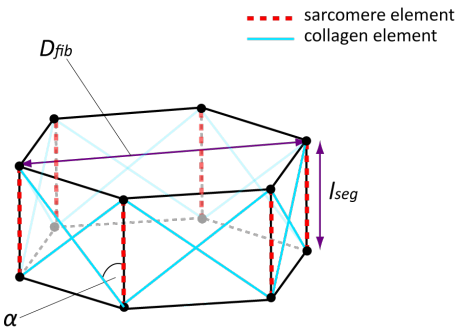

Fig. 4: Parameters within a single hexagonal prism element, the red dotted lines represent the sarcomere elements that contract, the light blue elements represent the collagen fiber elements that form the endomysium in the model. The black dots indicate the nodes within a single hexagonal prism, the volume enclosed by the black lines represents the constrained volume segment. D_{fib} indicates the fiber diameter, α indicates the braiding angle and l_{seg} represents the segment length.

250 model simulations were conducted in total for fiber and fascicle (see Appendix C).
The following set of linearised equations were used for the model [23] (See Appendix D for the definition and the derivation of the parameters in equation 1) :

$$\begin{bmatrix} \vec{K}+\vec{K}^b & \vec{\Omega}^T \\ \vec{\Omega} & \vec{0} \end{bmatrix} \begin{bmatrix} \Delta\vec{q} \\ \Delta\vec{\lambda} \end{bmatrix} = \begin{bmatrix} \vec{f}^e - \vec{f} + \vec{\Omega}^T\vec{\lambda} \\ -\vec{C}(\vec{q}) \end{bmatrix}; \quad (1)$$

The solution is found by using the Newton-Raphson iteration scheme [23], with k representing the iteration.

$$\vec{q}^{(k+1)} = \vec{q}^{(k)} + (\vec{K}+\vec{K}^b)^{-1}(\vec{q}^{(k)})[\vec{f}^e - \vec{f}(\vec{q}^{(k)}) + \vec{\Omega}^T\vec{\lambda}^{(k)}] \quad (2)$$

Three different convergence criteria are used as described in [24]:

$$|\vec{f}^e - \vec{f}| < \varepsilon_1 \quad (3)$$

$$|\vec{C}(\vec{q})| < \varepsilon_2 \quad (4)$$

$$|\vec{\lambda}^{(k)} - \vec{\lambda}^{(k-1)}| < \varepsilon_3 \quad (5)$$

D. Input Parameters

The model has two input parameters, an activation input and an external force. For this model, activation a is used as the main input parameter, where the external force input f^e was mainly used as an extra input to allow for calculation of stiffness as an output parameter. Activation is represented on a scale between 0 (no activation) and 1 (maximal activation). To simulate a real muscle fiber contraction, the activation level was be coupled to the human muscle force-length relationship. The contraction force is therefore dependent on sarcomere length. For a fascicle an activation level can be assigned per fiber.
A normalized force-length relationship of a muscle fiber was assumed as well as that maximum isometric stress occurs at optimal fiber length. Lastly, the assumption was made that the active fiber stress scales linearly with the activation level, which varies from 0 to 1. The contraction force is induced by modelling the longitudinal elements as pretensioned springs of which the initial length l_0 is adapted according to the force exerted by the force-length relationship for that sarcomere length. The length-tension relationship is implemented as an asymmetric Gaussian function (Figure 5). The Gaussian is parametrized according to the method described in [25]. Where a parameter mapping method is described that results in a parameter set with clear physical meanings. More details can be found in Appendix D.

E. Model Parameters

The model is subject to several model parameters. Some of these parameters were chosen to remain constant and others were tuned for the scenario analysis and parameter sensitivity analysis. Because there is uncertainty in most of these parameters, a range of parameter values was defined from literature to allow for a substantiated choice in values used, see table I.
Varying parameters:

TABLE I: Literary Range

Parameter	Name	Literature Range	Model values	Unit	Source
E_{col}	Collagen modulus	200 - 860	200 - 860	MPa	[21]
r_{col}	Thickness endomysium (radius)	0.1 - 0.5	0.25 - 0.4	μm	[9]
p_{col}	Collagen percentage (of muscle dry weight)	0.47 - 1.20	0.5 - 1.27 (in fascicle)	%	[20]
D_{fib}	Fiber diameter	1 - 100	30	μm	[26]
ℓ_{rest}	Sarcomere resting length	1.97 - 3.01	2.64	μm	[27]
σ_{max}	Maximum Isometric Tension	98 - 490	280	kPa	[28], [29]

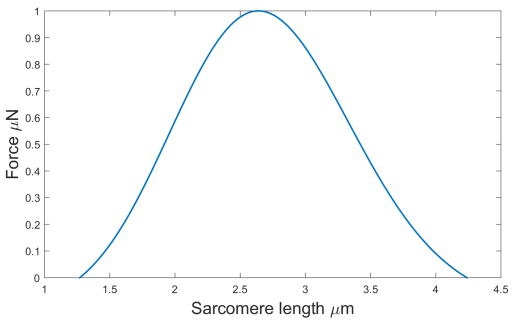

Fig. 5: The Gaussian force-length relationship used in the model (normalized for force). Derived using assymmetric Gaussian model and the method of parametrization by [25] (see Appendix D).

- initial collagen braiding angle α_{init}
- collagen modulus E_{col}
- collagen cross-sectional area r_{col}
- external spring stiffness k_{ex}

Constant parameters:

- maximum isometric tension σ_{max}
- initial external spring length ℓ_{ex}
- starting fiber diameter D_{fib}
- sarcomere resting length ℓ_{rest}

1) Collagen Modulus: The collagen radius for the endomysium specifically has not been determined, therefore reported values for collagen fiber in general were used. The reported values lie in the range of 200-860MPa [21], [30]–[33] where the most reported range would be 250 to 570 MPa. Therefore 250MPa, 400MPa and 570MPa are chosen for the simulations to span the range of collagen moduli. In the simulation where the collagen is the main variation parameter, the full range from 200 - 860 was used.

2) Collagen radius and volume percentage: In the model setup a fixed choice of collagen fiber radius results in the collagen content differing per discretization. To compensate for this the radius was adapted to have the same percentage as the reference configuration with an initial braiding angle of 54.44°. To account for potential bias due to collagen content compensation, uncompensated simulations were conducted as well. In literature the thickness of the endomysium ranges from 0.2-1μm and the collagen content from 0.47-1.20%. For the reference configuration a radius r_{col} of 0.25μm and 0.4μm are chosen, these values result in a collagen content p_{col} of 0.5% and 1.27%. The collagen content is calculated relative to the volume of the fascicle model since the endomysium walls are shared between muscle fibers in real muscle. Because it can be expected that the relative content for a whole muscle will be even lower than the fascicle setup, the 1.27% is acceptable.

3) External Spring Stiffness and Length: The external spring stiffness k_{ex} was subject to a sensitivity analysis to determine the best value for the model simulations. It is important that it is chosen to allow for sufficient contraction without losing stability. The external spring length ℓ_{ex} was chosen beforehand to be twice the total fiber length.

4) Maximum Isometric Tension and Sarcomere resting length: Maximum isometric tension is an important parameter since it determines the maximum force in the force-length relationship. For this model a maximum isometric tension σ_{max} of 280kPa is assumed.

5) Fiber Diameter: The diameter of a fiber can range between 1μm and 100μm [26], a diameter D_{fib} of 30μm was chosen for the model simulations.

F. Output Parameters

To be able to fully analyze the model a range of output parameters was defined. Some relate to the fiber of fascicle as a whole, but others relate to single members and therefore need to be averaged.

- resulting displacements δ
- total length change ΔL
- work W_{tot}
- segmental pressure λ
- final braiding angle α_{end}
- longitudinal stiffness E_{stiff}
- endpoint force F_{end}
- final sarcomere length $\ell_{sarc_{end}}$
- collagen strain ε_{col}

1) Averaged Output Parameters: The resulting displacements as well as the segmental pressure are direct output parameters, but because the system is discrete, some of the output parameters require additional calculations to acquire. To find the final braiding angle α_{end}, sarcomere lengths l_{sarc}, pressures λ, and collagen strain ε_{col} an average value was calculated. The outer segments of the fiber are excluded from analysis because the values in these segments can differ extensively due to boundary conditions. This is implemented by disregarding the results of the outer u segments on both the top and bottom of the fiber. The number of segments to disregard was determined proportional to the total number of segments in the discretization to be able to analyze the same part of the fiber in all set-ups, see Appendix D. For all of these parameters a mean value is calculated as well as the standard deviation.

2) Force and Work: Both the endpoint force F_{end} and the work in the system were be calculated. The endpoint force can be distracted from the length difference in the external springs in combination with its stiffness (eq.6). Two work parameters, the potential energy in the endomysium and the

potential energy in the external springs, were calculated to determine the total energy in the system after contraction. Both are found by doing a summation of the potential energy of all elements in the system. This is shown in equation 7, with q being the total amount of external springs, n is the total amount of segments and m is the number of crossed elements within one segment.

$$F_{end} = \sum_{p=1}^{q} k_{ex_p} \delta l_{ex_p} \tag{6}$$

$$W_{tot} = \sum_{p=1}^{q} \frac{1}{2} k_{ex_p} \delta l_{ex_p}^2 + \sum_{i=1}^{n} \sum_{j=1}^{m} \frac{1}{2} k_{col_i,j} \delta l_{col_i,j}^2 \tag{7}$$

3) Muscle stiffness: Finally muscle stiffness properties were examined. This is quite complex since the definition of muscle stiffness can have multiple interpretations. In this case the longitudinal stiffness of both fiber and fascicle was analyzed. To acquire this data a contraction was simulated until the end configuration was reached. This active configuration was used as the input for a new simulation where a force was put on each node of the fiber in longitudinal direction. Since the force input is known, as a result a displacement is found. To be able to extrapolate the data, stiffness is calculated as a modulus using the following method:

$$E_{stiff} = \frac{f^e L_0}{A_0 \Delta L} \tag{8}$$

G. Fascicle Model

In essence the fascicle model is the same model as the single fiber model, however in the fascicle model multiple fibers are connected. This requires an extra consideration for the connection between the fibers. Since the endomysial layer separating the two muscle fibers is a single layer, joined at the nodes between adjacent fibers [7], here the decision was made for neighbouring fibers to share nodes. This implies that some nodes have two or three sarcomere elements exert force on them. This was compensated by increasing the stiffness of the external springs at these nodes.

The fascicle model allows for contraction with different levels of activation. To analyze force transmission a configuration was used where only the central fiber was activated. Because the resulting work in the system can only result from sarcomere contraction in the central fiber, potential energy found in the surrounding fibers has to be the result of myofascial force transmission. A calculation was done of the amount of potential energy in certain parts of the fiber, this way the percentage of force transmission was determined.

III. Results

A. Initial Braiding Angle

In Figure 6 and 7 visualization are given of the initial model configurations and the end configurations for three simulations with various initial braiding angles. Figure 6 shows a 3D view and Figure 7 shows the x-y-view (top) of a typical model end configuration for the different initial orientation angles. The shapes vary quite extensively as a rectangular shape can be identified for the smallest angle, a hexagonal shape for the 54.44° model and a circular shape for the largest initial angle.

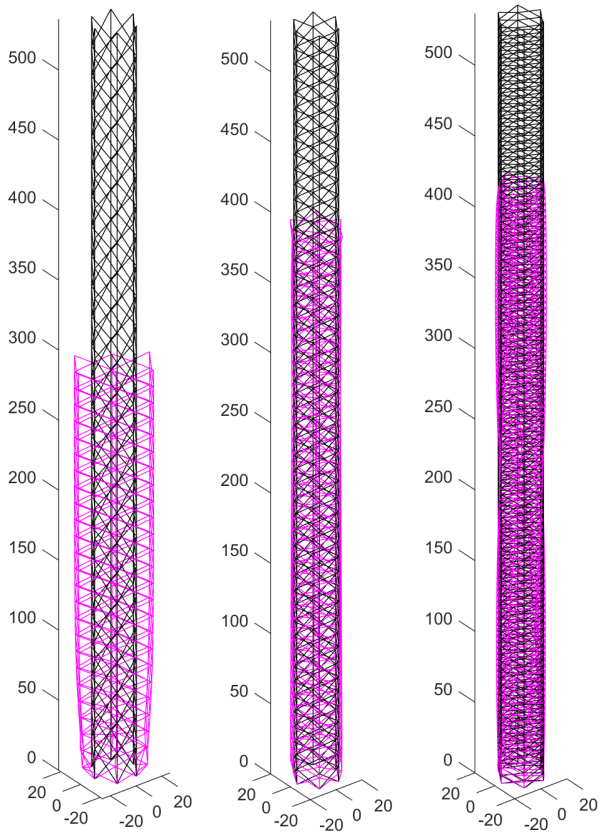

(a) 34.97° (b) 54.44° (c) 70.33°

Fig. 6: Typical simulation output images for the three angles 34.97°, 54.44°, 70.33° respectively. In black the original position of the fiber elements is indicated and in magenta the resulting shape. All axes are displayed in μm

B. Collagen Modulus

Most of the figures in this section display results for several configurations. This includes various angles as well as several stiffness moduli and collagen radii. The 54.44° configuration was used as a reference for the volume compensation. Where an S is indicated in the legend it indicates the strongest collagen modulus E_{col} = 570MPa in combination with the thickest compensated radius accounting for a volume percentage of p_{col} = 1.27%. Where a W is indicated this implies the weakest configuration with E_{col} = 250MPa and p_{col} = 0.5%. Where a U is indicated behind the first letter, it indicates the uncompensated state.

In Figure 8 an overview is given of different output parameters for collagen moduli ranging from 200MPa to 860MPa. All three angle configurations are displayed for two different collagen diameters of 0.4μm and 0.25μm, and the equivalent volume-compensated values for the 34.97°, and 70.33° angles. In Figure 8d) the potential energy stored in the collagen fibers as well as the external spring are displayed.

C. Fiber vs. fascicle

In Figure 9 several figures are displayed comparing the output parameter of fibers and fascicles. In these simulations the fascicle is always equally activated.

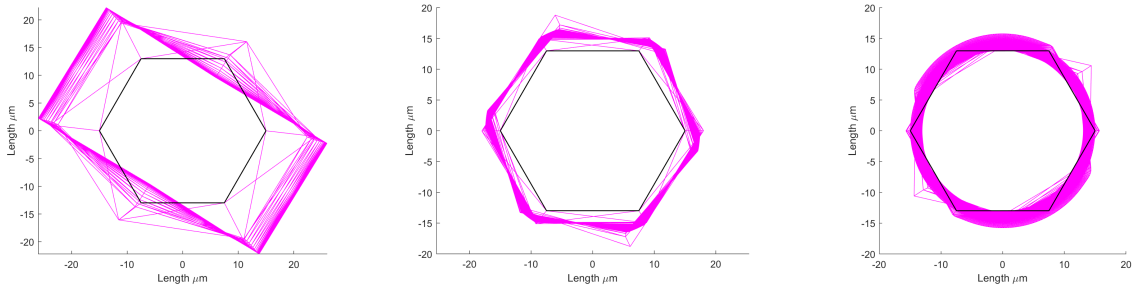

(a) Typical Shape Result for 34.97° (x-y view)

(b) Typical Shape Result for 54.44° (x-y view)

(c) Typical Shape Result for 70.33° (x-y view)

Fig. 7: Top view of the end-configuration of the various initial angle models after contraction. The black hexagon indicates the initial position before contraction and in magenta the end configuration is shown. The circular shape in 7c is the result of torsion, and slight torsion can also be seen in 7b

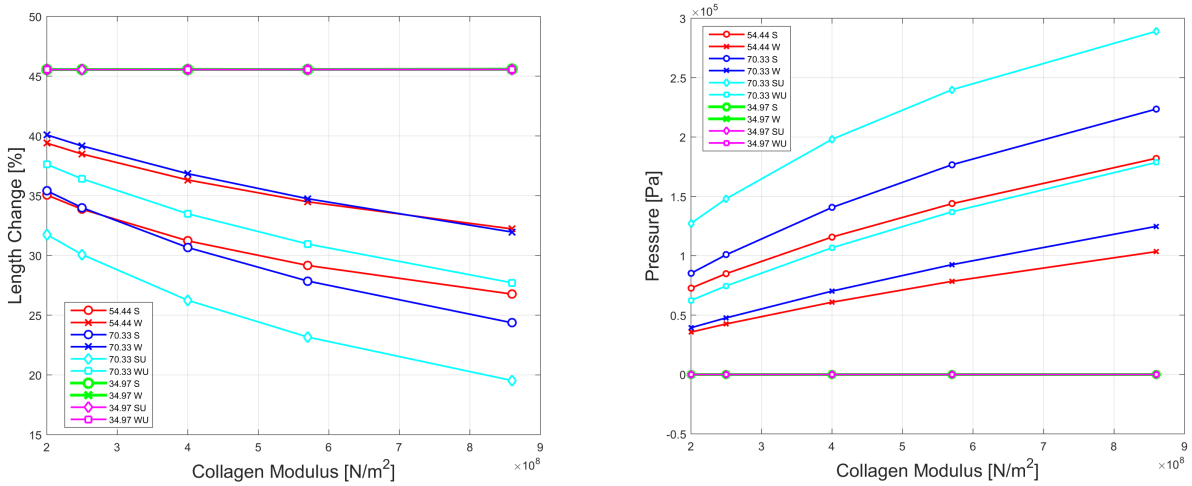

(a) Collagen modulus vs. Percentage of length change for all configurations with k_{ex}=1e^{-5} N/m

(b) Collagen Stiffness vs. Average Compartmental Pressure for all configurations with k_{ex}=1e^{-5} N/m

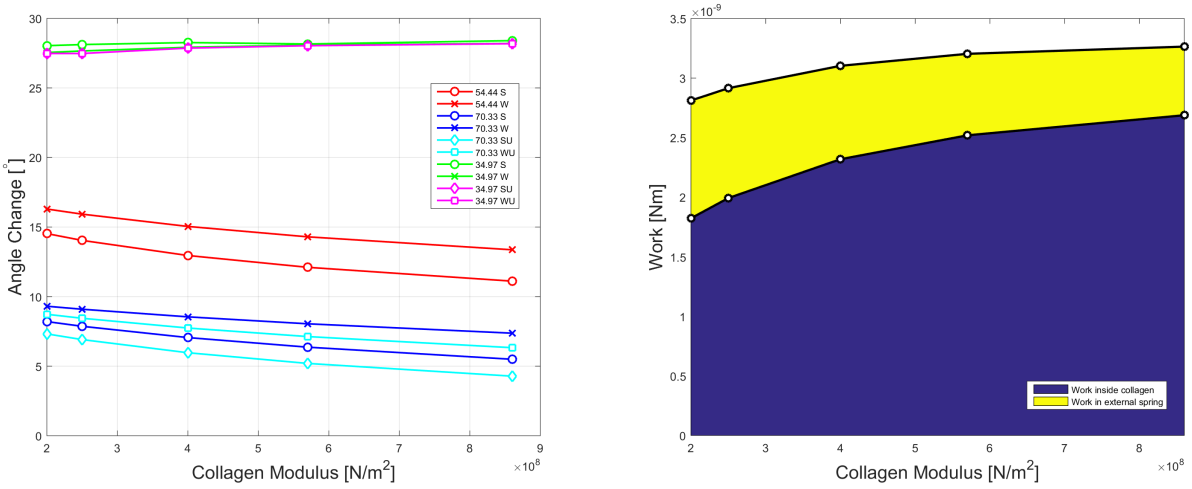

(c) Collagen Stiffness vs. Change in Orientation Angle for all configurations with k_{ex}=1e^{-5} N/m

(d) Stacked work diagram for different collagen moduli with α_{init}=54.44°, E_{col}=570MPa, r_{col}=0.4μm.

Fig. 8: Different Output Parameters for Collagen Stiffness Moduli Ranging from 200MPa to 860MPa

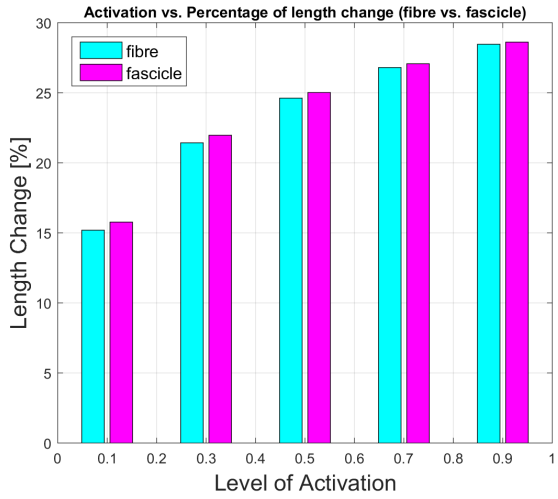

(a) Level of activation vs. length change for fiber and fascicle

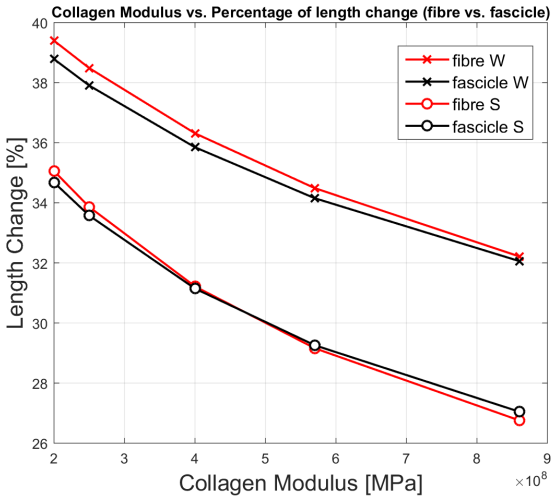

(b) Collagen modulus vs. length change for fiber and fascicle

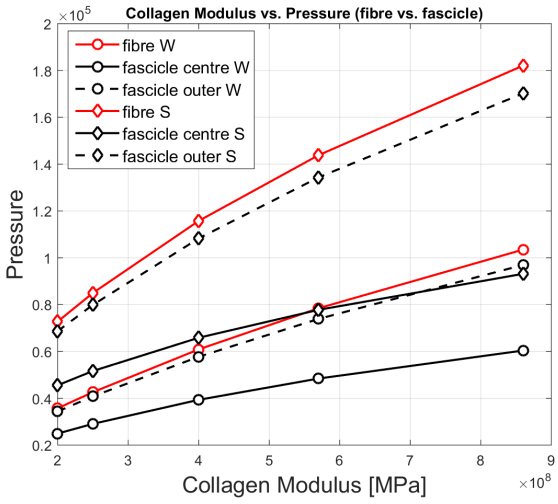

(c) Level of activation vs. pressure for fiber and fascicle. For the fascicle the pressure inside the central fiber is given as well as the average pressure in the surrounding fibers.

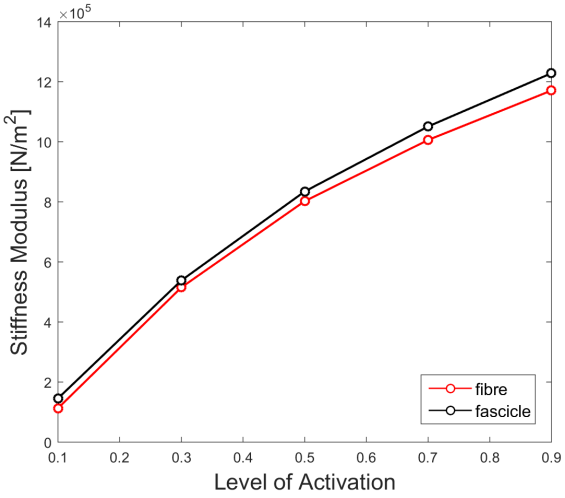

(d) Comparison of the stiffness modulus for a fascicle with a fiber in the same configuration.

Fig. 9: Comparison between fiber and fascicle for varying output parameters. (a)Level of activation vs. length change for the 54.44° configuration with r_{col}=0.4μm and E_{stiff}=570MPa, (b)Collagen modulus vs. length change for the 54.44° configuration with r_{col}=0.25μm & r_{col}=0.4μm, (c)Collagen modulus vs. pressure for the 54.44° configuration with r_{col}=0.25μm & r_{col}=0.4μm, (d)Level of activation vs. Stiffness modulus for the 54.44° configuration with r_{col}=0.4μm and E_{stiff}=570MPa. In the line plots the fiber is always indicated in red and the fascicle in black.

1) Force-Length Relationship: From the simulation results the ascending limb of the force-length relationship was reconstructed for both the fiber and fascicle model. This can be seen in Figure 10 where the normalized fiber force is plotted against percentage of length change of the fiber.

D. Myofascial Force Transmission

To analyze the effect of force transmission, a work analysis was done for a simulation where only the central fiber is activated. From analyzing the amount of work stored in the external springs as well as the collagen fiber it was found that 64.64% of the work in the system was found in the outer fibers. Since the endomysium surrounding the middle fiber is shared.

E. Sensitivity Analysis

A sensitivity analysis was conducted for all varying model parameters. In Figure 12 the results for the external spring stiffness sensitivity are displayed with the x-axis on a logarithmic scale, from this figure it is visible that external spring stiffness is a very important parameter in the model. In Figure 13 a sensitivity analysis was conducted for activation level. The results look like as expected. The sensitivity analysis for collagen modulus (Figure 8a) has already been given in the section about collagen stiffness.

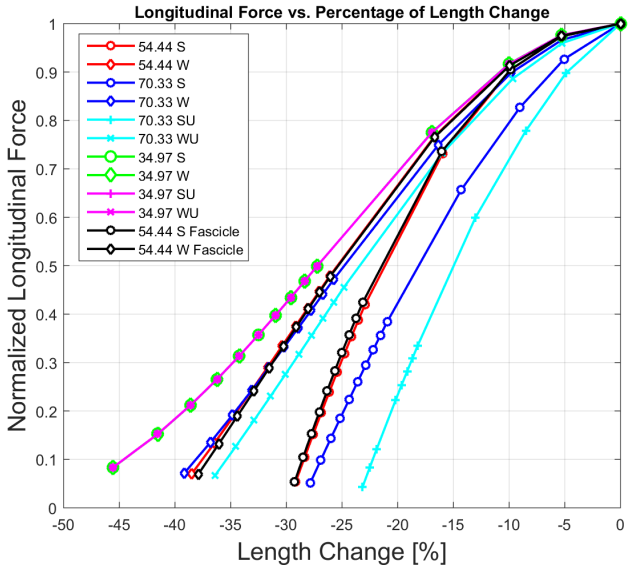

Fig. 10: Normalized Force-Length relationship for the fiber model in three different angles in the strongest and weakest configuration in both compensated (S,W) and uncompensated (SU,WU) state. The black lines indicate the fascicle model with an initial angle of 54.44° in both strong and weak configuration.

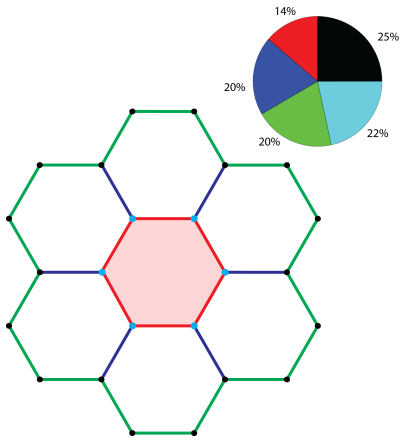

Fig. 11: Overview of the potential energy percentages for different areas of the fascicle after a simulation where only the central fiber (red) is activated. The lines indicate the collagen structure and the dots indicate the external springs. In the pie chart the percentages of the total work are stated. Summing the potential energy in the structures that do not directly surround the central fiber, a percentage of 65% is found.

More results can be found in Appendix E and the raw output data can be found in Appendix C.

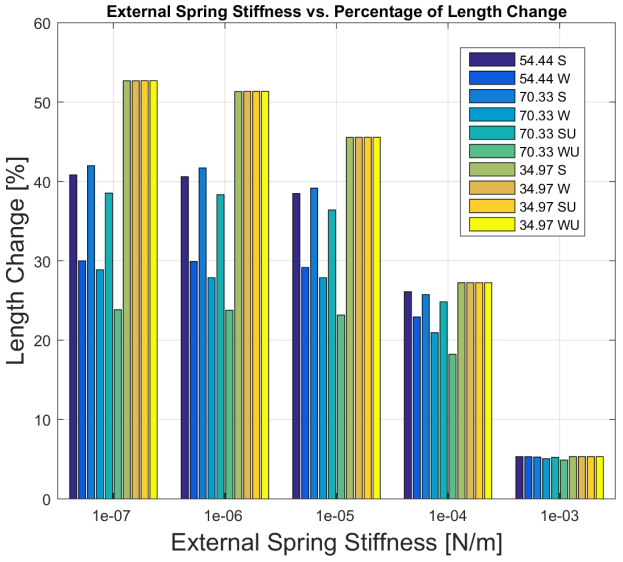

Fig. 12: External Spring Stiffness vs. Percentage of length change for weakest configuration $E_{col} = 250MPa, r_{col} = 0.25$ and strongest configuration $E_{col} = 570MPa, r_{col} = 0.4$ with k_{ex}=1e$^-$5 N/m

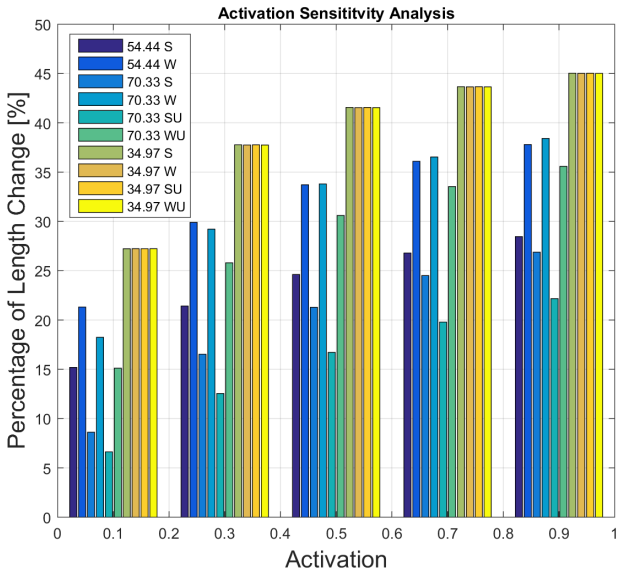

Fig. 13: Activation vs. Percentage of length change for weakest configuration $E_{col} = 250MPa, r_{col} = 0.25$ and strongest configuration $E_{col} = 570MPa, r_{col} = 0.4$ with k_{ex}=1e$^-$5 N/m

IV. Discussion

A. Model review

The model runs smoothly and convergence was good in most cases. The computational intensiveness increases with the amount of segments as well as the amount of fibers and is also dependent on the convergence. In Appendix F model convergence and computational intensiveness are thoroughly discussed. The convergence was relatively poor for the lowest angle configuration due to reaching the end of the force length-relationship, this is a numerical problem.

1) Influence of braiding angle: The first data is generated by creating a plot from the resulting coordinates of the model (Figure 6). It is evident that the different initial angles lead to different results. From the top view in Figure 7 it is very noticeable that the resulting shapes of the simulations differ quite extensively per initial angle. In the 34.97° angle configuration a shape can be seen that would be described as elliptic if the fiber were round. The 54.44° configuration largely remains hexagonal and in the 70.33° configuration a circular top view can be noticed. This circular image is in fact the result of torsion within the stacked elements leading to a circular look. Furthermore we can find that the smaller the initial braiding angle, the larger the contraction. This was expected, since for the highest angles, fiber contraction can only result in straining of the collagen lattice. whereas for the smallest angle a large rotation can take place before straining the collagen. This leads to the force-length relationship being dominant for the smallest angle and the passive collagen lattice becoming more dominant for higher initial angles.

The expectation that 54.44° angle would play an important role in terms of strain levels was not completely fulfilled. This could partly be attributed to the relatively larger error in the 34.97° model as well as all angles being a mean value. For the 34.97 angle configurations the mean strain levels remained negative, however when looking at only the positive values the following figure could be created (Figure 14). Positive strain levels start to arise around the expected value for the strong configuration, however for the weak configuration strain levels only start to increase around 60°. Because of the poor convergence for this model setup, model errors are relatively large. This could be an explanation for the discrepancy.

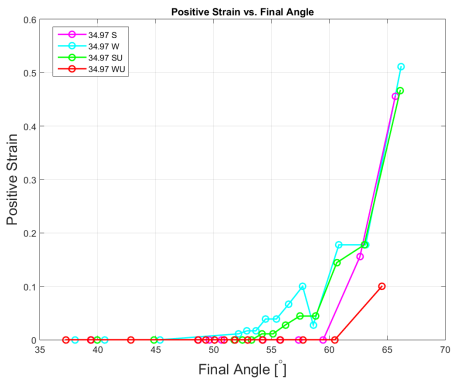

Fig. 14: Positive strain values vs. Orientation angle for different configurations in the 34.97° model.

2) Influence of collagen stiffness: To observe the effect of collagen modulus, this value was plotted against several other parameters. In Figure 8a collagen modulus is plotted against length change. In this figure we find that collagen modulus does not affect the 34.97° configuration, since the length change is the same for every collagen modulus. For the other angles there is a clear effect; length change decreases with increasing collagen modulus. Furthermore the weaker configurations undergo a larger contraction than the stronger configurations. This is exactly as expected. Interesting in this figure is that the lines of the compensated 70.33° configuration and the 54.44° configuration cross. For the lowest stiffness modulus both blue lines are above the red, even though the collagen strain is higher in the 70.33° configuration due to the higher initial angle. This is likely the effect of the compensation resulting in a lower collagen stiffness due to a decreased fiber thickness as the uncompensated configurations remain below the red lines. The collagen in the model was assumed to be linearly elastic, however in reality it is highly nonlinear and its strength increases with stress levels [34], this is likely to increase differences between the 54.44° and 70.33° configurations. In Figure 8 collagen modulus is plotted against average compartmental pressure and in Figure (8b) against change in orientation angle. When we look at pressure what stands out is that for the 54.44° and 70.33° configurations the pressures are positive and increasing with collagen modulus. This is what was expected since the pressure within the fiber is induced by straining of the collagen fibers. A higher collagen modulus will therefore lead to a higher pressure. Interesting is that the effect that was visible in the previous Figure 8a with the red and blue lines crossing is not present in this figure for pressure. For the 34.97° configuration however, all pressures are slightly negative but very close to 0, and collagen strain levels have an average negative value. Because of the assumption of collagen only resisting deformation in tension this means there is no resistance in the collagen fibers. The slightly negative pressure indicates that the constraint forces are pulling the nodes inwards. The shortening of the fiber is therefore only the result of rotation and it is likely that the elliptic shape allows for the largest amount of collagen fiber rotation without straining. The contraction action is ended because of the sarcomeres reaching the left end of the force-length relationship and therefore cannot deliver contraction force anymore. When we look at the angle reorientation (8c) we can see that the 34.97° configuration is subject to the largest angle change and the 70.33° configuration encounters the least rotation but has a relatively high standard deviation (see Appendix E.1). The collagen modulus has a negative correlation with angle change for the larger angle configurations. These results are as expected. For the smallest angle, the angle change actually seems to increase slightly with angle change, this is likely the effect of model variance as the standard deviation also decreases with collagen stiffness here.

3) Work: When we reflect back to Figure 8a,8c, we found that in some cases length change was larger for the 70.33° configuration whereas the pressure was also higher. This can be explained by looking at the work levels in the system. Even thought the length change is slightly higher, the collagen potential energy is higher for the 70.33° configuration. This is the effect of a higher strain level for this configuration despite the lower stiffness.
In figure 8d the amount of work is plotted against collagen

stiffness for a single configuration. Here the division is shown between potential energy in the collagen lattice and the external springs. From this figure it can be found that work in the external springs decreases with collagen stiffness, this is due to the collagen limiting the contraction and therefore the strain in the external springs. Furthermore we find we find that work generally increases with collagen stiffness. Generally since this is the case in most scenarios tested, there are however exceptions. When we look at the formula for calculating potential energy in a linear spring $W = \frac{1}{2}ke^2$ we find that the elongation e is quadratically related to potential energy and stiffness is not, so when the collagen stiffness becomes so high that it extensively limits the strain levels, the potential energy could decrease for an increasing collagen modulus. This effect can be observed in the strongest configuration of 70.33° in Appendix E.1.1. So for we can conclude that in the model, the end result is always a balance between the contraction force from the sarcomeres and the passive contribution of the collagen fiber as well as the external spring.

B. Fiber vs. Fascicle Model

The fascicle model was made for two reasons; to compare its results to the fiber model as well as analyzing myofascial force transmission, therefore these results were presented.

In Figure 9a one can see that in general the length change in a fiber is higher than in a fascicle. The difference increases with lower levels of activation. This can likely be explained by the fact that the relative collagen content is larger in a fiber since the fibers in the fascicle share their endomysial walls. When activation decreases the relative contribution of the sarcomeres decreases where the passive property influence of the endomysium remain the same. Since the passive content is relatively higher in a single fiber this has more impact than in a fascicle. When we look at Figure 9b we find that in the weak condition the length change is always higher in a fiber, but the difference becomes smaller with increasing collagen modulus. For the strong condition an actual shift can be seen. A thing that stands out with the fascicle model is the difference in pressure between the central and surrounding fibers. This is represented in 9c where one can see that the pressure inside the central fiber is generally lower than in the outer fibers. When compared to the single fiber model the average pressure in the outer fibers is slightly lower and the pressure in the central fiber is extensively lower. The pressure difference can be explained by the fact that any width expansion within the central fiber will result in pressure on the outer fibers, these are therefore forced to expand even further resulting in higher collagen strain. The higher collagen strain is also the likely explanation for the shift in length change for higher collagen moduli in Figure 9b. This effect is expected to be larger on a regular fascicle or whole muscle scale. Finally the stiffness of both models was compared for different activation levels in Figure 9d. The fascicle model has a higher stiffness modulus that increases with activation. The higher stiffness could however also be the result of the difference in length change that can be seen in 9b for the strong configuration at E_{stiff}=570MPa, therefore the stiffness results are inconclusive.

C. Force-Length Relationship

In Figure 10 the force-length relationship was reconstructed for different model configurations. From this figure we can conclude that for the 34.97° configuration all lines are on top of one another and therefore the collagen stiffness does not influence the results. This means that the force-length relationship for this initial angle can solely be attributed to the force-length relationship of a sarcomere. To check this the normalized curves for 34.97° were compared to the normalized force-length relationship used as input for the model and both aligned (see Appendix E.2). For the other configurations a shift can be seen towards the right, for a higher collagen stiffness, the half parabola is closer to the rest length axis. This means that here the collagen does affect the outcome and therefore the total length change decreases for the same force level. This is caused by a larger amount of the work generated by the sarcomere elements being stored in the collagen fiber structure, therefore decreasing the operating range for these configurations. This is a similar effect to what can be observed in the active force-length relationship for whole muscle where the amount of length change generally does not surpass 40% [35], [36].

What can also be noticed is that the curve for the 54.44° angle is steeper than the ones for 70.33°. The black lines indicate the results for a fascicle with an initial angle of 54.44°. The fascicle results are similar to the single fiber results for the same configuration.

D. Force Transmission

The force transmission was analyzed in the fascicle model. The results are displayed Figure 11. In a configuration where only the central fiber was fully activated 64.64% of the work in the system was found in the outer fibers. This does not include the work found in the collagen surrounding the central fiber (red lines in the figure), even though this layer is shared with the surrounding fibers. When 50% of the potential energy in this layer is accredited to the neighbours, a transmission percentage of 71.5% is found. Similar studies calculated force transmission in a slightly different way. Findley [14] compared radial stress to longitudinal stress and found a ratio of 50%. Sharafi [13] found a lateral force transmission percentage of 80% in intrafascicularly terminating muscle fibers. The found values here are right in between those studies, however it needs to be stressed that the calculation method differs quite extensively and it is therefore difficult to compare results.

E. Sensitivity Analysis

In Figure 12 a sensitivity analysis for the external spring stiffness was conducted. The finding here is that the external spring stiffness can influence the length change quite extensively. The value that was chosen to be used for the simulations was chosen to be $1e^{-5}$N/m, because it allows for quite some extension while remaining stable

in all configurations whereas the smaller two values led to instabilities in the fascicle models. In Figure 13 the results for the activation sensitivity analysis are displayed. From this it can be concluded that length change increases with activation which was to be expected.

F. Model Validation

Since the data that were modeled are not available experimentally validation methods were limited. Therefore validation will be have to be attributed to the model largely behaving like expected and the use of model parameters from literature. We hypothesized that for a smaller braiding angle, strain, pressure and internal work would be lower and displacements would be larger than in a higher angle configuration. This was confirmed by the model results. Furthermore the expectation that a higher collagen stiffness resulted in less contraction turned out to be right. No contra-intuitive behaviour was found as lower activation resulted in less contraction and when activation was completely removed the model moved back to its initial position. Furthermore muscle contraction resulted in radial expansion and an increased stiffness for the external spring resulted in less contraction.
In Appendix G different discretizations were compared, a completely fair comparison was not possible however as far as the comparison could be made results agreed well. In Appendix H a comparison was done with experimental data on active muscle stiffness for different levels of activation. It was found that the experimental values fell well within the range of the modeling output values for the 54.44° model. In Appendix I model data and data from Purslow (1994) on numerically-weighted mean fibril orientation of the endomysium for different sarcomere lengths were collated. This also turned out to be a good fit despite the slight difference in initial braiding angle.

G. Comparison to other models

This model is dissimilar to most other models used in muscle modeling. As mentioned in the introduction, this model addresses the strong relationship between muscle architecture and functional capabilities. This model was built to gain a better understanding on the influence of the myofascia on muscle function and the results suggest the influence can be substantial. The relevance of the findings in this study for other models is very much dependent on model function. As far as the Hill model goes, the causality between different parameters that were found from this study can likely be applied, however before this can be done the model needs to be further validated.

H. Limitations

The model described in the paper is limited to static model simulations for only three different initial angle configurations. Ideally more angle configurations would be tested, however this was not possible due to time constraints. Furthermore the model input possibilities were restricted to force inputs only. This made it difficult to compare stiffness for the different model configurations. Because of the force-length relationship, the length from which the stiffness is measured needs to be the same to make a fair stiffness comparison. With a displacement input this would have been possible, however with a force input only possibilities were limited. The discretization method of the model was not ideal since the initial angle configuration determined the discretization of the system. It was therefore difficult to make a fair comparison between the different discretizations used in the model(see Appendix G). This also limited the amount of angle configurations that could be tested as not every configuration would result in the same muscle fiber length in the model. Another limitation for creating the model was that relatively little experimental data is available on the topic, especially on the endomysium. Therefore many assumptions had to be made to come to a model and validation possibilities were limited. An important simplification that was done was to neglect the waviness of collagen fiber and assume it to be linearly elastic. The waviness would make it possible for the material to deform without straining the collagen, allowing for much easier movement. What needs to be kept in mind however is that this does not exclude radial stiffness which is likely to be most important in this model. In future improvements this characteristic could be implemented. Barring the waviness, collagen fiber is never linearly elastic in practice. It has been a long known fact that collagen exhibits highly nonlinear stress-strain behaviour [34], its stiffness being known to increase with load. Another simplification was that the force-length relationship was assumed to scale equally with activation, however in reality the force-length relationship exhibits activation-dependent shifts [37]. This could also be an addition to a future model. Finally in the fascicle model it was assumed that neighbouring fibers share nodes, however in real muscle fibers a complex network of costameres connects fibers with the endomysium.

V. Conclusion

The goal of this study was to develop a model incorporating the properties of the collagen braiding structure and analyzing the sensitivity of the kinematic properties in the model. Most expectations came out of the data and the main finding of this study is that collagen braiding angle as well as collagen stiffness have a strong effect on model outcomes. Because validation is challenging it is difficult to directly relate model output to skeletal muscle behaviour.

Conclusions

- The model runs smooth but validation possibilities were limited
- Initial braiding angle influences the shape, displacement, pressure, work and strain of the fiber model output
- For smaller initial braiding angles the active contractile properties are more dominant than the passive properties
- Collagen stiffness influences displacement, pressure, work and strain only for larger angle configurations
- Slight differences were found between fiber and fascicle in terms of length change and stiffness.
- Large pressure difference were found between fibers in the fascicle

- Outer fibers within fascicle are subject to larger strain values due to radial extension of all muscle fibers
- Myofascial force transmission was found to be at least 65%
- The expected strain effect at the 54.44° could not clearly be extrapolated from the data

VI. Recommendations

The recommendations consist of two parts, the first one being adaptions to improve the model and the second one gathering more experimental data so model validation will be more accessible in the future.

Model Adaptions

- Expand the model to apply a displacement input to accurately assess stiffness
- Add passive component and calibrate it to use model in passive as well as active conditions
- Make the model dynamic
- Continuum model where mesh is independent from fiber angle
- Extend the model scale to a larger fascicle

Further research

- More anatomic research is needed since the amount of studies on endomysium and perimysium very limited
- New experimental techniques must be developed that enable measurements on myofascia material properties

References

[1] G. A. Meyer and R. L. Lieber, "Elucidation of Extracellular Matrix Mechanics from Muscle Fibers and Fiber Bundles," *Journal of Biomechanics*, vol. 44, no. 4, pp. 771–773, 2011.

[2] T. J. Patel and R. L. Lieber, "Force transmission in skeletal muscle: from actomyosin to external tendons.," *Exercise and sport sciences reviews*, vol. 25, pp. 321–63, jan 1997.

[3] P. A. Huijing, "Epimuscular myofascial force transmission: A historical review and implications for new research. International society of biomechanics Muybridge award lecture, Taipei, 2007," *Journal of Biomechanics*, vol. 42, pp. 9–21, jan 2009.

[4] P. P. Purslow, "The structure and functional significance of variations in the connective tissue within muscle," *Comparative Biochemistry and Physiology Part A: Molecular & Integrative Physiology*, vol. 133, pp. 947–966, dec 2002.

[5] M. D. Grounds, L. Sorokin, and J. White, "Strength at the extracellular matrix-muscle interface," *Scandinavian Journal of Medicine and Science in Sports*, vol. 15, no. 6, pp. 381–391, 2005.

[6] A. R. Gillies and R. L. Lieber, "Structure and function of the skeletal muscle extracellular matrix," *Muscle nerve*, vol. 44, no. 3, pp. 318–331, 2012.

[7] P. Fratzl, *Collagen Structure and Mechanics*. Springer, 2008.

[8] B. Van der Linden, "Mechanical modeling of skeletal muscle functioning.," pp. 1–147, 1998.

[9] P. Purslow and J. A. Trotter, "The morphology and mechanical properties of endomysium in series-fibred muscles: variations with muscle length," *Journal of Muscle Research and Cell Motility*, vol. 15, jun 1994.

[10] P. P. Purslow, "Strain-induced reorientation of an intramuscular connective tissue network: Implications for passive muscle elasticity," *Journal of Biomechanics*, vol. 22, pp. 21–31, jan 1989.

[11] R. B. Clark and J. B. Cowey, "Factors Controlling the Change of Shape of Certain Nemertean and Turbellarian Worms," *J Exp Biol*, vol. 35, pp. 731–748, 1958.

[12] G. Scarr, "Fascial hierarchies and the relevance of crossed-helical arrangements of collagen to changes in the shape of muscles," *Journal of Bodywork and Movement Therapies*, vol. 20, no. 2, pp. 377–387, 2015.

[13] B. Sharafi and S. S. Blemker, "A mathematical model of force transmission from intrafascicularly terminating muscle fibers.," *Journal of biomechanics*, vol. 44, pp. 2031–9, jul 2011.

[14] T. Findley, H. Chaudhry, and S. Dhar, "Transmission of muscle force to fascia during exercise.," *Journal of bodywork and movement therapies*, vol. 19, pp. 119–23, jan 2015.

[15] C. A. Yücesoy, *Myofascial Force Transmission a Combined Finite Element Modeling and Experimental Approach*. 2003.

[16] C. Zhang and Y. Gao, "Finite element analysis of mechanics of lateral transmission of force in single muscle fiber.," *Journal of biomechanics*, vol. 45, pp. 2001–6, jul 2012.

[17] J. A. Hodgson, "Finite Element Modeling of Passive Material Influence on the Deformation and Force Output of Skeletal Muscle," *J Mech Behav Biomed Mater.*, vol. 29, no. 6, pp. 997–1003, 2012.

[18] S. S. Blemker, P. M. Pinsky, and S. L. Delp, "A 3D model of muscle reveals the causes of nonuniform strains in the biceps brachii.," *Journal of biomechanics*, vol. 38, pp. 657–65, apr 2005.

[19] B. Sharafi and S. S. Blemker, "A micromechanical model of skeletal muscle to explore the effects of fiber and fascicle geometry.," *Journal of biomechanics*, vol. 43, pp. 3207–13, dec 2010.

[20] P. P. Purslow, "Muscle fascia and force transmission.," *Journal of bodywork and movement therapies*, vol. 14, pp. 411–7, oct 2010.

[21] J. Gindre, M. Takaza, K. M. Moerman, and C. K. Simms, "A structural model of passive skeletal muscle shows two reinforcement processes in resisting deformation.," *Journal of the mechanical behavior of biomedical materials*, vol. 22, pp. 84–94, jun 2013.

[22] D. Rassier, B. MacIntosh, and W. Herzog, "Length dependence of active force production in skeletal muscle," no. 127, pp. 626–634, 1999.

[23] O. Bauchau, *Flexible Multibody Dynamics*, vol. 176. Springer, 2011.

[24] R. Avilés, G. Ajuria, V. Gómez-Garay, and S. Navalpotro, "Comparison among nonlinear optimization methods for the static equilibrium analysis of multibody systems with rigid and elastic elements," *Mechanism and Machine Theory*, vol. 35, no. 8, pp. 1151–1168, 2000.

[25] G. A. Mohammed and M. Hou, "Optimization of Active Muscle Force-Length Models Using Least Squares Curve Fitting," *IEEE Transactions on Biomedical Engineering*, vol. 63, no. 3, pp. 630–635, 2016.

[26] E. N. Marieb and K. Hoehn, *Human Anatomy & Physiology*. 2013.

[27] A. Cutts, "The range of sarcomere lengths in the muscles of the human lower limb.," *Journal of anatomy*, vol. 160, pp. 79–88, 1988.

[28] V. Decostre, P. Bianco, V. Lombardi, and G. Piazzesi, "Effect of temperature on the working stroke of muscle myosin.," *Proceedings of the National Academy of Sciences of the United States of America*, vol. 102, no. 39, pp. 13927–13932, 2005.

[29] R. I. Close, "Dynamic Mammalian Properties of Skeletal Muscles," *Physiological Reviews*, vol. 52, no. 1, pp. 129–197, 1972.

[30] Y. P. Kato, D. L. Christiansen, R. A. Hahn, S. J. Shieh, J. D. Goldstein, and F. H. Silver, "Mechanical properties of collagen fibres: a comparison of reconstituted and rat tail tendon fibres," *Biomaterials*, vol. 10, no. 1, pp. 38–42, 1989.

[31] E. Gentleman, A. N. Lay, D. A. Dickerson, E. A. Nauman, G. A. Livesay, and K. C. Dee, "Mechanical characterization of collagen fibers and scaffolds for tissue engineering," *Biomaterials*, vol. 24, no. 21, pp. 3805–3813, 2003.

[32] J. A. J. Van Der Rijt, K. O. Van Der Werf, M. L. Bennink, P. J. Dijkstra, and J. Feijen, "Micromechanical testing of individual collagen fibrils," *Macromolecular Bioscience*, vol. 6, no. 9, pp. 699–702, 2006.

[33] Z. L. Shen, M. R. Dodge, H. Kahn, R. Ballarini, and S. J. Eppell, "Stress-strain experiments on individual collagen fibrils.," *Biophysical journal*, vol. 95, no. 8, pp. 3956–63, 2008.

[34] A. J. Licup, S. Münster, A. Sharma, M. Sheinman, L. M. Jawerth, B. Fabry, D. a. Weitz, and F. C. MacKintosh, "Stress controls the mechanics of collagen networks," *Proceedings of the National Academy of Sciences*, vol. 112, no. 31, p. 201504258, 2015.

[35] C. N. Maganaris and C. N. Maganaris, "Force-length characteristics of in vivo human skeletal muscle," *Acta physiologica Scandinavica*, vol. 172, no. 4, pp. 279–285, 2001.

[36] H. Gareis, S. Moshe, R. Baratta, R. Best, and R. D'Ambrosia, "The isometric length-force models of nine different skeletal muscles," *Journal of Biomechanics*, vol. 25, no. 8, pp. 903–916, 1992.

[37] N. C. Holt and E. Azizi, "What drives activation-dependent shifts in the force-length curve?," *Biology letters*, vol. 10, pp. 20140651–, sep 2014.

A

Background

A.1. Anatomic Background

Skeletal muscle generally consists of skeletal muscle fibers, connective tissue, neural tissue and structures for blood supply. In figure A.1a the general structure of muscle fibers and the myofascia is displayed. the structures will be discussed from the outside to the inside starting with the largest unit, the muscle itself. The muscle is wrapped in a connective tissue sheath called the epimysium. The epimysium is continuous with the tendon that connects muscle to bone. On a smaller scale fascicles are found, these are bundles of muscle fibers. Fascicles are surrounded by a second connective tissue sheath called the perimysium. The smallest structure indicated in figure A.1a is the muscle fiber. Muscle fibers can also be referred to as 'muscle cells' and are therefore the basic structural and functional unit of skeletal muscle tissue. Muscle fibers are embedded in a connective tissue network called the endomysium, a connective tissue sheath mainly consisting of collagen fibers. The epimysium, perimysium and endomyium together are called the myofascia. For this study we are mainly interested in the endomysium and only slightly in the perimysium. The epimysium will therefore not be discussed any further.

A.1.1. Muscle contraction

To acquire an understanding of the principle of muscle contraction, we need to zoom in to the microscopic level of a single muscle fiber. Muscle fibers are constructed of smaller units called myofibrils which can also be seen in figure A.1a but are not indicated. Myofibrils are rodlike structures running in parallel to the length direction of the fiber. All myofibrils are wrapped by the sarcolemma to form a single fiber structure. Myobrils are composed of sarcomere units running in series along the length of the myofibril. Sarcomeres are the functional units of muscle contraction [5], this is where movement is originated. In figure A.1b the structure is displayed. Sarcomeres are composed of myofilaments that can be further divided into two main groups of thick and thin filaments. The thick filaments are large polymers of the protein myosin, and the thin filaments are composed of the protein actin. Within a sarcomere these protein polymers intertwine and form hexagonal lattices often referred to as "cross-bridges". These are the structures that in an active state produce muscle force and movement. This principle is described as the sliding filament theory because it involves the actin and myosin filaments sliding over each other. In A.2 the principle of sarcomere contraction is demonstrated.

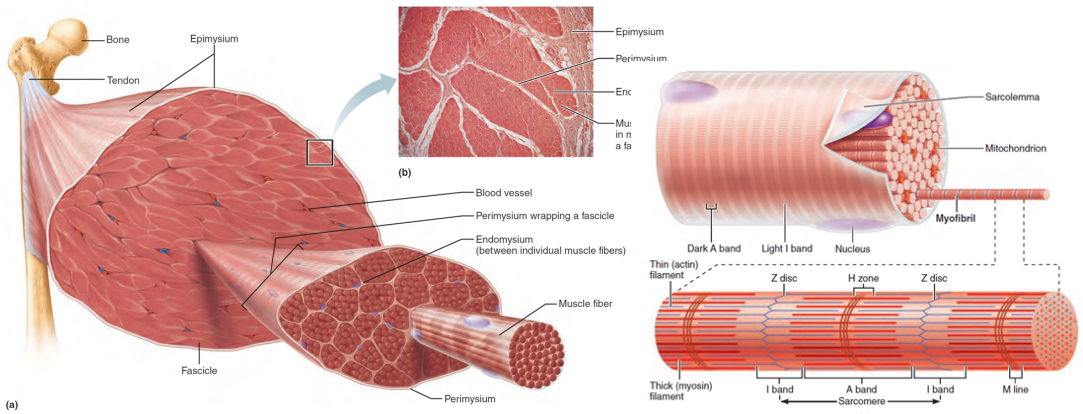

(a) Skeletal Muscle Anatomy [7]

(b) Muscle fibre and myofibril anatomy [7]

Figure A.1: Anatomy of muscle, fascicle, muscle fiber, myofibril and sarcomeres

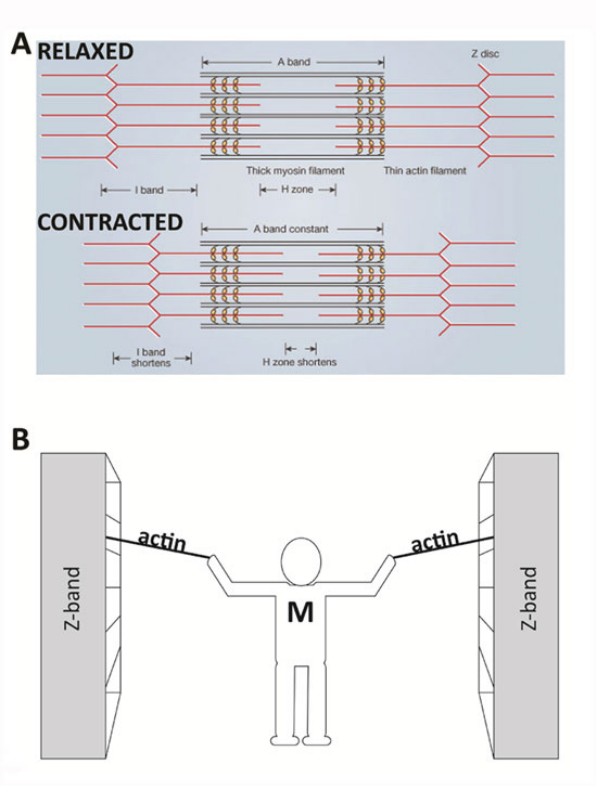

Figure A.2: (A) The basic organization of a sarcomere showing the location of myosin (A band). Actin and the z-discs are shown in red. (B) A conceptual figure representing the connectivity of molecules within a sarcomere. A person standing between two bookcases (z-discs) pulls them in via ropes (actin). Myosin (M) is analogous to the person and the pulling arms. ©Nature Publishing Group

A.1.2. Endomysium

From inside out, the endomysium is the first intramuscular connective tissue layer encountered as it surrounds every separate muscle fiber and is in direct contact with the sarcolemma. Therefore, force generated by the muscular fibers is transmitted directly to the endomysium [12, 15]. It forms a network in which the muscle fibers lie adjacent in hexagonally shaped compartments [17]. Throughout the endomysium, all fibers lie in the same plane, only at the junctional zones between the endomysium and perimysium this is not the case. The endomysium is composed of fibrillar collagen types I,III and

V and periodic filamentous collagen type IV [16]. The tissue is relatively constant in its structure and only varies slightly between different muscles.
The collagen fibrils are curvilinear and therefore will first have to be stretched to resist deformation. In figure A.3 a microscopic picture of the endomysium is displayed from which the hexagonal structure is clearly visible. The endomysium seems to be quite disordered as the collagen fibers run at almost every angle to the muscle fibre axis at resting length but it is not completely random [13]. In an experiment where the orientation angle of the endomysium was examined, the collagen fibrils were slightly biased towards the circumferential orientation with an average weighted orientation of 59 °. Since the tubular wall of the endomysial sheath is shared between adjacent fibers, the tensional force generated by contraction can be efficiently transmitted to adjacent tubes. This principle is also referred to as myofascial force transmission.

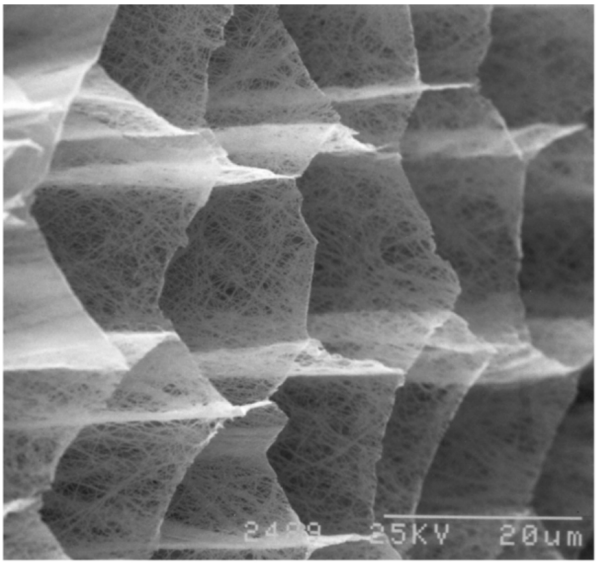

Figure A.3: Endomysium after removal of muscle fibres [12]

A.1.3. Perimysium

The perimysium is the structure that encapsulates each fascicle. Unlike the endomysium, the perimysium can vary greatly between and within muscles in size, shape and thickness. Fascicles are organized into primary- and secondary fascicles by the perimysium. Smaller fascicles are wrapped by primary perimysium and the bigger ones by secondary perimysium. The perimysium has a slightly different collagen composition as it contains collagen types I, III, VI, and XII [9]. The collagen fibers in the perimysium have a diameter up to ten times greater than the collagen fibers of the endomysium [11]. Unlike the endomysium, the perimysium has a clear orientation structure of its collagen fibers. The collagen fibrils run in the plane of the perimysium and in each so-called layer, the collagen fibers lie parallel to one another at an angle of 55° to the muscle fiber axis when at resting length. This represents the optimum fiber angle for carrying simultaneously the radial and longitudinal stresses in composite materials [3]. The fiber orientation drastically changes with muscle activation. Like the endomysium, the perimysium is compliant in the longitudinal direction untill the fibers are straightened out. At this point the perimysium is capable of carrying a large load in tension, but this only happens in ranges beyond the physiological length [12].

A.2. Myofascial force transmission

Myofascial force transmission is a means of lateral force transmission trough the fascia within or surrounding the muscle. When a fiber is activated a network of intermediate filaments and costameres transmits the action of the myofibril onto the neighbouring myofibrils and this is then passed on to the sarcolemma, the first key point of transfer. From the sarcolemma force is transferred laterally to the basement membrane and is then integrated with the connective tissue before being passed on to the tendon.

A.3. Clinical Background

Many patients experience spasticity as a result of an upper motor neuron lesion. Spasticity can be very disabling for patients. In conditions involving spasticity often a dramatic increase of muscle stiffness is found, in addition the morphology of the muscle appears to change [6]. The muscle fibre density decreases and an increase in the thickness of the passive sheath is often found [5]. The myofascia therefore play a large role in muscle remodeling as a result of spasticity. To achieve a better insight in the remodeling process happening in spasticity, we first need to understand the functional role of the myofascia. For a physician is can be difficult to distinguish between the different elements contributing to joint stiffness. Furthermore it can be difficult to distinguish collageneous tissue from fat. As different treatment methods are advisable for different causes of the increased joint resistance and spasticity, it is important to get a better insight into the contribution of passive tissue sheath to muscle mechanics.

B

Matlab Code

B.1. General Matlab Script

```
clear all
close all
clc

prompt = {'Enter number of segments:','Enter total fibre diameter:',...
            'Initial sarcomere length','Enter initial collagen angle (degrees):',...
            'Collagen Stiffness:','External spring stiffness:','Activation [0-1]:',...
            'Fixed top? [0 1]','Fixed bottom? [0 1]'};
dlg_title = 'Model Parameters';
num_lines = [1 60];
defaultans = {'1','30','2.64','54.44','250','10','1','0','1'};
answer = inputdlg(prompt,dlg_title,num_lines,defaultans);

seg=str2num(answer{1});dia=str2num(answer{2});sarcrest=str2num(answer{3});
angle=str2num(answer{4});colstiff=str2num(answer{5});exstiff=str2num(answer{6});
act=str2num(answer{7});topfix=str2num(answer{8});bottomfix=str2num(answer{9});

%  Definition of Data
dim = 3;                                % dimensions
o= seg;                                 % # of elements
n=o+1;                                  % # of boundries

rib=dia/2;                              % half diameter
sepz=rib/tand(angle);                   % layer thickness
cline=tand(60)*(rib/2);                 % coordinate height
A_fib=(cline*(rib/2))*6;                % total fibre diameter area
A_sarc=A_fib/6;                         % Total area per sarcomere
pretbex=0;
prettex=0;

nx=6*n*3;                               % # of DOF's
numnod=6*n;                             % # of nodes
numco=6*3;                              % # of DOF's in one layer
E=colstiff;
A=(0.2)^2*pi;
EA = E*A;                               % spring stiffness (endomysium)
EAx = exstiff;                          % spring stiffness (external spring)
EAf = 100;                              % force stiffness
```

```
labda = ones(o,1)*0;                % initial value of lambda
sigmamax=0.28*act;                  % Maximum sarcomere tension (280 kPa)
fe=(sigmamax*A_sarc);               % sarcomere force
l_ex=sepz*o*2;                      % external spring length

%Other angles
newangle=atand(rib/(sepz*2));
%% Generating coordinate points
xA =sym('xA',[n 1]);yA =sym('yA',[n 1]);zA =sym('zA',[n 1]);% Gen sym 'A' nodes
xB =sym('xB',[n 1]);yB =sym('yB',[n 1]);zB =sym('zB',[n 1]);% Gen sym 'B' nodes
xC =sym('xC',[n 1]);yC =sym('yC',[n 1]);zC =sym('zC',[n 1]);% Gen sym 'C' nodes
xD =sym('xD',[n 1]);yD =sym('yD',[n 1]);zD =sym('zD',[n 1]);% Gen sym 'D' nodes
xE =sym('xE',[n 1]);yE =sym('yE',[n 1]);zE =sym('zE',[n 1]);% Gen sym 'E' nodes
xF =sym('xF',[n 1]);yF =sym('yF',[n 1]);zF =sym('zF',[n 1]);% Gen sym 'F' nodes

% External spring connection points
syms sbxA sbyA sbzA sbxB sbyB sbzB sbxC sbyC sbzC
syms sbxD sbyD sbzD sbxE sbyE sbzE sbxF sbyF sbzF
syms stxA styA stzA stxB styB stzB stxC styC stzC
syms stxD styD stzD stxE styE stzE stxF styF stzF

% Create vertices (symbolic)
A=[xA yA zA];   % Generate symbolic 'A' vertices
B=[xB yB zB];   % Generate symbolic 'B' vertices
C=[xC yC zC];   % Generate symbolic 'C' vertices
D=[xD yD zD];   % Generate symbolic 'D' vertices
E=[xE yE zE];   % Generate symbolic 'E' vertices
F=[xF yF zF];   % Generate symbolic 'F' vertices

% Initial Conditions (apply initial dimensions to node locations)
xA0=ones(n,1)*-rib/2;    yA0=ones(n,1)*cline;        zA0=(0:sepz:o*sepz).';
xB0=ones(n,1)*rib/2;     yB0=ones(n,1)*cline;        zB0=(0:sepz:o*sepz).';
xC0=ones(n,1)*rib;       yC0=zeros(n,1);             zC0=(0:sepz:o*sepz).';
xD0=ones(n,1)*rib/2;     yD0=ones(n,1)*-cline;       zD0=(0:sepz:o*sepz).';
xE0=ones(n,1)*-rib/2;    yE0=ones(n,1)*-cline;       zE0=(0:sepz:o*sepz).';
xF0=ones(n,1)*-rib;      yF0=zeros(n,1);             zF0=(0:sepz:o*sepz).';

A0=[xA0 yA0 zA0];   % Generate initial numeric 'A' vertices
B0=[xB0 yB0 zB0];   % Generate initial numeric 'B' vertices
C0=[xC0 yC0 zC0];   % Generate initial numeric 'C' vertices
D0=[xD0 yD0 zD0];   % Generate initial numeric 'D' vertices
E0=[xE0 yE0 zE0];   % Generate initial numeric 'E' vertices
F0=[xF0 yF0 zF0];   % Generate initial numeric 'F' vertices

% Coordinates
coord(1:6,:)=[A0(1,:);B0(1,:);C0(1,:);D0(1,:);E0(1,:);F0(1,:)];
coord_sym(1:6,:)=[A(1,:);B(1,:);C(1,:);D(1,:);E(1,:);F(1,:)];
for ii=2:n
    % numeric coordinate matrix
    coord=[coord;A0(ii,:);B0(ii,:);C0(ii,:);D0(ii,:);E0(ii,:);F0(ii,:)];
    % symbolic coordinate matrix
    coord_sym=[coord_sym;A(ii,:);B(ii,:);C(ii,:);D(ii,:);E(ii,:);F(ii,:)];
end
nco = [[1:dim:nx].' [2:dim:nx].' [3:dim:nx].'];% create node location vector
```

```
[j] = size(nco,1);
for i=1:j
    x0(nco(i,:)) = coord(i,:);        % generalized coordinates numeric
    x(nco(i,:)) = coord_sym(i,:);     % generalized coordinates symbolic
end
% initial conditions generalized coordinates (without external springs)
x0_init = reshape(x0,nx,1);
% generalized coordinates (symbolic) (with external springs)
x_init = reshape(x,nx,1);

%% External spring coordinates
nex=nx+12*3;
% create node location vector
nxco = [[nco(end,1)+3:dim:nex].' [nco(end,2)+3:dim:nex].' [nco(end,3)+3:dim:nex].'];

% External spring element fixed nodes(bottom)
bxA=x0_init(1:3)-[0;0;l_ex];
bxB=x0_init(4:6)-[0;0;l_ex];
bxC=x0_init(7:9)-[0;0;l_ex];
bxD=x0_init(10:12)-[0;0;l_ex];
bxE=x0_init(13:15)-[0;0;l_ex];
bxF=x0_init(16:18)-[0;0;l_ex];
bx=[bxA,bxB,bxC,bxD,bxE,bxF];

% External spring element fixed nodes(top)
txA=x0_init(end-17:end-15)+[0;0;l_ex];
txB=x0_init(end-14:end-12)+[0;0;l_ex];
txC=x0_init(end-11:end-9)+[0;0;l_ex];
txD=x0_init(end-8:end-6)+[0;0;l_ex];
txE=x0_init(end-5:end-3)+[0;0;l_ex];
txF=x0_init(end-2:end)+[0;0;l_ex];
tx=[txA,txB,txC,txD,txE,txF];

x=[x_init;sbxA;sbyA;sbzA;sbxB;sbyB;sbzB;sbxC;sbyC;sbzC;sbxD;sbyD;sbzD;sbxE;
    sbyE;sbzE;sbxF;sbyF;sbzF;stxA;styA;stzA;stxB;styB;stzB;stxC;styC;stzC;
    stxD;styD;stzD;stxE;styE;stzE;stxF;styF;stzF];
x0=[x0_init;bxA;bxB;bxC;bxD;bxE;bxF;txA;txB;txC;txD;txE;txF];
coords=[coord;bx.';tx.'];

lda = sym('labda',[o 1]); % symbolic lambda variables
q0 = [x0;labda];% initial numeric generalized coordinates (incl lambda's)
q  = [x;lda];   % symbolic  generalized coordinates (incl lambda's)



%% Volume Constraint

for ii=1:o
T1(ii)= 1/6*det([B(ii+1,:).',A(ii,:).',  F(ii+1,:).',E(ii,:).'   ; 1, 1, 1, 1]);
T2(ii)= 1/6*det([A(ii,:).',  A(ii+1,:).',B(ii+1,:).',F(ii+1,:).' ; 1, 1, 1, 1]);
T3(ii)= 1/6*det([E(ii,:).',  B(ii+1,:).',E(ii+1,:).',F(ii+1,:).' ; 1, 1, 1, 1]);
T4(ii)= 1/6*det([A(ii,:).',  E(ii,:).',  F(ii,:).',  F(ii+1,:).' ; 1, 1, 1, 1]);
T5(ii)= 1/6*det([A(ii,:).',  B(ii,:).',  E(ii,:).',  B(ii+1,:).' ; 1, 1, 1, 1]);

T6(ii)= 1/6*det([E(ii+1,:).',D(ii,:).',  C(ii+1,:).',B(ii,:).'   ; 1, 1, 1, 1]);
T7(ii)= 1/6*det([D(ii,:).',  D(ii+1,:).',E(ii+1,:).',C(ii+1,:).' ; 1, 1, 1, 1]);
```

```
T8(ii)= 1/6*det([B(ii,:).',  E(ii+1,:).',B(ii+1,:).',C(ii+1,:).' ; 1, 1, 1, 1]);
T9(ii)= 1/6*det([D(ii,:).',  B(ii,:).',  C(ii,:).',  C(ii+1,:).' ; 1, 1, 1, 1]);
T10(ii)=1/6*det([D(ii,:).',  E(ii,:).',  B(ii,:).',  E(ii+1,:).' ; 1, 1, 1, 1]);
% Total volume vector (per segment)
V(ii)=T1(ii)+T2(ii)+T3(ii)+T4(ii)+T5(ii)+T6(ii)+T7(ii)+T8(ii)+T9(ii)+T10(ii);

V_0(ii)=double(subs(V(ii),x,x0));
end

% Constraint and Jacobian
Co_T=V.'-V_0.';                         % Set constraint
Omega_T=jacobian(Co_T,x);               % Constraint Jacobian

% Save symbolic derivation to script file.
if exist('symb_Omega_T.m', 'file')
    ! del symb_Omega_T.m
end
diary symb_Omega_T.m;
    disp('Omega_T = ['), disp(Omega_T), disp('];');
diary off

Kb_T=jacobian(Omega_T.'*lda,q);     % constraint stiffness matrix
% Save symbolic derivation to script file.
if exist('symb_Kb_T.m', 'file')
    ! del symb_Kb_T.m
end
diary symb_Kb_T.m;
    disp('Kb_T = ['), disp(Kb_T), disp('];');
diary off

% Save symbolic derivation to script file.
if exist('symb_Co_T.m', 'file')
    ! del symb_Co_T.m
end
diary symb_Co_T.m
    disp('Co_T = ['), disp(Co_T), disp('];');
diary off


%% Element connectivity (endomysium)
num=1:6:6*o;
rcon1=1:1:6;        rcon2=[(8:1:12),7];
lcon1=[(2:1:6),1];  lcon2=7:1:12;
for ii=2:o
rcon1=[rcon1,(num(ii):1:num(ii)+5)];
rcon2=[rcon2,(num(ii)+7:1:num(ii)+11),(num(ii)+6)];
lcon1=[lcon1,(num(ii)+1:1:num(ii)+5),(num(ii))];
lcon2=[lcon2,(num(ii)+6:1:num(ii)+11)];
end
con=[rcon1.',rcon2.';lcon1.',lcon2.'];% endomysium node connection vector

% Force connectivity
num2=1:6:6*n;
fcon1=num2(1):1:(num2(end-1)+5);
fcon2=num2(2):1:(num2(end)+5);
fcon=[fcon1.',fcon2.'];                 % sarcomere force connection vector
```

```
%External spring connectivity
conbx=[1 numnod+1;2 numnod+2;3 numnod+3;4 numnod+4;5 numnod+5;6 numnod+6];
contx=[numnod-5 numnod+7;numnod-4 numnod+8;numnod-3 numnod+9;
       numnod-2 numnod+10;numnod-1 numnod+11;numnod numnod+12];

%% Element location vector (endo)
ncox=[nco;nxco];
[j,k] = size(con);
% Create element endomysium locationvector
for i=1:j
    xloc(i,:) = [ncox(con(i,1),:) ncox(con(i,2),:)];
end
% Create element sarcomere locationvector
[j,k] = size(fcon);
for i=1:j
    fxloc(i,:) = [ncox(fcon(i,1),:) ncox(fcon(i,2),:)];
end

% External spring elements
% Create element bottom spring locationvector
[j,k] = size(conbx);
for i=1:j
    bxloc(i,:) = [ncox(conbx(i,1),:) ncox(conbx(i,2),:)];
end
% Create element top sprig locationvector
[j,k] = size(contx);
for i=1:j
    txloc(i,:) = [ncox(contx(i,1),:) ncox(contx(i,2),:)];
end

%% Calculate initial spring element lengths (endomysium)
[j,k] = size(con);
for i=1:j
    xi =x0(xloc(i,:));
    d(:,i) = xi(4:6)-xi(1:3);                   % Element vector
    l0(i) = norm(d(:,i));                       % Unstretched length array
    lcon(i)=l0(i);
    S(i) = EA/l0(i);                            % Element stiffness array
end
[j,k] = size(fcon);
for i=1:j
    xi =x0(fxloc(i,:));
    dfc(:,i) = xi(4:6)-xi(1:3);                 % Element vector center
    l0_ref(i) = norm(dfc(:,i));                 % reference length
    Sf(i) = EAf/(l0_ref(i)/2);                  % Element stiffness array
    lf(i)=l0_ref(i);
    strain(i)= 0;
    l_sarc=sarcrest*(1+strain);
    [l0f(i),fact(i)]=Gaussian_scaled(l_sarc(i),sigmamax,A_sarc,lf(i),Sf(i),act);
end

[j,k] = size(conbx);
for i=1:j
    xi =x0(bxloc(i,:));
    dbx = xi(4:6)-xi(1:3);                       % Element vector center
```

```
    l0bx(i) = norm(dbx);                          % Unstretched length array
    l0bx(i) = (l0bx(i)/(100+pretbex))*100;        % add pretension
    Sbx(i) = EAx/l0bx(i);                         % Element stiffness array
end
[j,k] = size(contx);
for i=1:j
    xi =x0(txloc(i,:));
    dtx = xi(4:6)-xi(1:3);                        % Element vector center
    l0tx(i) = norm(dtx);                          % Unstretched length array
    l0tx(i) = (l0tx(i)/(100+prettex))*100;        % add pretension
    Stx(i) = EAx/l0tx(i);                         % Element stiffness array
end

    S=[S,Sf,Sbx,Stx];
    l0=[l0,l0f,l0bx,l0tx];
    con=[con;fcon;conbx;contx];
    xloc=[xloc;fxloc;bxloc;txloc];

%% Calculate angle
for ii=1:length(dfc)
    dxl=dfc(:,ii);
    dyl=d(:,ii+length(dfc));
    thetal(ii)=acosd(dot(dxl,dyl)/(norm(dxl)*norm(dyl)));
end

for ii=2:length(dfc)
    dxr=dfc(:,ii);
    dyr=d(:,ii-1);
    thetar(ii)=acosd(dot(dxr,dyr)/(norm(dxr)*norm(dyr)));
end
dx=dfc(:,1);
dy=d(:,length(dfc));
thetar(1)=acosd(dot(dx,dy)/(norm(dx)*norm(dy)));

thetas=[thetal,thetar];

%% Plot all present elements in initial condition
X=[];
Y=[coords.'];
co=[con].';
s=co(1,:);
t=co(2,:);
for i=1:3
    M=[Y(i,s);Y(i,t); repmat(NaN,size(s))];
    X(:,i)=M(:);
end
endo=X(1:36*o,:);
sarc=X(size(endo,1)+1:end-36,:);
bext=X(end-36+1:end-18,:);
text=X(end-18+1:end,:);

figure(101)
plot3(endo(:,1),endo(:,2),endo(:,3),'r','LineWidth',1.0)
hold on
plot3(sarc(:,1),sarc(:,2),sarc(:,3),'k:','LineWidth',1.5)
```

```
if bottomfix == 0
    plot3(bext(:,1),bext(:,2),bext(:,3),'c--','LineWidth',1.0)
end
legend('Endomysium','Sarcomeres')
axis('equal');
grid on

%% Fixed nodes
if bottomfix > 0 && topfix == 0
    fixed = [A(1,:),B(1,:),C(1,:),D(1,:),E(1,:),F(1,:)];
elseif bottomfix > 0 && topfix > 0
    fixed = [A(1,:),B(1,:),C(1,:),D(1,:),E(1,:),F(1,:),A(end,:),B(end,:),...
            C(end,:),D(end,:),E(end,:),F(end,:)];
elseif topfix > 0 && bottomfix == 0
    fixed = [A(end,:),B(end,:),C(end,:),D(end,:),E(end,:),F(end,:)];
        else fixed =[];
end
x0loc=[];
for ii=1:length(fixed)
    [row(ii),col(ii)] = find(coord_sym==fixed(ii));
    x0loc(ii)=nco(row(ii),col(ii));          % Fixed coordinate numbers
end
x0loc=[x0loc,(nx+1:1:nx+12*3)];
% Free nodes
xfloc = reshape(ncox',1,numel(ncox));        % Shape matrix into vector
xfloc(x0loc)=[];                             % Remove fixed coordinates

%% Applied forces
fa = zeros(nex,1);



%% Initial Stiffness Matrix
f = zeros(nex,1);
K = zeros(nex,nex);

[j,k] = size(con);
for i=1:j
    loc = xloc(i,:);
    xi = x0(loc);
p1 = xi(1:3);
p2 = xi(4:6);
d = reshape(p2-p1,3,1);
l = norm(d);                 % actual length
r = d./l;                    % unit length vector
e = l-l0(i);                 % elongation
N = S(i)*e;                  % normal force
D = [-r.' r.'];              % jacobian de/dx
fi = D.'*N;                  % nodal forces

% stiffness matrices
A = r*r.';
Ks = S(i).*[ A -A; -A A];    % material stiffness matrix
B = (eye(3)-A)./l;
Kg = N.*[ B -B; -B B];       % geometrical stiffness matrix
Kij = Ks+Kg;
```

```
f(loc) = f(loc)+fi;
K(loc,loc) = K(loc,loc)+Kij;
end

X = q;
values = q0;
for k = 1:numel(X)
    eval(sprintf('%s=values(%d)',char(X(k)),k));
end

symb_Omega_T;
exist('symb_Kb_T.m', 'file');
symb_Kb_T;
symb_Co_T;

K=[K,zeros(length(x),o)];      % expand K
K=K+Kb_T;                      % symbolic stiffness matrix

tic
%%  Iterate
maxiterat = 250;               % set maximum number of iterations
freltol = 1e-6;                % set relative force error
vreltol = 1e-6;

ferr=[];
verr=[];
lerr=[];

qx=q0;
dq=zeros(size(qx));
dV=0;

for iterat = 1:maxiterat
    fb(:,iterat)= Omega_T.'*labda;  % constraint reaction forces (per iteration)
    fiv(:,iterat)= f;               % stiffness matrix forces (per iteration)
    labdav(:,iterat)= labda;        % labda's (per iteration)
    f = fiv(:,iterat) +fb(:,iterat);% total internal forces (for this iteration)
    fav(:,iterat)=fa;               % external forces (per iteration)
    fv(:,iterat)= f;                % total internal force (per iteration)
    df(:,iterat) = fa-f;            % determine df (per iteration)
    qv(:,iterat)= qx;               % generalized coordinate vector (per iteration)
    dlabda = dq(end-(o-1):end);     % determine dlabda
    dlabdav(:,iterat) = dlabda;     % dlabda vector
    l0v(:,iterat)= l0;              % l0 (per iteration)
    factv(:,iterat)=fact;
    l_sarcv(:,iterat)=l_sarc;
    dV = Co_T;                      % volume difference (for this iteration)

    ferr(iterat) = max(abs(df(xfloc,iterat)));
    verr(iterat)= max(abs(dV));
    lerr(iterat) = max(abs(dlabda));

    % check convergence and when ok then exit the loop
    if ferr(iterat)<freltol && verr(iterat)<vreltol && lerr(iterat)<freltol;
       break
    end
```

```
% EOM
M1=[K(xfloc,xfloc) Omega_T(:,xfloc).';
    Omega_T(:,xfloc) zeros(size(Omega_T(:,xfloc),1),size(Omega_T(:,xfloc),1))];
M2=[df(xfloc,iterat); -Co_T];
sol=M1\M2;
dq(xfloc)=sol(1:end-o);
dq(end-(o-1):end)=sol(end-(o-1):end);

% update the nodal coordinates
    qx=qx+dq;                                % update generalized coordinates
    labda= labda + dq(end-(o-1):end);        % update lambda
    x=qx(1:nex);                             % isolate position coordinates
    f = zeros(nex,1);                        % reset force vector
    K = zeros(size(K));                      % reset stiffness matrix

% Calculate the nodal forces and stiffnes matrix for the next iteration
[j,k] = size(con);
for i=1:j
    loc = xloc(i,:);
    xi = x(loc);
p1 = xi(1:3);
p2 = xi(4:6);
d = reshape(p2-p1,3,1);
l = norm(d);                 % actual length
r = d./l;                    % unit length vector
if i < o*12+1
    strainc=(l-lcon(i))/lcon(i);
if strainc < 0
    l0(i)=l;
else l0(i)=lcon(i);
end
end
if i > (o*12) & i < (o*12+o*6+1)
     strain=(l-l0_ref(i-(o*12)))/l0_ref(i-(o*12));
     l_sarc(i-(o*12))=sarcrest*(1+strain);
[l0(i),fact(i-(o*12))]=Gaussian_scaled(l_sarc(i-(o*12)),...
                                          sigmamax,A_sarc,l,S(i),act);
end

e = l-l0(i);                 % elongation
N = S(i)*e;                  % normal force
D = [-r.' r.'];              % jacobian de/dx
fi = D.'*N;                  % nodal forces
strain(i)=l/l0(i)-1;

% stiffness matrices
A = r*r.';
Ks = S(i).*[ A -A; -A A];    % material stiffness matrix
B = (eye(3)-A)./l;
Kg = N.*[ B -B; -B B];       % geometrical stiffness matrix
Kij = Ks+Kg;
f(loc) = f(loc)+fi;
K(loc,loc) = K(loc,loc)+Kij;
end
```

```
X = q;
values = qx;
for k = 1:numel(X)
    eval(sprintf('%s=values(%d)',char(X(k)),k));
end

symb_Omega_T;
symb_Kb_T;
symb_Co_T;

K=K+Kb_T;                       % symbolic stiffness matrix
end

%% plot
numit=length(ferr)
Vend=double(subs(V,q,qx));  % test volume
dV=double(Vend-V_0);        % test volume

x=qx((1:end-o));
enit=zeros(3, length(x)/3);
id=1:3:length(x);
for i=1:length(x)/3
    enit(:,i)=x(id(i):id(i)+2);
end

X=[];
Cor=[coords.';enit];
s=co(1,:);
t=co(2,:);
for i=1:6
    M=[Cor(i,s);Cor(i,t); repmat(NaN,size(s))];
    X(:,i)=M(:);
end
if bottomfix == 1
    X(end-36+1:end-18,:)=[];
end
figure(1)
plot3(X(:,1),X(:,2),X(:,3),'k',X(:,4),X(:,5),X(:,6),'m');
axis('equal');

%% plot
X=[];
numit=length(ferr);
Vend=double(subs(V,q,qx));
dV=double(Vend-V_0);

x=qx((1:end-o),:);
enit=zeros(3, length(x)/3);
id=1:3:length(x);
for i=1:length(x)/3
    enit(:,i)=x(id(i):id(i)+2);
end

Cor=[coords.';enit];
s=co(1,:);
t=co(2,:);
```

```
for i=1:6
    M=[Cor(i,s);Cor(i,t); repmat(NaN,size(s))];
    X(:,i,:)=M(:);
end

X=X(1:end-36,:,:);

nA=1:18:length(x);nB=4:18:length(x);nC=7:18:length(x);nD=10:18:length(x);
nE=13:18:length(x);nF=16:18:length(x);
for ii=1:n
    As(:,ii)=x(nA(ii):nA(ii)+2);    As0(:,ii)=x0(nA(ii):nA(ii)+2);
    Bs(:,ii)=x(nB(ii):nB(ii)+2);    Bs0(:,ii)=x0(nB(ii):nB(ii)+2);
    Cs(:,ii)=x(nC(ii):nC(ii)+2);    Cs0(:,ii)=x0(nC(ii):nC(ii)+2);
    Ds(:,ii)=x(nD(ii):nD(ii)+2);    Ds0(:,ii)=x0(nD(ii):nD(ii)+2);
    Es(:,ii)=x(nE(ii):nE(ii)+2);    Es0(:,ii)=x0(nE(ii):nE(ii)+2);
    Fs(:,ii)=x(nF(ii):nF(ii)+2);    Fs0(:,ii)=x0(nF(ii):nF(ii)+2);
end

CM = hsv(n);
figure(5)
plot3(X(:,1),X(:,2),X(:,3),'k')
hold on
plot3(X(:,4),X(:,5),X(:,6),'m','LineWidth',1.0)
axis equal

%% Andere Plots
%errors
iter=1:1:iterat;
nul=zeros(length(iterat));
figure(4)
loglog(iter,ferr,'r',iter,lerr,'g',iter,verr,'b',iter,nul,'k')
legend('Force Error','Pressure Error','Volume Error')

%% Calculate work
for ii=1:o*12
    loc = xloc(ii,:);
    xi = qx(loc);
p1 = xi(1:3);
p2 = xi(4:6);
d = reshape(p2-p1,3,1);
l = norm(d);                % actual length
e = l-l0(ii);               % elongation
Work(ii)=1/2*S(ii)*e^2;     % normal force
end
WU=sum(Work);

% Calculate work for external springs
for ii=1:size(contx,1)
    loc = txloc(ii,:);
    xi = qx(loc);
p1 = xi(1:3);
p2 = xi(4:6);
d = reshape(p2-p1,3,1);
l = norm(d);                        % actual length
e = l-l0tx(ii);                     % elongation
Workex(ii)=1/2*EAx*e^2;             % potential energy
```

```
end
WUex=sum(Workex);                    % Total work done by external springs
Wtot=WU+WUex;

%%
% Length change
range=length(x_init):-3:length(x_init)-6*3+1;
faslength=mean(qx(range));
faslength0=sepz*o;                           % initial fascicle length
perc=100-(faslength/(faslength0/100));       % total strain
sarcomerelength=mean(l_sarc);

% Force
force=[];
for ii=length(con)-5:length(con)
    loc = xloc(ii,:);
    xi = qx(loc);
p1 = xi(1:3);
p2 = xi(4:6);
d = reshape(p2-p1,3,1);
l = norm(d);                         % actual length
e = l-l0(ii);                        % elongation
cstrain(ii)=e/l0(ii);
force(ii-(length(con)-5)+1)=(EAx/l0tx((ii-(length(con)-5)+1)))*e;
end
force=sum(force);

%%

% Mean area
vec1=1:1:nx;                         % extract vector
vec2=3:3:nx;
vec1(vec2)=[];
nums=1:12:length(vec1);
for ii=1:n
sum1=sum([qx(vec1(nums(ii)))*qx(vec1(nums(ii)+3));
          qx(vec1(nums(ii)+2))*qx(vec1(nums(ii)+5));
          qx(vec1(nums(ii)+4))*qx(vec1(nums(ii)+7));
          qx(vec1(nums(ii)+6))*qx(vec1(nums(ii)+9));
          qx(vec1(nums(ii)+8))*qx(vec1(nums(ii)+11));
          qx(vec1(nums(ii)+10))*qx(vec1(nums(ii)+1))]);
sum2=sum([qx(vec1(nums(ii)+1))*qx(vec1(nums(ii)+2));
          qx(vec1(nums(ii)+3))*qx(vec1(nums(ii)+4));
          qx(vec1(nums(ii)+5))*qx(vec1(nums(ii)+6));
          qx(vec1(nums(ii)+7))*qx(vec1(nums(ii)+8));
          qx(vec1(nums(ii)+9))*qx(vec1(nums(ii)+10));
          qx(vec1(nums(ii)+11))*qx(vec1(nums(ii)))]);
Area(ii)=abs(sum1-sum2)/2;
end
meanA=mean(Area(3:end-1));

% Mean angle
[j,k] = size(con);
for i=1:j
    xi =qx(xloc(i,:));
    d(:,i) = xi(4:6)-xi(1:3);                        % Element vector
```

```
end
[j,k] = size(fcon);
for i=1:j
    xi =qx(fxloc(i,:));
    dfc(:,i) = xi(4:6)-xi(1:3);                    % Element vector
end

for ii=1:length(dfc)
    dxl=dfc(:,ii);
    dyl=d(:,ii+length(dfc));
    thetal(ii)=acosd(dot(dxl,dyl)/(norm(dxl)*norm(dyl)));
end

for ii=2:length(dfc)
    dxr=dfc(:,ii);
    dyr=d(:,ii-1);
    thetar(ii)=acosd(dot(dxr,dyr)/(norm(dxr)*norm(dyr)));
end
dx=dfc(:,1);
dy=d(:,length(dfc));
thetar(1)=acosd(dot(dx,dy)/(norm(dx)*norm(dy)));

thetas=[thetal,thetar];
mean(thetas)

toc
```

B.2. Gaussian Force-Length Relationship

```
function [l0,f] = Gaussian_scaled(l_sarc,sigmamax,A_sarc,lf,Sf,act)
fm=sigmamax*A_sarc;
l=l_sarc;

la = 1.27;      % minimum length
lb = 4.24-la;   % maximum length
lm = 2.64;      % optimum length
r = 1.088*10;   % slope at la

syms c0
eqn=((4*c0*(la+lb-lm))/(lb*(lm-la))*log((fm+c0)/c0))== r;
solx = solve(eqn,c0);
c0=double(real(solx));

c1=fm+c0;
a=sqrt(log(c1/c0));

c2=lm;
c4=(2*la+lb-2*lm)/(a*lb);
c3=lb*(lm-la)/(a*lb)-la*c4;

f=-c0+c1*exp(-(((l-c2)/(c3+c4*l)))^2);
f=f*act;
l0=lf-(f/Sf);
end
```

C

Excel Data

The raw data form the simulations was stored into an excel sheet to get a good overview of the results. The following parameters can be found in the excel sheets, in sequence of display:

Input
act = activation
alpha_in = initial braiding angle in ˚
E_col = collagen modulus in MPa
colrad = collagen radius in m
k_ex = external spring stiffness in Nm
col_proportion = collagen volume proportion in %

Output
alpha_end = average final braiding angle in ˚
std_alpha = standard deviation of final braiding angle in ˚
delta alpha = difference in angle orientation in ˚
L_end = final fibre length in m
Delta L = absolute length difference in m
delta L = relative length difference in %
l_sarc = average final sarcomere length in m
std_l_sarc = standard deviation sarcomere length in m
labda = average compartmental pressure in Pa
std_labda = standard deviation compartmental pressure in Pa
e_col = average collagen strain
std_ecol = standard deviation collagen strain
W_col = work inside collagen in J
W_ex = work inside external springs in J
W_tot = total internal work in J
A_end = average final area in m^2
f_end = endpoint force in N
sigma = endpoint tension in Pa

Convergence
numit = number of iterations needed
ferr = force error in N
verr = volume error in m^3

Fascicle
act = activation of fiber 1 to 7 respectively labda_cent = average compartmental pressure in central fibre within fascicle in Pa
labda_out = average compartmental pressure in outer fibres within fascicle in Pa

Stiffness
L_end = Fiber length when starting stiffness simulation in m
Fex_tot = Total external force divided over the different top noded in N
dlength = difference in length before and after stiffness simulation in m
lstiff = longitudinal model stiffness in N/m
Estiff = longitudinal stiffness modulus in N/m^2
perc = percentage of length change during stiffness simulation
sarclength = resulting mean sarcomere length after stiffness simulation
sarclength = standard deviation mean sarcomere length after stiffness simulation

act	alpha	E_col	colrad	k_ex	col_pr	alpha_	std_a	delta	L_end	Delta L	delta L	l_sarc	std_l_sar	labda	std_la	e_col	std_ecol	W_col	W_ex	W_tot	A_end	f_end	sigma	num	ferr	verr
Inp	Model Parameters					Output Parameters																		Convergence		
Collagen stiffness																										
1	70.33	2.00E+08	3.04E-07	1.00E-05	1.27%	78.535	17.71	8.205	3.46E-04	1.90E-04	35.41%	1.70E-06	1.28E-09	-8.52E+04	0.90	5.53E-02	4.44E-02	2.78E-09	1.01E-09	3.79E-09	6.17E-10	1.06E-05	1.72E+04	76	2.73E-11	5.18E-29
1	70.33	2.50E+08	3.04E-07	1.00E-05	1.27%	78.196	17.23	7.866	3.54E-04	1.82E-04	34.00%	1.74E-06	9.94E-10	-1.01E+05	0.34	5.24E-02	4.24E-02	3.14E-09	9.31E-10	4.07E-09	6.14E-10	1.02E-05	1.66E+04	75	2.23E-11	4.64E-29
1	70.33	4.00E+08	3.04E-07	1.00E-05	1.27%	77.385	16.10	7.055	3.72E-04	1.64E-04	30.66%	1.83E-06	5.19E-10	-1.41E+05	0.82	4.58E-02	3.76E-02	3.88E-09	7.58E-10	4.64E-09	6.08E-10	9.21E-06	1.52E+04	77	2.32E-11	3.87E-29
1	70.33	5.70E+08	3.04E-07	1.00E-05	1.27%	76.695	15.15	6.365	3.87E-04	1.49E-04	27.86%	1.91E-06	3.1E-10	-1.77E+05	0.78	4.04E-02	3.36E-02	4.36E-09	6.26E-10	4.99E-09	6.02E-10	8.37E-06	1.39E+04	84	2.44E-11	9.69E-29
1	70.33	8.60E+08	3.04E-07	1.00E-05	1.27%	75.826	13.95	5.496	4.06E-04	1.31E-04	24.36%	2.00E-06	2.94E-10	-2.24E+05	0.33	3.40E-02	2.86E-02	4.71E-09	4.79E-10	5.19E-09	5.95E-10	7.32E-06	1.23E+04	103	2.63E-11	2.42E-28
1	70.33	2.00E+08	4.00E-07	1.00E-05	3.07%	77.651	16.47	7.321	3.66E-04	1.70E-04	31.75%	1.80E-06	1.57E-10	-1.27E+05	0.69	4.79E-02	3.92E-02	3.66E-09	8.12E-10	4.47E-09	6.10E-10	9.53E-06	1.56E+04	75	2.67E-11	4.77E-29
1	70.33	2.50E+08	4.00E-07	1.00E-05	3.07%	77.241	15.90	6.911	3.75E-04	1.61E-04	30.07%	1.85E-06	1.85E-10	-1.48E+05	0.85	4.46E-02	3.68E-02	4.00E-09	7.29E-10	4.72E-09	6.06E-10	9.03E-06	1.49E+04	78	2.39E-11	6.82E-29
1	70.33	4.00E+08	4.00E-07	1.00E-05	3.07%	76.296	14.59	5.966	3.95E-04	1.41E-04	26.24%	1.95E-06	2.43E-10	-1.98E+05	0.59	3.74E-02	3.13E-02	4.56E-09	5.56E-10	5.11E-09	5.99E-10	7.89E-06	1.32E+04	92	2.72E-11	2.20E-28
1	70.33	5.70E+08	4.00E-07	1.00E-05	3.07%	75.528	13.54	5.198	4.12E-04	1.24E-04	23.17%	2.04E-06	2.77E-10	-2.40E+05	0.21	3.19E-02	2.69E-02	4.76E-09	4.34E-10	5.19E-09	5.93E-10	6.97E-06	1.17E+04	111	2.58E-11	4.17E-28
1	70.33	8.60E+08	4.00E-07	1.00E-05	3.07%	74.612	12.29	4.282	4.32E-04	1.05E-04	19.52%	2.13E-06	3E-10	-2.89E+05	0.26	2.56E-02	2.18E-02	4.66E-09	3.09E-10	4.97E-09	5.86E-10	5.88E-06	1.00E+04	218	2.62E-11	4.77E-29
1	70.33	2.00E+08	1.90E-07	1.00E-05	0.50%	79.638	19.30	9.308	3.21E-04	2.15E-04	40.08%	1.58E-06	2.86E-09	-3.94E+04	6.14	6.54E-02	5.10E-02	1.49E-09	1.29E-09	2.78E-09	6.26E-10	1.20E-05	1.92E+04	112	2.72E-11	4.46E-29
1	70.33	2.50E+08	1.90E-07	1.00E-05	0.50%	79.422	18.99	9.092	3.26E-04	2.10E-04	39.16%	1.60E-06	2.4E-09	-4.77E+04	4.55	6.33E-02	4.97E-02	1.75E-09	1.23E-09	2.99E-09	6.24E-10	1.17E-05	1.88E+04	98	2.45E-11	3.00E-29
1	70.33	4.00E+08	1.90E-07	1.00E-05	0.50%	78.875	18.20	8.545	3.39E-04	1.98E-04	36.84%	1.66E-06	1.63E-09	-7.02E+04	1.93	5.83E-02	4.64E-02	2.40E-09	1.09E-09	3.49E-09	6.19E-10	1.11E-05	1.78E+04	82	2.31E-11	3.50E-29
1	70.33	5.70E+08	1.90E-07	1.00E-05	0.50%	78.375	17.49	8.045	3.50E-04	1.86E-04	34.74%	1.72E-06	1.14E-09	-9.25E+04	0.56	5.39E-02	4.34E-02	2.95E-09	9.72E-10	3.92E-09	6.15E-10	1.04E-05	1.69E+04	75	2.61E-11	4.59E-29
1	70.33	8.60E+08	1.90E-07	1.00E-05	0.50%	77.701	16.54	7.371	3.65E-04	1.71E-04	31.95%	1.80E-06	6.75E-10	-1.25E+05	0.66	4.83E-02	3.94E-02	3.61E-09	8.23E-10	4.44E-09	6.10E-10	9.59E-06	1.57E+04	75	2.56E-11	5.91E-29
1	70.33	2.00E+08	2.50E-07	1.00E-05	1.20%	79.059	18.46	8.729	3.34E-04	2.02E-04	37.62%	1.64E-06	1.07E-10	-6.24E+04	2.66	5.99E-02	4.75E-02	2.19E-09	1.14E-09	3.32E-09	6.21E-10	1.13E-05	1.82E+04	86	2.49E-11	3.14E-29
1	70.33	2.50E+08	2.50E-07	1.00E-05	1.20%	78.773	18.05	8.443	3.41E-04	1.95E-04	36.41%	1.68E-06	9.44E-11	-7.46E+04	1.58	5.74E-02	4.58E-02	2.52E-09	1.07E-09	3.58E-09	6.19E-10	1.09E-05	1.77E+04	80	2.34E-11	5.28E-29
1	70.33	4.00E+08	2.50E-07	1.00E-05	1.20%	78.072	17.06	7.742	3.57E-04	1.80E-04	33.48%	1.75E-06	1.28E-10	-1.07E+05	0.35	5.13E-02	4.16E-02	3.26E-09	9.03E-10	4.17E-09	6.13E-10	1.01E-05	1.64E+04	74	2.66E-11	4.09E-29
1	70.33	5.70E+08	2.50E-07	1.00E-05	1.20%	77.457	16.20	7.127	3.70E-04	1.66E-04	30.95%	1.82E-06	1.70E-10	-1.37E+05	0.80	4.63E-02	3.80E-02	3.82E-09	7.72E-10	4.60E-09	6.08E-10	9.30E-06	1.53E+04	76	2.64E-11	6.28E-29
1	70.33	8.60E+08	2.50E-07	1.00E-05	1.20%	76.658	15.09	6.328	3.88E-04	1.49E-04	27.71%	1.91E-06	2.22E-10	-1.79E+05	0.76	4.01E-02	3.34E-02	4.38E-09	6.19E-10	5.00E-09	6.02E-10	8.32E-06	1.38E+04	85	2.32E-11	1.06E-28
External spring stiffness																										
1	70.33	5.70E+08	3.04E-07	1.00E-07	1.27%	76.939	15.57	6.609	3.81E-04	1.55E-04	28.86%	1.88E-06	2.26E-10	-1.85E+05	0.74	4.24E-02	3.48E-02	4.74E-09	6.72E-12	4.75E-09	6.04E-10	8.67E-08	1.44E+02	82	2.37E-11	1.51E-28
1	70.33	5.70E+08	3.04E-07	1.00E-06	1.27%	76.916	15.53	6.586	3.82E-04	1.54E-04	28.76%	1.88E-06	2.3E-10	-1.84E+05	0.75	4.22E-02	3.47E-02	4.71E-09	6.68E-11	4.77E-09	6.03E-10	8.64E-07	1.43E+03	82	2.43E-11	1.61E-28
1	70.33	5.70E+08	3.04E-07	1.00E-05	1.27%	76.695	15.15	6.365	3.87E-04	1.49E-04	27.86%	1.91E-06	3.1E-10	-1.77E+05	0.78	4.04E-02	3.36E-02	4.36E-09	6.26E-10	4.99E-09	6.02E-10	8.37E-06	1.39E+04	84	2.44E-11	9.69E-29
1	70.33	5.70E+08	3.04E-07	2.00E-05	1.27%	76.463	14.74	6.133	3.92E-04	1.44E-04	26.91%	1.93E-06	2.14E-10	-1.69E+05	0.80	3.86E-02	3.25E-02	4.01E-09	1.17E-09	5.18E-09	6.01E-10	1.62E-05	2.69E+04	86	2.72E-11	1.10E-28
1	70.33	5.70E+08	3.04E-07	3.00E-05	1.27%	76.244	14.34	5.914	3.97E-04	1.39E-04	26.01%	1.96E-06	2.07E-10	-1.61E+05	0.81	3.69E-02	3.14E-02	3.70E-09	1.64E-09	5.34E-09	6.00E-10	2.34E-05	3.91E+04	89	2.62E-11	7.73E-29
1	70.33	5.70E+08	3.04E-07	4.00E-05	1.27%	76.041	13.97	5.711	4.01E-04	1.35E-04	25.16%	1.98E-06	2.00E-10	-1.54E+05	0.81	3.53E-02	3.04E-02	3.42E-09	2.04E-09	5.47E-09	5.99E-10	3.02E-05	5.05E+04	100	2.40E-11	4.41E-29
1	70.33	5.70E+08	3.04E-07	5.00E-05	1.27%	75.849	13.62	5.519	4.06E-04	1.31E-04	24.36%	2.00E-06	1.92E-10	-1.48E+05	0.81	3.38E-02	2.94E-02	3.17E-09	2.40E-09	5.56E-09	5.98E-10	3.66E-05	6.13E+04	108	2.65E-11	7.69E-29
1	70.33	5.70E+08	3.04E-07	6.00E-05	1.27%	75.667	13.27	5.337	4.10E-04	1.27E-04	23.60%	2.02E-06	1.85E-10	-1.42E+05	0.82	3.24E-02	2.85E-02	2.94E-09	2.70E-09	5.64E-09	5.97E-10	4.26E-05	7.13E+04	100	2.52E-11	1.06E-28
1	70.33	5.70E+08	3.04E-07	7.00E-05	1.27%	75.493	12.94	5.163	4.13E-04	1.23E-04	22.89%	2.04E-06	1.77E-10	-1.36E+05	0.82	3.11E-02	2.76E-02	2.73E-09	2.96E-09	5.69E-09	5.96E-10	4.81E-05	8.08E+04	100	2.64E-11	7.14E-29
1	70.33	5.70E+08	3.04E-07	8.00E-05	1.27%	75.328	12.63	4.998	4.17E-04	1.19E-04	22.20%	2.06E-06	1.70E-10	-1.31E+05	0.82	2.99E-02	2.68E-02	2.55E-09	3.18E-09	5.73E-09	5.95E-10	5.34E-05	8.97E+04	103	2.36E-11	8.73E-29
1	70.33	5.70E+08	3.04E-07	9.00E-05	1.27%	75.170	12.32	4.840	4.21E-04	1.16E-04	21.56%	2.07E-06	1.62E-10	-1.26E+05	0.82	2.88E-02	2.61E-02	2.38E-09	3.38E-09	5.75E-09	5.94E-10	5.83E-05	9.81E+04	105	2.41E-11	8.41E-29
1	70.33	5.70E+08	3.04E-07	1.00E-04	1.27%	75.020	12.02	4.690	4.24E-04	1.12E-04	20.94%	2.09E-06	1.55E-10	-1.21E+05	0.81	2.77E-02	2.53E-02	2.22E-09	3.54E-09	5.76E-09	5.94E-10	6.29E-05	1.06E+05	108	2.53E-11	4.96E-29
1	70.33	5.70E+08	3.04E-07	2.50E-04	1.27%	73.394	8.75	3.064	4.59E-04	7.67E-05	14.30%	2.26E-06	2.1E-10	-7.53E+04	13.13	1.73E-02	1.72E-02	9.39E-10	4.13E-09	5.07E-09	5.86E-10	1.07E-04	1.83E+05	171	2.65E-11	8.23E-29
1	70.33	5.70E+08	3.04E-07	5.00E-04	1.27%	72.088	6.56	1.758	4.88E-04	4.84E-05	9.02%	2.40E-06	3E-10	-4.50E+04	19.02	1.04E-02	1.03E-02	3.37E-10	3.28E-09	3.62E-09	5.74E-10	1.35E-04	2.36E+05	250	5.15E-11	1.02E-28
1	70.33	5.70E+08	3.04E-07	1.00E-03	1.27%	71.121	4.98	0.791	5.09E-04	2.71E-05	5.05%	2.51E-06	3.7E-10	-2.24E+04	18.90	5.19E-03	5.20E-03	8.51E-11	2.06E-09	2.14E-09	5.65E-10	1.52E-04	2.68E+05	250	2.57E-09	1.12E-25
1	70.33	2.50E+08	1.90E-07	1.00E-07	0.50%	80.064	20.06	9.734	3.11E-04	2.25E-04	41.98%	1.53E-06	1.67E-10	-5.26E+04	4.34	6.98E-02	5.29E-02	2.07E-09	1.42E-11	2.09E-09	6.28E-10	1.26E-07	2.01E+02	95	2.49E-11	3.46E-29
1	70.33	2.50E+08	1.90E-07	1.00E-06	0.50%	80.000	19.95	9.670	3.13E-04	2.24E-04	41.70%	1.53E-06	1.68E-10	-5.21E+04	4.37	6.91E-02	5.26E-02	2.04E-09	1.40E-10	2.18E-09	6.28E-10	1.25E-06	1.99E+03	95	2.58E-11	3.68E-29
1	70.33	2.50E+08	1.90E-07	1.00E-05	0.50%	79.422	18.99	9.092	3.26E-04	2.10E-04	39.16%	1.60E-06	2.4E-09	-4.77E+04	4.55	6.33E-02	4.97E-02	1.75E-09	1.23E-09	2.99E-09	6.24E-10	1.17E-05	1.88E+04	98	2.45E-11	3.00E-29
1	70.33	2.50E+08	1.90E-07	2.00E-05	0.50%	78.881	18.05	8.551	3.39E-04	1.97E-04	36.82%	1.66E-06	1.91E-10	-4.37E+04	4.73	5.82E-02	4.70E-02	1.51E-09	2.18E-09	3.69E-09	6.21E-10	2.21E-05	3.56E+04	102	2.46E-11	2.68E-29
1	70.33	2.50E+08	1.90E-07	3.00E-05	0.50%	78.415	17.22	8.085	3.49E-04	1.87E-04	34.84%	1.71E-06	2.07E-10	-4.04E+04	5.06	5.39E-02	4.48E-02	1.33E-09	2.93E-09	4.26E-09	6.18E-10	3.14E-05	5.07E+04	107	2.70E-11	4.96E-29
1	70.33	2.50E+08	1.90E-07	4.00E-05	0.50%	78.002	16.47	7.672	3.59E-04	1.78E-04	33.11%	1.76E-06	2.23E-10	-3.76E+04	5.54	5.02E-02	4.29E-02	1.18E-09	3.53E-09	4.70E-09	6.16E-10	3.97E-05	6.45E+04	111	2.72E-11	4.37E-29
1	70.33	2.50E+08	1.90E-07	5.00E-05	0.50%	77.632	15.78	7.302	3.67E-04	1.69E-04	31.57%	1.80E-06	2.40E-10	-3.52E+04	6.17	4.71E-02	4.12E-02	1.05E-09	4.01E-09	5.06E-09	6.14E-10	4.74E-05	7.71E+04	115	2.71E-11	4.68E-29
1	70.33	2.50E+08	1.90E-07	6.00E-05	0.50%	77.297	15.14	6.967	3.74E-04	1.62E-04	30.19%	1.84E-06	2.54E-10	-3.31E+04	6.89	4.43E-02	3.96E-02	9.50E-10	4.40E-09	5.35E-09	6.13E-10	5.44E-05	8.87E+04	120	2.46E-11	5.68E-29
1	70.33	2.50E+08	1.90E-07	7.00E-05	0.50%	76.991	14.55	6.661	3.81E-04	1.55E-04	28.94%	1.87E-06	2.66E-10	-3.12E+04	7.65	4.18E-02	3.82E-02	8.62E-10	4.72E-09	5.58E-09	6.11E-10	6.08E-05	9.94E+04	124	2.53E-11	3.14E-29
1	70.33	2.50E+08	1.90E-07	8.00E-05	0.50%	76.710	14.00	6.380	3.87E-04	1.49E-04	27.79%	1.90E-06	2.76E-10	-2.95E+04	8.43	3.95E-02	3.69E-02	7.86E-10	4.97E-09	5.76E-09	6.10E-10	6.67E-05	1.09E+05	128	2.64E-11	8.28E-29
1	70.33	2.50E+08	1.90E-07	9.00E-05	0.50%	76.450	13.49	6.120	3.93E-04	1.43E-04	26.73%	1.93E-06	2.84E-10	-2.80E+04	9.26	3.75E-02	3.57E-02	7.21E-10	5.17E-09	5.89E-09	6.09E-10	7.22E-05	1.18E+05	133	2.51E-11	3.77E-29
1	70.33	2.50E+08	1.90E-07	1.00E-04	0.50%	76.210	13.01	5.880	3.98E-04	1.38E-04	25.74%	1.95E-06	2.95E-10	-2.66E+04	10.35	3.57E-02	3.45E-02	6.63E-10	5.33E-09	6.00E-09	6.08E-10	7.72E-05	1.27E+05	142	2.70E-11	4.55E-29
1	70.33	2.50E+08	1.90E-07	2.50E-04	0.50%	73.890	9.21	3.560	4.48E-04	8.77E-05	16.36%	2.20E-06	9.9E-10	-1.60E+04	16.11	2.14E-02	2.13E-02	2.45E-10	5.38E-09	5.63E-09	5.90E-10	1.23E-04	2.08E+05	215	2.60E-11	4.32E-29
1	70.33	2.50E+08	1.90E-07	5.00E-04	0.50%	72.280	6.65	1.950	4.84E-04	5.26E-05	9.80%	2.38E-06	1.31E-09	-8.96E+03	19.11	1.21E-02	1.21E-02	7.86E-11	3.87E-09	3.95E-09	5.76E-10	1.47E-04	2.55E+05	222	2.68E-11	3.32E-28
1	70.33	2.50E+08	1.90E-07	1.00E-03	0.50%	71.185	4.87	0.855	5.08E-04	2.83E-05	5.27%	2.50E-06	1.7E-09	-4.28E+03	16.67	5.90E-03	5.91E-03	1.88E-11	2.24E-09	2.25E-09	5.66E-10	1.58E-04	2.79E+05	250	1.78E-10	7.80E-26
1	70.33	2.50E+08	2.50E-07	1.00E-07	1.20%	79.269	18.9	8.94	3.30E-04	2.07E-04	38.54%	1.6E-06	9.2E-11	-8.08E+04	1.53	6.20E-02	4.83E-02	2.89E-09	1.20E-11	2.90E-09	6.22E-10	1.16E-07	1.86E+02	77	2.25E-11	4.2E-29
1	70.33	2.50E+08	2.50E-07	1.00E-06	1.20%	79.221	18.81	8.891	3.31E-04	2.06E-04	38.33%	1.62E-06	9.27E-11	-8.02E+04	1.54	6.16E-02	4.80E-02	2.85E-09	1.18E-10	2.97E-09	6.22E-10	1.15E-06	1.85E+03	77	2.38E-11	4.32E-29
1	70.33	2.50E+08	2.50E-07	1.00E-05	1.20%	78.773	18.05	8.443	3.41E-04	1.95E-04	36.41%	1.68E-06	9.44E-11	-7.46E+04	1.58	5.74E-02	4.58E-02	2.52E-09	1.07E-09	3.58E-09	6.19E-10	1.09E-05	1.77E+04	80	2.34E-11	5.28E-29
1	70.33	2.50E+08	2.50E-07	2.00E-05	1.20%	78.333	17.29	8.003	3.51E-04	1.85E-04	34.54%	1.72E-06	9.39E-11	-6.94E+04	1.60	5.33E-02	4.37E-02	2.22E-09	1.92E-09	4.14E-09	6.16E-10	2.07E-05	3.37E+04	83	2.49E-11	6.28E-29
1	70.33	2.50E+08	2.50E-07	3.00E-05	1.20%	77.944	16.59	7.614	3.60E-04	1.76E-04	32.89%	1.77E-06	9.36E-11	-6.48E+04	1.64	4.99E-02	4.18E-02	1.98E-09	2.61E-09	4.59E-09	6.14E-10	2.96E-05	4.82E+04	86	2.68E-11	5.87E-29
1	70.33	2.50E+08	2.50E-07	4.00E-05	1.20%	77.592	15.95	7.262	3.68E-04	1.68E-04	31.42%	1.81E-06	9.42E-11	-6.08E+04	1.74	4.69E-02	4.01E-02	1.77E-09	3.18E-09	4.95E-09	6.12E-10	3.77E-05	6.16E+04	90	2.47E-11	4.87E-29
1	70.33	2.50E+08	2.50E-07	5.00E-05	1.20%	77.270	15.35	6.940	3.75E-04	1.61E-04	30.08%	1.84E-06	9.59E-11	-5.73E+04	1.91	4.42E-02	3.86E-02	1.60E-09	3.64E-09	5.25E-09	6.10E-10	4.51E-05	7.40E+04	93	2.71E-11	3.73E-29
1	70.33	2.50E+08	2.50E-07	6.00E-05	1.20%	76.974	14.79	6.644	3.81E-04	1.55E-04	28.86%	1.87E-06	9.83E-11	-5.41E+04	2.14	4.18E-02	3.72E-02	1.46E-09	4.02E-09	5.48E-09	6.09E-10	5.20E-05	8.53E+04	97	2.62E-11	5.23E-29
1	70.33	2.50E+08	2.50E-07	7.00E-05	1.20%	76.700	14.27	6.370	3.87E-04	1.49E-04	27.74%	1.90E-06	1.01E-10	-5.12E+04	2.40	3.96E-02	3.59E-02	1.33E-09	4.34E-09	5.67E-09	6.08E-10	5.83E-05	9.59E+04	104	2.50E-11	4.41E-29
1	70.33	2.50E+08	2.50E-07	8.00E-05	1.20%	76.446	13.77	6.116	3.93E-04	1.43E-04	26.70%	1.93E-06	1.04E-10	-4.86E+04	2.70	3.76E-02	3.47E-02	1.22E-09	4.59E-09	5.81E-09	6.07E-10	6.41E-05	1.06E+05	109	2.41E-11	5.05E-29
1	70.33	2.50E+08	2.50E-07	9.00E-05	1.20%	76.209	13.30	5.879	3.98E-04	1.38E-04	25.74%	1.96E-06	1.06E-10	-4.63E+04	3.03	3.58E-02	3.36E-02	1.12E-09	4.80E-09	5.92E-09	6.06E-10	6.95E-05	1.15E+05	113	2.49E-11	4.68E-29
1	70.33	2.50E+08	2.50E-07	1.00E-04	1.20%	75.988	12.86	5.658	4.03E-04	1.33E-04	24.83%	1.98E-06	1.09E-10	-4.41E+04	3.43	3.41E-02	3.25E-02	1.03E-09	4.97E-09	6.00E-09	6.05E-10	7.45E-05	1.23E+05	117	2.55E-11	4.68E-29
1	70.33	2.50E+08	2.50E-07	2.50E-04	1.20%	73.801	9.12	3.471	4.50E-04	8.57E-05	15.99%	2.21E-06	6.81E-10	-2.66E+04	20.46	2.06E-02	2.05E-02	3.95E-10	5.14E-09	5.54E-09	5.89E-10	1.20E-04	2.04E+05	192	2.59E-11	5.14E-29
1	70.33	2.50E+08	2.50E-07	5.00E-04	1.20%	72.245	6.66	1.915	4.84E-04	5.19E-05	9.67%	2.38E-06	9.10E-10	-1.51E+04	24.84	1.18E-02	1.17E-02	1.29E-10	3.76E-09	3.89E-09	5.75E-10	1.45E-04	2.52E+05	232	2.61E-11	1.39E-28
1	70.33	2.50E+08	2.50E-07	1.00E-03	1.20%	71.170	4.93	0.840	5.08E-04	2.81E-05	5.24%	2.50E-06	1.17E-09	-7.28E+03	23.38	5.74E-03	5.76E-03	3.08E-11	2.21E-09	2.24E-09	5.66E-10	1.57E-04	2.78E+05	250	3.01E-10	7.57E-26
1	70.33	5.70E+08	4.00E-07	1.00E-07	3.07%	75.692	13.83	5.362	4.08E-04	1.28E-04	23.84%	2.02E-06	2.8E-10	-2.49E+05	0.19	3.31E-02	2.78E-02	5.10E-09	4.59E-12	5.10E-09	5.94E-10	7.17E-08	1.21E+02	108	2.63E-11	3.84E-28
1	70.33	5.70E+08	4.00E-07	1.00E-06	3.07%	75.677	13.80	5.347	4.09E-04	1.27E-04	23.78%	2.02E-06	2.8E-10	-2.48E+05	0.19	3.30E-02	2.77E-02	5.06E-09	4.57E-11	5.11E-09	5.94E-10	7.15E-07	1.20E+03	109	2.28E-11	2.79E-28
1	70.33	5.70E+08	4.00E-07	1.00E-05	3.07%	75.528	13.54	5.198	4.12E-04	1.24E-04	23.17%	2.04E-06	2.77E-10	-2.40E+05	0.21	3.19E-02	2.69E-02	4.76E-09	4.34E-10	5.19E-09	5.93E-10	6.97E-06	1.17E+04	111	2.58E-11	4.17E-28
1	70.33	5.70E+08	4.00E-07	2.00E-05	3.07%	75.368	13.26	5.038	4.15E-04	1.21E-04	22.52%	2.05E-06	2.70E-10	-2.31E+05	0.22	3.07E-02	2.62E-02	4.44E-09	8.20E-10	5.26E-09	5.92E-10	1.35E-05	2.29E+04	112	2.67E-11	6.80E-28
1	70.33	5.70E+08	4.00E-07	3.00E-05	3.07%	75.216	12.98	4.886	4.19E-04	1.17E-04	21.90%	2.07E-06	2.63E-10	-2.23E+05	0.24	2.96E-02	2.54E-02	4.15E-09	1.16E-09	5.32E-09	5.91E-10	1.98E-05	3.34E+04	116	2.57E-11	4.47E-28
1	70.33	5.70E+08	4.00E-07	4.00E-05	3.07%	75.070	12.72	4.740	4.22E-04	1.14E-04	21.31%	2.08E-06	2.6E-10	-2.15E+05	0.25	2.86E-02	2.47E-02	3.88E-09	1.47E-09	5.35E-09	5.90E-10	2.56E-05	4.34E+04	116	2.57E-11	4.47E-28
1	70.33	5.70E+08	4.00E-07	5.00E-05	3.07%	74.933	12.46	4.603	4.25E-04	1.11E-04	20.74%	2.10E-06	2.5E-10	-2.07E+05	0.27	2.76E-02	2.40E-02	3.64E-09	1.74E-09	5.38E-09	5.90E-10	3.12E-05	5.29E+04	154	2.69E-11	4.27E-29
1	70.33	5.70E+08	4.00E-07	6.00E-05	3.07%	74.804	12.22	4.474	4.28E-04	1.08E-04	20.19%	2.11E-06	2.41E-10	-2.00E+05	0.29	2.66E-02	2.33E-02	3.41E-09	1.98E-09	5.39E-09	5.89E-10	3.64E-05	6.19E+04	154	2.69E-11	4.27E-29
1	70.33	5.70E+08	4.00E-07	7.00E-05	3.07%	74.679	11.98	4.349	4.31E-04	1.05E-04	19.66%	2.13E-06	2.34E-10	-1.93E+05	0.31	2.57E-02	2.27E-02	3.21E-09	2.19E-09	5.39E-09	5.88E-10	4.14E-05	7.04E+04	149	2.65E-11	3.59E-29
1	70.33	5.70E+08	4.00E-07	8.00E-05	3.07%	74.558	11.75	4.228	4.33E-04	1.03E-04	19.16%	2.14E-06	2.27E-10	-1.87E+05	0.33	2.49E-02	2.21E-02	3.01E-09	2.38E-09	5.39E-09	5.88E-10	4.61E-05	7.85E+04	147	2.53E-11	4.32E-29
1	70.33	5.70E+08	4.00E-07	9.00E-05	3.07%	74.442	11.52	4.112	4.36E-04	1.00E-04	18.68%	2.15E-06	2.19E-10	-1.80E+05	0.35	2.40E-02	2.15E-02	2.83E-09	2.54E-09	5.37E-09	5.87E-10	5.06E-05	8.61E+04	145	2.69E-11	5.41E-29
1	70.33	5.70E+08	4.00E-07	1.00E-04	3.07%	74.331	11.30	4.001	4.39E-04	9.77E-05	18.21%	2.16E-06	2.12E-10	-1.75E+05	0.36	2.33E-02	2.09E-02	2.67E-09	2.69E-09	5.35E-09	5.87E-10	5.48E-05	9.34E+04	145	2.63E-11	9.14E-29
1	70.33	5.70E+08	4.00E-07	2.50E-04	3.07%	73.082	8.64	2.752	4.66E-04	6.99E-05	13.03%	2.30E-06	1.22E-10	-1.12E+05	0.57	1.49E-02	1.47E-02	1.20E-09	3.44E-09	4.64E-09	5.82E-10	9.81E-05	1.68E+05	172	2.72E-11	2.32E-28
1	70.33	5.70E+08	4.00E-07	5.00E-04	3.07%	71.961	6.48	1.631	4.91E-04	4.55E-05	8.49%	2.42E-06	1.52E-10	-6.91E+04	10.77	9.21E-03	9.21E-03	4.63E-10	2.91E-09	3.37E-09	5.73E-10	1.28E-04	2.23E+05	250	1.34E-10	2.74E-28
1	70.33	5.70E+08	4.00E-07	1.00E-03	3.07%	71.083	4.97	0.753	5.10E-04	2.62E-05	4.90%	2.51E-06	1.69E-10	-3.56E+04	10.36	4.76E-03	4.77E-03	1.24E-10	1.93E-09	2.06E-09	5.65E-10	1.47E-04	2.60E+05	250	7.88E-09	1.55E-25
Activity																										
0.1	70.33	2.50E+08	1.90E-07	1.00E-05	0.50%	74.344	11.32	4.014	4.38E-04	9.78E-05	18.24%	2.16E-06	2.11E-10	-1.74E+04	0.04	2.33E-02	2.10E-02	2.66E-10	2.69E-10	5.35E-10	5.87E-10	5.49E-06	9.35E+03	250	3.32E-09	3.18E-27
0.3	70.33	2.50E+08	1.90E-07	1.00E-05	0.50%	77.049	15.36	6.719	3.80E-04	1.57E-04	29.22%	1.87E-06	1.38E-10	-3.21E+04	0.22	4.29E-02	3.63E-02	8.51E-10	6.88E-10	1.54E-09	6.07E-10	8.77E-06	1.45E+04	143	7.64E-12	4.91E-29
0.5	70.33	2.50E+08	1.90E-07	1.00E-05	0.50%	78.156	17.04	7.826	3.55E-04	1.81E-04	33.80%	1.74E-06	9.64E-11	-3.90E+04	0.58	5.19E-02	4.25E-02	1.22E-09	9.20E-10	2.14E-09	6.15E-10	1.01E-05	1.65E+04	110	1.29E-11	4.50E-29
0.7	70.33	2.50E+08	1.90E-07	1.00E-05	0.50%	78.806	18.04	8.476	3.40E-04	1.96E-04	36.54%	1.67E-06	1.09E-10	-4.34E+04	1.99	5.76E-02	4.62E-02	1.47E-09	1.07E-09	2.55E-09	6.19E-10	1.10E-05	1.77E+04	102	1.73E-11	4.96E-29
0.9	70.33	2.50E+08	1.90E-07	1.00E-05	0.50%	79.248	18.72	8.918	3.30E-04	2.06E-04	38.41%	1.62E-06	1.54E-10	-4.64E+04	3.67	6.17E-02	4.87E-02	1.67E-09	1.19E-09	2.86E-09	6.23E-10	1.15E-05	1.85E+04	99	2.26E-11	3.46E-29
0.1	70.33	2.50E+08	2.50E-07	1.00E-05	1.20%	73.546	10.42	3.216	4.55E-04	8.10E-05	15.11%	2.25E-06	2.47E-10	-2.34E+04	0.01	1.83E-02	1.63E-02	2.80E-10	1.85E-10	4.65E-10	5.79E-10	4.55E-06	7.86E+03	250	5.56E-09	8.49E-27
0.3	70.33	2.50E+08	2.50E-07	1.00E-05	1.20%	76.198	14.25	5.868	3.98E-04	1.38E-04	25.80%	1.96E-06	2.03E-10	-4.72E+04	0.28	3.65E-02	3.11E-02	1.08E-09	5.37E-10	1.61E-09	5.99E-10	7.75E-06	1.29E+04	145	8.03E-12	4.05E-29
0.5	70.33	2.50E+08	2.50E-07	1.00E-05	1.20%	77.378	15.98	7.048	3.72E-04	1.64E-04	30.60%	1.83E-06	1.50E-10	-5.91E+04	0.35	4.56E-02	3.78E-02	1.64E-09	7.55E-10	2.39E-09	6.08E-10	9.19E-06	1.51E+04	103	1.35E-11	3.64E-29
0.7	70.33	2.50E+08	2.50E-07	1.00E-05	1.20%	78.088	17.03	7.758	3.56E-04	1.80E-04	33.54%	1.75E-06	1.15E-10	-6.68E+04	0.27	5.14E-02	4.19E-02	2.05E-09	9.06E-10	2.96E-09	6.14E-10	1.01E-05	1.64E+04	89	1.78E-11	3.91E-29
0.9	70.33	2.50E+08	2.50E-07	1.00E-05	1.20%	78.578	17.76	8.248	3.45E-04	1.91E-04	35.59%	1.70E-06	9.67E-11	-7.24E+04	1.06	5.56E-02	4.47E-02	2.38E-09	1.02E-09	3.40E-09	6.17E-10	1.07E-05	1.73E+04	82	2.37E-11	3.64E-29
0.1	70.33	5.70E+08	3.04E-07	1.00E-05	1.27%	71.890	8.44	1.560	4.90E-04	4.62E-05	8.62%	2.43E-06	2.46E-10	-3.49E+04	0.04	8.18E-03	7.16E-03	1.87E-10	6.10E-11	2.48E-10	5.64E-10	2.61E-06	4.62E+03	250	1.35E-09	3.40E-24
0.3	70.33	5.70E+08	3.04E-07	1.00E-05	1.27%	73.865	11.18	3.535	4.48E-04	8.86E-05	16.53%	2.21E-06	2.91E-10	-8.90E+04	0.07	2.06E-02	1.78E-02	1.17E-09	2.22E-10	1.39E-09	5.80E-10	4.98E-06	8.58E+03	216	7.73E-12	6.50E-29
0.5	70.33	5.70E+08	3.04E-07	1.00E-05	1.27%	75.060	12.84	4.730	4.22E-04	1.14E-04	21.29%	2.09E-06	2.81E-10	-1.24E+05	0.07	2.86E-02	2.44E-02	2.23E-09	3.67E-10	2.60E-09	5.90E-10	6.40E-06	1.09E+04	124	1.21E-11	4.64E-29
0.7	70.33	5.70E+08	3.04E-07	1.00E-05	1.27%	75.865	13.97	5.535	4.05E-04	1.31E-04	24.51%	2.00E-06	2.57E-10	-1.49E+05	0.28	3.43E-02	2.89E-02	3.17E-09	4.85E-10	3.66E-09	5.96E-10	7.37E-06	1.24E+04	103	1.69E-11	7.00E-29
0.9	70.33	5.70E+08	3.04E-07	1.00E-05	1.27%	76.454	14.80	6.124	3.92E-04	1.44E-04	26.88%	1.93E-06	2.32E-10	-1.69E+05	0.62	3.86E-02	3.22E-02	3.99E-09	5.83E-10	4.57E-09	6.00E-10	8.08E-06	1.35E+04	89	2.11E-11	6.87E-29
0.1	70.33	5.70E+08	4.00E-07	1.00E-05	3.07%	71.386	7.78	1.056	5.01E-04	3.55E-05	6.63%	2.48E-06	2.27E-10	-3.80E+04	1.21	5.17E-03	4.52E-03	1.29E-10	3.63E-11	1.65E-10	5.60E-10	2.01E-06	3.59E+03	250	7.77E-09	8.83E-22
0.3	70.33	5.70E+08	4.00E-07	1.00E-05	3.07%	72.857	9.86	2.527	4.69E-04	6.73E-05	12.54%	2.32E-06	2.86E-10	-1.05E+05	0.02	1.42E-02	1.23E-02	9.64E-10	1.28E-10	1.09E-09	5.72E-10	3.78E-06	6.62E+03	250	1.26E-10	4.50E-29
0.5	70.33	5.70E+08	4.00E-07	1.00E-05	3.07%	73.908	11.30	3.578	4.47E-04	8.96E-05	16.72%	2.21E-06	3.00E-10	-1.56E+05	0.12	2.09E-02	1.80E-02	2.08E-09	2.27E-10	2.30E-09	5.80E-10	5.04E-06	8.68E+03	169	1.32E-11	6.46E-29
0.7	70.33	5.70E+08	4.00E-07	1.00E-05	3.07%	74.681	12.37	4.351	4.30E-04	1.06E-04	19.79%	2.13E-06	2.96E-10	-1.95E+05	0.16	2.61E-02	2.22E-02	3.20E-09	3.17E-10	3.52E-09	5.86E-10	5.96E-06	1.02E+04	132	1.82E-11	3.23E-28
0.9	70.33	5.70E+08	4.00E-07	1.00E-05	3.07%	75.277	13.19	4.947	4.17E-04	1.19E-04	22.17%	2.06E-06	2.8E-10	-2.26E+05	0.15	3.02E-02	2.55E-02	4.26E-09	3.97E-10	4.66E-09	5.91E-10	6.67E-06	1.13E+04	117	2.22E-11	2.95E-28

act	alpha	E_col	colrad	k_ex	col_pr	alpha_	std_a	delta a	L_end	Delta L	delta L	l_sarc	std_l_sar	labda	std_la	e_col	std_ecol	W_col	W_ex	W_tot	A_end	f_end	sigma	num	ferr	verr
inpu	Model Parameters					Output Parameters																			Convergence	
Collagen stiffness																										
1	54.44	2.00E+08	4.00E-07	1.00E-05	1.27%	68.969	4.88	14.529	3.48E-04	1.88E-04	35.06%	1.71E-06	1.46E-10	-7.27E+04	11.03	4.60E-02	3.42E-02	1.82E-09	9.89E-10	2.81E-09	8.35E-10	1.05E-05	1.26E+04	40	2.62E-11	6.00E-29
1	54.44	2.50E+08	4.00E-07	1.00E-05	1.27%	68.481	4.42	14.041	3.55E-04	1.82E-04	33.86%	1.74E-06	1.20E-10	-8.50E+04	9.80	4.32E-02	3.17E-02	1.99E-09	9.22E-10	2.92E-09	8.26E-10	1.02E-05	1.23E+04	39	2.59E-11	4.37E-29
1	54.44	4.00E+08	4.00E-07	1.00E-05	1.27%	67.395	3.51	12.955	3.69E-04	1.67E-04	31.22%	1.81E-06	6.83E-11	-1.16E+05	6.40	3.73E-02	2.64E-02	2.32E-09	7.84E-10	3.10E-09	8.07E-10	9.37E-06	1.16E+04	37	2.62E-11	4.27E-29
1	54.44	5.70E+08	4.00E-07	1.00E-05	1.27%	66.546	2.89	12.106	3.80E-04	1.56E-04	29.16%	1.87E-06	3.89E-11	-1.44E+05	4.25	3.29E-02	2.26E-02	2.52E-09	6.84E-10	3.20E-09	7.91E-10	8.75E-06	1.11E+04	40	1.96E-11	5.28E-29
1	54.44	8.60E+08	4.00E-07	1.00E-05	1.27%	65.552	2.27	11.112	3.93E-04	1.43E-04	26.76%	1.93E-06	2.53E-11	-1.82E+05	4.75	2.81E-02	1.84E-02	2.69E-09	5.76E-10	3.26E-09	7.72E-10	8.03E-06	1.04E+04	45	2.23E-11	4.09E-29
1	54.44	2.00E+08	2.50E-07	1.00E-05	0.50%	70.736	6.88	16.296	3.25E-04	2.11E-04	39.40%	1.59E-06	2.01E-10	-3.57E+04	4.09	5.70E-02	4.34E-02	1.11E-09	1.25E-09	2.36E-09	8.63E-10	1.18E-05	1.37E+04	44	2.65E-11	1.02E-25
1	54.44	2.50E+08	2.50E-07	1.00E-05	0.50%	70.367	6.39	15.927	3.30E-04	2.06E-04	38.48%	1.62E-06	2.36E-10	-4.26E+04	5.65	5.45E-02	4.15E-02	1.27E-09	1.19E-09	2.46E-09	8.58E-10	1.15E-05	1.35E+04	44	2.48E-11	6.43E-26
1	54.44	4.00E+08	2.50E-07	1.00E-05	0.50%	69.484	5.39	15.044	3.41E-04	1.95E-04	36.31%	1.68E-06	1.70E-10	-6.09E+04	11.72	4.90E-02	3.69E-02	1.63E-09	1.06E-09	2.69E-09	8.44E-10	1.09E-05	1.29E+04	42	2.43E-11	2.32E-28
1	54.44	5.70E+08	2.50E-07	1.00E-05	0.50%	68.737	4.66	14.297	3.51E-04	1.85E-04	34.49%	1.73E-06	1.34E-10	-7.84E+04	10.49	4.47E-02	3.30E-02	1.91E-09	9.57E-10	2.86E-09	8.31E-10	1.03E-05	1.25E+04	40	2.20E-11	4.18E-29
1	54.44	8.60E+08	2.50E-07	1.00E-05	0.50%	67.805	3.84	13.365	3.63E-04	1.73E-04	32.22%	1.79E-06	8.65E-11	-1.03E+05	7.72	3.95E-02	2.84E-02	2.20E-09	8.35E-10	3.04E-09	8.14E-10	9.67E-06	1.19E+04	38	2.35E-11	4.18E-29
External spring stiffness																										
1	54.44	5.70E+08	4.00E-07	1.00E-07	1.27%	66.871	3.14	12.431	3.75E-04	1.61E-04	29.98%	1.85E-06	4.12E-11	-1.52E+05	4.43	3.46E-02	2.40E-02	2.81E-09	7.23E-12	2.81E-09	7.97E-10	9.00E-08	1.13E+02	58	2.52E-11	4.27E-29
1	54.44	5.70E+08	4.00E-07	1.00E-06	1.27%	66.841	3.11	12.401	3.76E-04	1.60E-04	29.91%	1.85E-06	4.10E-11	-1.51E+05	4.41	3.45E-02	2.39E-02	2.78E-09	7.20E-11	2.85E-09	7.96E-10	8.97E-07	1.13E+03	57	2.52E-11	6.09E-29
1	54.44	5.70E+08	4.00E-07	1.00E-05	1.27%	66.546	2.89	12.106	3.80E-04	1.56E-04	29.16%	1.87E-06	3.89E-11	-1.44E+05	4.25	3.29E-02	2.26E-02	2.52E-09	6.84E-10	3.20E-09	7.91E-10	8.75E-06	1.11E+04	40	1.96E-11	5.28E-29
1	54.44	5.70E+08	4.00E-07	2.00E-05	1.27%	66.228	2.68	11.788	3.84E-04	1.52E-04	28.36%	1.89E-06	3.70E-11	-1.36E+05	4.13	3.13E-02	2.12E-02	2.26E-09	1.29E-09	3.55E-09	7.85E-10	1.70E-05	2.17E+04	39	2.67E-11	6.00E-29
1	54.44	5.70E+08	4.00E-07	3.00E-05	1.27%	65.920	2.48	11.480	3.88E-04	1.48E-04	27.59%	1.91E-06	3.52E-11	-1.29E+05	4.01	2.98E-02	1.99E-02	2.03E-09	1.84E-09	3.87E-09	7.79E-10	2.48E-05	3.19E+04	39	2.64E-11	5.09E-29
1	54.44	5.70E+08	4.00E-07	4.00E-05	1.27%	65.623	2.30	11.183	3.92E-04	1.44E-04	26.85%	1.93E-06	3.36E-11	-1.22E+05	3.90	2.84E-02	1.87E-02	1.82E-09	2.32E-09	4.14E-09	7.74E-10	3.22E-05	4.16E+04	39	2.65E-11	4.73E-29
1	54.44	5.70E+08	4.00E-07	5.00E-05	1.27%	65.334	2.13	10.894	3.96E-04	1.40E-04	26.14%	1.95E-06	3.20E-11	-1.16E+05	3.78	2.70E-02	1.75E-02	1.64E-09	2.75E-09	4.39E-09	7.68E-10	3.92E-05	5.10E+04	39	2.69E-11	6.18E-29
1	54.44	5.70E+08	4.00E-07	6.00E-05	1.27%	65.055	1.97	10.615	4.00E-04	1.36E-04	25.45%	1.97E-06	3.06E-11	-1.10E+05	3.66	2.57E-02	1.65E-02	1.47E-09	3.13E-09	4.60E-09	7.63E-10	4.58E-05	6.00E+04	40	1.99E-11	4.09E-29
1	54.44	5.70E+08	4.00E-07	7.00E-05	1.27%	64.785	1.83	10.345	4.03E-04	1.33E-04	24.79%	1.98E-06	2.93E-11	-1.04E+05	3.54	2.45E-02	1.55E-02	1.32E-09	3.46E-09	4.78E-09	7.58E-10	5.21E-05	6.87E+04	40	2.07E-11	4.82E-29
1	54.44	5.70E+08	4.00E-07	8.00E-05	1.27%	64.522	1.70	10.082	4.07E-04	1.29E-04	24.14%	2.00E-06	2.81E-11	-9.86E+04	3.42	2.33E-02	1.45E-02	1.19E-09	3.75E-09	4.94E-09	7.53E-10	5.79E-05	7.69E+04	40	2.17E-11	5.09E-29
1	54.44	5.70E+08	4.00E-07	9.00E-05	1.27%	64.268	1.58	9.828	4.10E-04	1.26E-04	23.52%	2.02E-06	2.70E-11	-9.35E+04	3.31	2.22E-02	1.37E-02	1.07E-09	4.01E-09	5.08E-09	7.48E-10	6.35E-05	8.49E+04	40	2.30E-11	5.73E-29
1	54.44	5.70E+08	4.00E-07	1.00E-04	1.27%	64.022	1.47	9.582	4.13E-04	1.23E-04	22.92%	2.03E-06	2.60E-11	-8.86E+04	3.20	2.11E-02	1.28E-02	9.66E-10	4.23E-09	5.19E-09	7.44E-10	6.88E-05	9.24E+04	40	2.45E-11	6.28E-29
1	54.44	5.70E+08	4.00E-07	2.50E-04	1.27%	61.132	0.55	6.692	4.51E-04	8.56E-05	15.97%	2.22E-06	2.34E-11	-4.13E+04	2.86	1.04E-02	5.38E-03	2.17E-10	5.13E-09	5.34E-09	6.92E-10	1.20E-04	1.73E+05	46	2.46E-11	4.00E-29
1	54.44	5.70E+08	4.00E-07	5.00E-04	1.27%	58.570	0.16	4.130	4.83E-04	5.29E-05	9.87%	2.38E-06	2.21E-11	-1.44E+04	3.02	3.82E-03	1.70E-03	2.76E-11	3.92E-09	3.95E-09	6.48E-10	1.48E-04	2.28E+05	40	2.72E-11	3.18E-29
1	54.44	5.70E+08	4.00E-07	1.00E-03	1.27%	56.660	0.03	2.220	5.08E-04	2.85E-05	5.32%	2.50E-06	9.10E-12	-3.46E+03	1.06	9.57E-04	3.87E-04	1.68E-12	2.27E-09	2.27E-09	6.18E-10	1.59E-04	2.58E+05	81	2.69E-11	4.37E-29
1	54.44	2.50E+08	2.50E-07	1.00E-07	0.50%	71.287	7.60	16.847	3.17E-04	2.19E-04	40.83%	1.56E-06	1.99E-10	-4.77E+04	5.44	6.06E-02	4.63E-02	1.58E-09	1.34E-11	1.59E-09	8.71E-10	1.22E-07	1.41E+02	52	2.44E-11	3.64E-27
1	54.44	2.50E+08	2.50E-07	1.00E-06	0.50%	71.197	7.48	16.757	3.18E-04	2.18E-04	40.60%	1.56E-06	2.01E-10	-4.72E+04	5.44	6.00E-02	4.58E-02	1.54E-09	1.33E-10	1.68E-09	8.70E-10	1.22E-06	1.40E+03	51	2.42E-11	6.07E-27
1	54.44	2.50E+08	2.50E-07	1.00E-05	0.50%	70.367	6.39	15.927	3.30E-04	2.06E-04	38.48%	1.62E-06	2.36E-10	-4.26E+04	5.65	5.45E-02	4.15E-02	1.27E-09	1.19E-09	2.46E-09	8.58E-10	1.15E-05	1.35E+04	44	2.48E-11	6.43E-26
1	54.44	2.50E+08	2.50E-07	2.00E-05	0.50%	69.563	5.47	15.123	3.41E-04	1.95E-04	36.46%	1.67E-06	1.90E-10	-3.85E+04	11.48	4.95E-02	3.73E-02	1.04E-09	2.14E-09	3.18E-09	8.45E-10	2.19E-05	2.59E+04	38	2.37E-11	4.52E-28
1	54.44	2.50E+08	2.50E-07	3.00E-05	0.50%	68.854	4.75	14.414	3.50E-04	1.86E-04	34.69%	1.72E-06	1.84E-10	-3.50E+04	11.58	4.54E-02	3.35E-02	8.64E-10	2.90E-09	3.77E-09	8.33E-10	3.12E-05	3.75E+04	34	2.66E-11	5.28E-29
1	54.44	2.50E+08	2.50E-07	4.00E-05	0.50%	68.219	4.17	13.779	3.59E-04	1.78E-04	33.11%	1.76E-06	1.79E-10	-3.20E+04	11.53	4.18E-02	3.03E-02	7.24E-10	3.53E-09	4.25E-09	8.22E-10	3.97E-05	4.84E+04	32	2.12E-11	4.91E-29
1	54.44	2.50E+08	2.50E-07	5.00E-05	0.50%	67.643	3.69	13.203	3.66E-04	1.70E-04	31.68%	1.80E-06	1.75E-10	-2.94E+04	11.40	3.87E-02	2.75E-02	6.12E-10	4.04E-09	4.65E-09	8.11E-10	4.75E-05	5.86E+04	30	2.22E-11	9.37E-29
1	54.44	2.50E+08	2.50E-07	6.00E-05	0.50%	67.116	3.27	12.676	3.73E-04	1.63E-04	30.39%	1.83E-06	1.71E-10	-2.71E+04	11.21	3.59E-02	2.51E-02	5.20E-10	4.46E-09	4.98E-09	8.02E-10	5.47E-05	6.82E+04	29	2.67E-11	6.00E-29
1	54.44	2.50E+08	2.50E-07	7.00E-05	0.50%	66.631	2.92	12.191	3.80E-04	1.57E-04	29.19%	1.86E-06	1.67E-10	-2.50E+04	10.97	3.34E-02	2.29E-02	4.45E-10	4.80E-09	5.24E-09	7.93E-10	6.13E-05	7.74E+04	29	2.32E-11	5.46E-29
1	54.44	2.50E+08	2.50E-07	8.00E-05	0.50%	66.181	2.62	11.741	3.86E-04	1.51E-04	28.09%	1.89E-06	1.63E-10	-2.32E+04	10.68	3.11E-02	2.09E-02	3.83E-10	5.08E-09	5.46E-09	7.84E-10	6.74E-05	8.60E+04	29	2.12E-11	7.46E-29
1	54.44	2.50E+08	2.50E-07	9.00E-05	0.50%	65.761	2.36	11.321	3.91E-04	1.45E-04	27.07%	1.92E-06	1.58E-10	-2.15E+04	10.35	2.91E-02	1.92E-02	3.30E-10	5.30E-09	5.63E-09	7.76E-10	7.31E-05	9.41E+04	29	2.02E-11	4.55E-29
1	54.44	2.50E+08	2.50E-07	1.00E-04	0.50%	65.368	2.13	10.928	3.96E-04	1.40E-04	26.11%	1.95E-06	1.54E-10	-2.00E+04	9.99	2.72E-02	1.77E-02	2.86E-10	5.48E-09	5.77E-09	7.69E-10	7.83E-05	1.02E+05	29	2.01E-11	5.46E-29
1	54.44	2.50E+08	2.50E-07	2.50E-04	0.50%	61.460	0.62	7.020	4.46E-04	8.97E-05	16.73%	2.19E-06	8.65E-11	-7.87E+03	4.59	1.15E-02	6.13E-03	4.63E-11	5.63E-09	5.67E-09	6.98E-10	1.25E-04	1.80E+05	34	2.08E-11	5.28E-29
1	54.44	2.50E+08	2.50E-07	5.00E-04	0.50%	58.618	0.16	4.178	4.83E-04	5.35E-05	9.98%	2.37E-06	3.05E-11	-2.54E+03	0.92	3.95E-03	1.84E-03	5.21E-12	4.00E-09	4.01E-09	6.49E-10	1.50E-04	2.31E+05	50	2.62E-11	4.18E-29
1	54.44	2.50E+08	2.50E-07	1.00E-03	0.50%	56.663	0.03	2.223	5.08E-04	2.85E-05	5.32%	2.50E-06	5.80E-12	-5.98E+02	0.05	9.89E-04	4.76E-04	3.41E-13	2.28E-09	2.28E-09	6.18E-10	1.60E-04	2.58E+05	69	2.52E-11	4.00E-29
Activity																										
0.1	54.44	2.50E+08	4.00E-07	1.00E-05	1.27%	61.966	0.79	7.526	4.39E-04	9.70E-05	18.09%	2.16E-06	1.88E-11	-2.32E+04	0.84	1.31E-02	7.14E-03	1.55E-10	2.63E-10	4.18E-10	7.06E-10	5.43E-06	7.68E+03	234	2.64E-11	5.73E-29
0.3	54.44	2.50E+08	4.00E-07	1.00E-05	1.27%	65.048	1.98	10.608	3.99E-04	1.37E-04	25.49%	1.97E-06	2.04E-11	-4.81E+04	1.11	2.57E-02	1.64E-02	6.45E-10	5.23E-10	1.17E-09	7.63E-10	7.65E-06	1.00E+04	101	2.69E-11	4.55E-29
0.5	54.44	2.50E+08	4.00E-07	1.00E-05	1.27%	66.518	2.87	12.078	3.80E-04	1.56E-04	29.06%	1.87E-06	4.62E-11	-6.28E+04	2.39	3.28E-02	2.24E-02	1.09E-09	6.79E-10	1.77E-09	7.90E-10	8.72E-06	1.10E+04	68	2.62E-11	2.82E-29
0.7	54.44	2.50E+08	4.00E-07	1.00E-05	1.27%	67.480	3.57	13.040	3.68E-04	1.68E-04	31.41%	1.81E-06	7.84E-11	-7.33E+04	5.03	3.78E-02	2.68E-02	1.49E-09	7.94E-10	2.28E-09	8.08E-10	9.42E-06	1.17E+04	52	2.63E-11	5.00E-29
0.9	54.44	2.50E+08	4.00E-07	1.00E-05	1.27%	68.188	4.16	13.748	3.58E-04	1.78E-04	33.14%	1.76E-06	1.07E-10	-8.15E+04	8.16	4.16E-02	3.02E-02	1.83E-09	8.84E-10	2.72E-09	8.21E-10	9.94E-06	1.21E+04	43	2.23E-11	3.27E-29
0.1	54.44	2.50E+08	2.50E-07	1.00E-05	0.50%	63.341	1.21	8.901	4.22E-04	1.14E-04	21.32%	2.08E-06	1.05E-11	-1.30E+04	0.22	1.83E-02	1.07E-02	1.22E-10	3.66E-10	4.87E-10	7.31E-10	6.40E-06	8.75E+03	242	2.70E-11	4.73E-29
0.3	54.44	2.50E+08	2.50E-07	1.00E-05	0.50%	66.885	3.11	12.445	3.76E-04	1.60E-04	29.90%	1.85E-06	8.03E-11	-2.61E+04	2.20	3.46E-02	2.40E-02	4.81E-10	7.19E-10	1.20E-09	7.97E-10	8.97E-06	1.13E+04	106	2.68E-11	3.91E-29
0.5	54.44	2.50E+08	2.50E-07	1.00E-05	0.50%	68.438	4.37	13.998	3.55E-04	1.81E-04	33.72%	1.75E-06	1.41E-10	-3.30E+04	5.38	4.30E-02	3.15E-02	7.69E-10	9.14E-10	1.68E-09	8.25E-10	1.01E-05	1.23E+04	73	2.58E-11	4.73E-29
0.7	54.44	2.50E+08	2.50E-07	1.00E-05	0.50%	69.405	5.31	14.965	3.43E-04	1.94E-04	36.10%	1.68E-06	1.76E-10	-3.77E+04	8.30	4.85E-02	3.64E-02	9.99E-10	1.05E-09	2.05E-09	8.42E-10	1.08E-05	1.29E+04	57	2.42E-11	5.28E-29
0.9	54.44	2.50E+08	2.50E-07	1.00E-05	0.50%	70.091	6.05	15.651	3.34E-04	2.03E-04	37.80%	1.64E-06	2.00E-10	-4.11E+04	10.23	5.27E-02	4.01E-02	1.19E-09	1.15E-09	2.34E-09	8.54E-10	1.13E-05	1.33E+04	47	2.50E-11	6.63E-28
0.1	54.44	4.00E+08	4.00E-07	1.00E-05	1.27%	61.250	0.63	6.810	4.48E-04	8.81E-05	16.42%	2.21E-06	3.70E-11	-3.00E+04	3.27	1.07E-02	5.59E-03	1.63E-10	2.17E-10	3.80E-10	6.94E-10	4.93E-06	7.10E+03	228	2.64E-11	4.82E-29
0.3	54.44	4.00E+08	4.00E-07	1.00E-05	1.27%	64.070	1.52	9.630	4.12E-04	1.24E-04	23.16%	2.03E-06	2.24E-11	-6.29E+04	1.73	2.14E-02	1.30E-02	6.94E-10	4.32E-10	1.13E-09	7.45E-10	6.95E-06	9.33E+03	98	2.68E-11	4.82E-29
0.5	54.44	4.00E+08	4.00E-07	1.00E-05	1.27%	65.467	2.22	11.027	3.94E-04	1.42E-04	26.53%	1.94E-06	2.36E-11	-8.33E+04	2.02	2.77E-02	1.81E-02	1.21E-09	5.66E-10	1.78E-09	7.71E-10	7.96E-06	1.03E+04	66	2.40E-11	4.37E-29
0.7	54.44	4.00E+08	4.00E-07	1.00E-05	1.27%	66.403	2.79	11.963	3.82E-04	1.54E-04	28.80%	1.88E-06	3.79E-11	-9.85E+04	2.93	3.22E-02	2.19E-02	1.68E-09	6.67E-10	2.35E-09	7.88E-10	8.64E-06	1.10E+04	50	2.55E-11	3.18E-29
0.9	54.44	4.00E+08	4.00E-07	1.00E-05	1.27%	67.102	3.29	12.662	3.73E-04	1.64E-04	30.50%	1.83E-06	5.81E-11	-1.11E+05	5.06	3.58E-02	2.50E-02	2.12E-09	7.48E-10	2.87E-09	8.01E-10	9.15E-06	1.14E+04	41	2.20E-11	3.55E-29
0.1	54.44	4.00E+08	2.50E-07	1.00E-05	0.50%	62.672	0.98	8.232	4.30E-04	1.06E-04	19.75%	2.12E-06	1.37E-11	-1.76E+04	0.39	1.57E-02	8.88E-03	1.41E-10	3.14E-10	4.54E-10	7.19E-10	5.92E-06	8.24E+03	239	2.65E-11	5.09E-29
0.3	54.44	4.00E+08	2.50E-07	1.00E-05	0.50%	65.999	2.52	11.559	3.87E-04	1.49E-04	27.77%	1.91E-06	4.06E-11	-3.59E+04	1.32	3.02E-02	2.02E-02	5.72E-10	6.20E-10	1.19E-09	7.81E-10	8.33E-06	1.07E+04	104	2.55E-11	6.91E-29
0.5	54.44	4.00E+08	2.50E-07	1.00E-05	0.50%	67.521	3.60	13.081	3.67E-04	1.69E-04	31.49%	1.81E-06	9.00E-11	-4.61E+04	4.00	3.80E-02	2.70E-02	9.41E-10	7.98E-10	1.74E-09	8.09E-10	9.45E-06	1.17E+04	71	2.37E-11	6.00E-29
0.7	54.44	4.00E+08	2.50E-07	1.00E-05	0.50%	68.494	4.43	14.054	3.55E-04	1.82E-04	33.88%	1.74E-06	1.31E-10	-5.32E+04	7.22	4.33E-02	3.18E-02	1.25E-09	9.23E-10	2.17E-09	8.26E-10	1.02E-05	1.23E+04	55	2.28E-11	4.37E-29
0.9	54.44	4.00E+08	2.50E-07	1.00E-05	0.50%	69.196	5.10	14.756	3.45E-04	1.91E-04	35.61%	1.70E-06	1.60E-10	-5.86E+04	10.38	4.73E-02	3.54E-02	1.51E-09	1.02E-09	2.53E-09	8.39E-10	1.07E-05	1.27E+04	45	2.33E-11	7.09E-29
0.1	54.44	5.70E+08	4.00E-07	1.00E-05	1.27%	60.721	0.53	6.281	4.55E-04	8.14E-05	15.19%	2.24E-06	6.54E-11	-3.59E+04	8.54	9.12E-03	4.60E-03	1.65E-10	1.86E-10	3.50E-10	6.84E-10	4.56E-06	6.66E+03	223	2.65E-11	6.73E-29
0.3	54.44	5.70E+08	4.00E-07	1.00E-05	1.27%	63.338	1.24	8.898	4.21E-04	1.15E-04	21.42%	2.08E-06	2.54E-11	-7.58E+04	2.21	1.83E-02	1.08E-02	7.13E-10	3.69E-10	1.08E-09	7.31E-10	6.43E-06	8.79E+03	96	2.50E-11	4.82E-29
0.5	54.44	5.70E+08	4.00E-07	1.00E-05	1.27%	64.669	1.80	10.229	4.04E-04	1.32E-04	24.62%	1.99E-06	2.40E-11	-1.02E+05	2.84	2.40E-02	1.51E-02	1.27E-09	4.87E-10	1.76E-09	7.56E-10	7.39E-06	9.77E+03	66	2.65E-11	3.37E-29
0.7	54.44	5.70E+08	4.00E-07	1.00E-05	1.27%	65.573	2.28	11.133	3.92E-04	1.44E-04	26.80%	1.93E-06	2.46E-11	-1.21E+05	3.03	2.82E-02	1.85E-02	1.79E-09	5.78E-10	2.37E-09	7.73E-10	8.04E-06	1.04E+04	52	2.41E-11	4.27E-29
0.9	54.44	5.70E+08	4.00E-07	1.00E-05	1.27%	66.258	2.70	11.818	3.84E-04	1.53E-04	28.46%	1.89E-06	3.28E-11	-1.37E+05	3.60	3.15E-02	2.13E-02	2.29E-09	6.52E-10	2.94E-09	7.86E-10	8.54E-06	1.09E+04	43	2.25E-11	3.82E-29
0.1	54.44	5.70E+08	2.50E-07	1.00E-05	0.50%	62.142	0.83	7.702	4.37E-04	9.92E-05	18.50%	2.15E-06	1.73E-11	-2.18E+04	0.66	1.38E-02	7.55E-03	1.52E-10	2.75E-10	4.27E-10	7.09E-10	5.55E-06	7.82E+03	235	2.68E-11	3.73E-29
0.3	54.44	5.70E+08	2.50E-07	1.00E-05	0.50%	65.286	2.11	10.846	3.96E-04	1.40E-04	26.06%	1.95E-06	2.27E-11	-4.48E+04	1.04	2.68E-02	1.73E-02	6.29E-10	5.46E-10	1.18E-09	7.67E-10	7.82E-06	1.02E+04	102	2.59E-11	3.18E-29
0.5	54.44	5.70E+08	2.50E-07	1.00E-05	0.50%	66.771	3.04	12.331	3.77E-04	1.59E-04	29.67%	1.86E-06	5.57E-11	-5.83E+04	2.76	3.41E-02	2.35E-02	1.06E-09	7.08E-10	1.77E-09	7.95E-10	8.90E-06	1.12E+04	69	2.42E-11	4.73E-29
0.7	54.44	5.70E+08	2.50E-07	1.00E-05	0.50%	67.737	3.78	13.297	3.64E-04	1.72E-04	32.03%	1.79E-06	9.07E-11	-6.79E+04	5.62	3.91E-02	2.80E-02	1.43E-09	8.25E-10	2.26E-09	8.13E-10	9.61E-06	1.18E+04	53	2.38E-11	4.18E-29
0.9	54.44	5.70E+08	2.50E-07	1.00E-05	0.50%	68.445	4.39	14.005	3.55E-04	1.81E-04	33.77%	1.75E-06	1.21E-10	-7.53E+04	8.85	4.30E-02	3.15E-02	1.76E-09	9.17E-10	2.67E-09	8.25E-10	1.01E-05	1.23E+04	43	2.64E-11	3.18E-29

act	alpha_	E_col	colrad	k_ex	col_pr	alpha_(	std_a	delta a	L_end	Delta L	delta L (	l_sarc	std_l_sarc	labda	std_lab	e_col	std_ecol	W_col	W_ex	W_tot	A_end	f_end	sigma	num	ferr	verr
Inpu	Model Parameters					Output Parameters																		Convergence		
	Collagen stiffness																									
1	34.97	2.00E+08	4.75E-07	1.00E-05	1.27%	63.006	1.53	28.036	2.92E-04	2.44E-04	45.56%	1.44E-06	9.47E-09	3.31E+01	37.86	-2.18E-02	3.48E-02	4.92E-16	1.67E-09	1.67E-09	1.07E-09	1.37E-05	1.27E+04	250	3.64E-08	5.49E-22
1	34.97	2.50E+08	4.75E-07	1.00E-05	1.27%	63.087	1.33	28.117	2.92E-04	2.44E-04	45.56%	1.44E-06	9.44E-09	3.29E+01	42.34	-1.96E-02	3.35E-02	4.95E-16	1.67E-09	1.67E-09	1.07E-09	1.37E-05	1.27E+04	250	4.39E-08	5.19E-22
1	34.97	4.00E+08	4.75E-07	1.00E-05	1.27%	63.231	0.96	28.261	2.92E-04	2.44E-04	45.57%	1.44E-06	9.15E-09	3.04E+01	49.10	-1.57E-02	3.14E-02	5.53E-16	1.67E-09	1.67E-09	1.07E-09	1.37E-05	1.27E+04	250	6.29E-08	4.27E-22
1	34.97	5.70E+08	4.75E-07	1.00E-05	1.27%	63.129	1.24	28.159	2.92E-04	2.44E-04	45.56%	1.44E-06	9.49E-09	3.29E+01	45.31	-1.85E-02	3.29E-02	2.59E-16	1.67E-09	1.67E-09	1.07E-09	1.37E-05	1.27E+04	500	4.82E-08	1.16E-22
1	34.97	8.60E+08	4.75E-07	1.00E-05	1.27%	63.243	0.88	28.273	2.92E-04	2.44E-04	45.57%	1.44E-06	8.86E-09	2.75E+01	47.07	-1.57E-02	3.07E-02	2.80E-16	1.67E-09	1.67E-09	1.07E-09	1.37E-05	1.27E+04	500	7.77E-08	1.31E-22
1	34.97	2.00E+08	4.00E-07	1.00E-05	0.90%	62.446	2.95	27.476	2.92E-04	2.44E-04	45.55%	1.44E-06	7.62E-09	2.74E+01	12.52	-3.84E-02	4.10E-02	2.41E-16	1.67E-09	1.67E-09	1.07E-09	1.37E-05	1.27E+04	500	1.45E-08	1.78E-22
1	34.97	2.50E+08	4.00E-07	1.00E-05	0.90%	62.078	4.13	27.108	2.92E-04	2.44E-04	45.54%	1.4E-06	5.34E-09	2.31E+01	5.08	-5.08E-02	4.64E-02	5.63E-17	1.67E-09	1.67E-09	1.07E-09	1.37E-05	1.27E+04	500	1.00E-08	5.9E-23
1	34.97	4.00E+08	4.00E-07	1.00E-05	0.90%	62.831	1.93	27.861	2.92E-04	2.44E-04	45.55%	1.44E-06	9.20E-09	3.20E+01	28.22	-2.67E-02	3.64E-02	2.47E-16	1.67E-09	1.67E-09	1.07E-09	1.37E-05	1.27E+04	500	2.61E-08	1.44E-22
1	34.97	5.70E+08	4.00E-07	1.00E-05	0.90%	63.005	1.53	28.035	2.92E-04	2.44E-04	45.56%	1.44E-06	9.49E-09	3.33E+01	38.24	-2.19E-02	3.49E-02	2.45E-16	1.67E-09	1.67E-09	1.07E-09	1.37E-05	1.27E+04	500	3.64E-08	1.35E-22
1	34.97	8.60E+08	4.00E-07	1.00E-05	0.90%	63.149	1.19	28.179	2.92E-04	2.44E-04	45.56%	1.44E-06	9.48E-09	3.28E+01	46.36	-1.79E-02	3.25E-02	2.63E-16	1.67E-09	1.67E-09	1.07E-09	1.37E-05	1.27E+04	500	5.10E-08	1.09E-22
1	34.97	2.00E+08	2.97E-07	1.00E-05	0.50%	62.517	2.74	27.547	2.92E-04	2.44E-04	45.55%	1.44E-06	8.03E-09	2.82E+01	14.77	-3.61E-02	3.99E-02	5.10E-16	1.67E-09	1.67E-09	1.07E-09	1.37E-05	1.27E+04	250	1.60E-08	6.99E-22
1	34.97	2.50E+08	2.97E-07	1.00E-05	0.50%	62.627	2.52	27.657	2.92E-04	2.44E-04	45.55%	1.44E-06	8.29E-09	3.03E+01	20.37	-3.29E-02	3.92E-02	4.71E-16	1.67E-09	1.67E-09	1.07E-09	1.37E-05	1.27E+04	250	1.96E-08	6.72E-22
1	34.97	4.00E+08	2.97E-07	1.00E-05	0.50%	62.892	1.80	27.922	2.92E-04	2.44E-04	45.55%	1.44E-06	9.35E-09	3.26E+01	31.52	-2.49E-02	3.61E-02	4.90E-16	1.67E-09	1.67E-09	1.07E-09	1.37E-05	1.27E+04	250	2.91E-08	5.85E-22
1	34.97	5.70E+08	2.97E-07	1.00E-05	0.50%	63.050	1.42	28.080	2.92E-04	2.44E-04	45.56%	1.44E-06	9.48E-09	3.31E+01	40.27	-2.06E-02	3.42E-02	5.04E-16	1.67E-09	1.67E-09	1.07E-09	1.37E-05	1.27E+04	250	4.02E-08	5.41E-22
1	34.97	8.60E+08	2.97E-07	1.00E-05	0.50%	63.168	1.13	28.198	2.92E-04	2.44E-04	45.56%	1.44E-06	9.48E-09	3.26E+01	46.91	-1.73E-02	3.19E-02	5.12E-16	1.67E-09	1.67E-09	1.08E-09	1.37E-05	1.27E+04	250	5.34E-08	3.97E-22
1	34.97	2.00E+08	2.50E-07	1.00E-05	0.35%	61.726	5.23	26.756	2.92E-04	2.44E-04	45.54%	1.44E-06	3.36E-09	1.78E+01	5.36	-6.29E-02	5.14E-02	7.80E-23	1.67E-09	1.67E-09	1.07E-09	1.37E-05	1.27E+04	500	8.00E-09	4.42E-22
1	34.97	2.50E+08	2.50E-07	1.00E-05	0.35%	60.461	4.52	25.491	2.92E-04	2.44E-04	45.53%	1.4E-06	5.59E-09	-3.16E+00	0.68	-9.68E-02	4.27E-02	0.00E+00	1.67E-09	1.67E-09	1.07E-09	1.37E-05	1.28E+04	559	9.30E-09	9.88E-23
1	34.97	4.00E+08	2.50E-07	1.00E-05	0.35%	62.277	3.51	27.307	2.92E-04	2.44E-04	45.55%	1.44E-06	6.55E-09	2.56E+01	8.30	-4.41E-02	4.37E-02	1.93E-16	1.67E-09	1.67E-09	1.07E-09	1.37E-05	1.27E+04	500	1.20E-08	2.03E-22
1	34.97	5.70E+08	2.50E-07	1.00E-05	0.35%	62.520	2.75	27.550	2.92E-04	2.44E-04	45.55%	1.44E-06	7.99E-09	2.83E+01	15.06	-3.61E-02	4.03E-02	2.57E-16	1.67E-09	1.67E-09	1.07E-09	1.37E-05	1.27E+04	500	1.60E-08	1.70E-22
1	34.97	8.60E+08	2.50E-07	1.00E-05	0.35%	62.760	2.12	27.790	2.92E-04	2.44E-04	45.55%	1.44E-06	8.98E-09	3.12E+01	24.82	-2.87E-02	3.78E-02	2.56E-16	1.67E-09	1.67E-09	1.07E-09	1.37E-05	1.27E+04	500	2.29E-08	1.55E-22
	External spring stiffness																									
1	34.97	2.50E+08	2.97E-07	1.00E-07	0.50%	66.700	2.83	31.730	2.54E-04	2.82E-04	52.68%	1.27E-06	2.54E-09	1.04E+00	6.72	-1.85E-02	3.38E-02	2.37E-13	2.23E-11	2.26E-11	1.21E-09	1.58E-07	1.30E+02	500	7.28E-09	2.57E-22
1	34.97	2.50E+08	2.97E-07	1.00E-06	0.50%	65.682	3.18	30.712	2.61E-04	2.75E-04	51.32%	1.29E-06	9.62E-09	5.62E-01	2.78	-2.93E-02	4.21E-02	6.55E-14	2.12E-10	2.12E-10	1.17E-09	1.54E-06	1.32E+03	383	9.99E-09	8.45E-23
1	34.97	2.50E+08	2.97E-07	1.00E-05	0.50%	62.627	2.52	27.657	2.92E-04	2.44E-04	45.55%	1.44E-06	8.29E-09	3.03E+01	20.37	-3.29E-02	3.92E-02	4.71E-16	1.67E-09	1.67E-09	1.07E-09	1.37E-05	1.27E+04	250	1.96E-08	6.72E-22
1	34.97	2.50E+08	2.97E-07	2.00E-05	0.50%	59.454	3.43	24.484	3.13E-04	2.23E-04	41.54%	1.54E-06	3.53E-09	3.44E+01	9.30	-6.25E-02	4.24E-02	0.00E+00	2.78E-09	2.78E-09	1.01E-09	2.49E-05	2.47E+04	500	1.65E-08	4.54E-22
1	34.97	2.50E+08	2.97E-07	3.00E-05	0.50%	57.323	3.07	22.353	3.29E-04	2.07E-04	38.58%	1.62E-06	3.24E-09	3.74E+01	11.26	-7.33E-02	3.88E-02	0.00E+00	3.59E-09	3.59E-09	9.61E-10	3.47E-05	3.61E+04	500	2.13E-08	6.13E-22
1	34.97	2.50E+08	2.97E-07	4.00E-05	0.50%	55.711	2.84	20.741	3.42E-04	1.94E-04	36.21%	1.68E-06	2.91E-09	3.99E+01	14.67	-7.78E-02	3.53E-02	0.00E+00	4.22E-09	4.22E-09	9.27E-10	4.35E-05	4.69E+04	500	2.74E-08	1.30E-21
1	34.97	2.50E+08	2.97E-07	5.00E-05	0.50%	54.246	2.56	19.276	3.53E-04	1.83E-04	34.22%	1.73E-06	2.79E-09	4.32E+01	17.36	-8.28E-02	3.21E-02	0.00E+00	4.71E-09	4.71E-09	8.98E-10	5.13E-05	5.72E+04	500	3.15E-08	2.16E-21
1	34.97	2.50E+08	2.97E-07	6.00E-05	0.50%	51.948	2.52	16.978	3.62E-04	1.74E-04	32.49%	1.8E-06	2.18E-09	3.39E+00	1.16	-1.06E-01	2.97E-02	0.00E+00	5.10E-09	5.10E-09	8.75E-10	5.85E-05	6.69E+04	500	8.67E-09	9.7E-23
1	34.97	2.50E+08	2.97E-07	7.00E-05	0.50%	51.771	2.13	16.801	3.70E-04	1.66E-04	30.97%	1.82E-06	2.66E-09	4.84E+01	22.39	-9.02E-02	2.70E-02	0.00E+00	5.40E-09	5.40E-09	8.55E-10	6.50E-05	7.61E+04	500	3.60E-08	5.71E-21
1	34.97	2.50E+08	2.97E-07	8.00E-05	0.50%	50.676	1.95	15.706	3.77E-04	1.59E-04	29.60%	1.85E-06	2.64E-09	5.01E+01	24.80	-9.34E-02	2.46E-02	0.00E+00	5.64E-09	5.64E-09	8.37E-10	7.11E-05	8.49E+04	500	3.66E-08	1.06E-20
1	34.97	2.50E+08	2.97E-07	9.00E-05	0.50%	49.636	1.79	14.666	3.84E-04	1.52E-04	28.37%	1.89E-06	2.63E-09	5.07E+01	26.62	-9.66E-02	2.28E-02	0.00E+00	5.82E-09	5.82E-09	8.22E-10	7.66E-05	9.31E+04	500	3.51E-08	3.05E-20
1	34.97	2.50E+08	2.97E-07	1.00E-04	0.50%	48.693	1.67	13.723	3.90E-04	1.46E-04	27.24%	1.92E-06	2.58E-09	1.27E+01	4.01	-9.91E-02	2.16E-02	0.00E+00	5.97E-09	5.97E-09	8.10E-10	8.17E-05	1.01E+05	500	1.24E-08	8.06E-21
1	34.97	2.50E+08	2.97E-07	2.50E-04	0.50%	42.866	0.84	7.896	4.45E-04	9.07E-05	16.93%	2.19E-06	2.52E-09	-3.06E-01	0.32	-7.26E-02	1.26E-02	0.00E+00	5.76E-09	5.76E-09	7.07E-10	1.27E-04	1.80E+05	262	9.99E-09	3.79E-24
1	34.97	2.50E+08	2.97E-07	5.00E-04	0.50%	39.408	0.50	4.438	4.83E-04	5.36E-05	10.01%	2.37E-06	1.92E-09	-1.06E+00	0.68	-4.64E-02	7.52E-03	0.00E+00	4.03E-09	4.03E-09	6.52E-10	1.50E-04	2.30E+05	134	9.92E-09	5.04E-24
1	34.97	2.50E+08	2.97E-07	1.00E-03	0.50%	37.256	0.24	2.286	5.08E-04	2.85E-05	5.32%	2.50E-06	1.03E-09	-8.03E-01	0.89	-2.59E-02	4.16E-03	0.00E+00	2.28E-09	2.28E-09	6.19E-10	1.60E-04	2.58E+05	109	9.96E-09	2.69E-24
1	34.97	2.50E+08	2.50E-07	1.00E-07	0.35%	65.012	8.26	30.042	2.56E-04	2.80E-04	52.17%	1.3E-06	1.60E-09	-1.01E+00	1.65	-7.44E-02	6.66E-02	2.79E-13	2.19E-11	2.22E-11	1.14E-09	1.57E-07	1.38E+02	500	4.12E-09	1.5E-22
1	34.97	2.50E+08	2.50E-07	1.00E-06	0.35%	64.519	7.43	29.549	2.61E-04	2.75E-04	51.32%	1.3E-06	2.57E-09	-4.37E+00	3.11	-7.59E-02	6.20E-02	1.44E-13	2.12E-10	2.12E-10	1.13E-09	1.54E-06	1.36E+03	500	4.12E-09	1.54E-22
1	34.97	2.50E+08	2.50E-07	1.00E-05	0.35%	60.461	4.52	25.491	2.92E-04	2.44E-04	45.53%	1.4E-06	5.59E-09	-3.16E+00	0.68	-9.68E-02	4.27E-02	0.00E+00	1.67E-09	1.67E-09	1.07E-09	1.37E-05	1.28E+04	559	9.30E-09	9.88E-23
1	34.97	2.50E+08	2.50E-07	2.00E-05	0.35%	57.726	3.24	22.756	3.13E-04	2.23E-04	41.53%	1.5E-06	4.40E-09	-2.15E+00	0.45	-1.05E-01	3.44E-02	0.00E+00	2.77E-09	2.77E-09	1.00E-09	2.49E-05	2.48E+04	559	9.09E-09	9.72E-23
1	34.97	2.50E+08	2.50E-07	3.00E-05	0.35%	55.760	2.70	20.79	3.29E-04	2.07E-04	38.58%	1.6E-06	3.55E-09	-1.04E+00	0.37	-1.08E-01	3.09E-02	0.00E+00	3.59E-09	3.59E-09	9.57E-10	3.47E-05	3.63E+04	543	6.63E-09	9.56E-23
1	34.97	2.50E+08	2.50E-07	4.00E-05	0.35%	54.219	2.47	19.249	3.42E-04	1.94E-04	36.21%	1.68E-06	3.12E-09	2.36E+00	0.74	-1.08E-01	2.97E-02	0.00E+00	4.22E-09	4.22E-09	9.21E-10	4.35E-05	4.72E+04	547	6.63E-09	9.56E-23
1	34.97	2.50E+08	2.50E-07	5.00E-05	0.35%	52.937	2.25	17.967	3.53E-04	1.83E-04	34.22%	1.73E-06	2.90E-09	2.44E+00	0.68	-1.08E-01	2.83E-02	0.00E+00	4.71E-09	4.71E-09	8.94E-10	5.13E-05	5.74E+04	559	6.18E-09	1.05E-22
1	34.97	2.50E+08	2.50E-07	6.00E-05	0.35%	51.847	2.06	16.877	3.62E-04	1.74E-04	32.49%	1.78E-06	2.80E-09	2.53E+00	0.67	-1.07E-01	2.73E-02	0.00E+00	5.10E-09	5.10E-09	8.71E-10	5.85E-05	6.72E+04	559	6.11E-09	9.20E-23
1	34.97	2.50E+08	2.50E-07	7.00E-05	0.35%	50.901	1.92	15.931	3.70E-04	1.66E-04	30.97%	1.82E-06	2.77E-09	2.60E+00	0.68	-1.05E-01	2.66E-02	0.00E+00	5.40E-09	5.40E-09	8.52E-10	6.50E-05	7.64E+04	559	6.32E-09	9.18E-23
1	34.97	2.50E+08	2.50E-07	8.00E-05	0.35%	50.060	1.84	15.09	3.77E-04	1.59E-04	29.60%	1.85E-06	2.65E-09	2.52E+00	0.63	-1.03E-01	2.59E-02	0.00E+00	5.64E-09	5.64E-09	8.35E-10	7.11E-05	8.51E+04	542	6.46E-09	8.65E-23
1	34.97	2.50E+08	2.50E-07	9.00E-05	0.35%	49.315	1.77	14.345	3.84E-04	1.52E-04	28.37%	1.89E-06	2.68E-09	2.49E+00	0.64	-1.01E-01	2.58E-02	0.00E+00	5.82E-09	5.82E-09	8.21E-10	7.66E-05	9.33E+04	770	7.76E-09	8.35E-23
1	34.97	2.50E+08	2.50E-07	1.00E-04	0.35%	48.643	1.72	13.673	3.90E-04	1.46E-04	27.24%	1.92E-06	2.78E-09	1.82E+00	0.58	-9.93E-02	2.59E-02	0.00E+00	5.97E-09	5.97E-09	8.08E-10	8.17E-05	1.01E+05	770	9.96E-09	3.46E-23
1	34.97	2.50E+08	2.50E-07	2.50E-04	0.35%	42.861	0.62	7.8909	4.45E-04	9.07E-05	16.92%	2.19E-06	2.78E-09	2.98E-01	0.37	-7.27E-02	1.08E-02	0.00E+00	5.76E-09	5.76E-09	7.06E-10	1.27E-04	1.80E+05	663	9.92E-09	4.65E-23
1	34.97	2.50E+08	2.50E-07	5.00E-04	0.35%	39.388	0.36	4.4176	4.83E-04	5.36E-05	10.01%	2.37E-06	1.87E-09	-3.65E-01	0.39	-4.67E-02	5.75E-03	0.00E+00	4.03E-09	4.03E-09	6.51E-10	1.50E-04	2.31E+05	663	9.94E-09	3.62E-24
1	34.97	2.50E+08	2.50E-07	1.00E-03	0.35%	37.237	0.27	2.267	5.08E-04	2.85E-05	5.32%	2.50E-06	1.54E-09	-2.78E-01	1.44	-2.61E-02	4.56E-03	0.00E+00	2.28E-09	2.28E-09	6.18E-10	1.60E-04	2.59E+05	663	9.94E-09	3.62E-24
1	34.97	5.70E+08	4.75E-07	1.00E-07	1.27%	66.889	2.34	31.919	2.54E-04	2.82E-04	52.67%	1.27E-06	2.35E-09	-3.33E+00	22.67	-1.11E-02	3.09E-02	4.93E-14	2.23E-11	2.24E-11	1.21E-09	1.58E-07	1.30E+02	500	7.52E-08	2.64E-22
1	34.97	5.70E+08	4.75E-07	1.00E-06	1.27%	66.178	0.98	31.208	2.61E-04	2.75E-04	51.35%	1.29E-06	9.55E-09	2.11E+00	33.13	-1.23E-02	2.98E-02	1.58E-14	2.12E-10	2.12E-10	1.18E-09	1.54E-06	1.30E+03	500	6.16E-08	2.06E-22
1	34.97	5.70E+08	4.75E-07	1.00E-05	1.27%	63.129	1.24	28.159	2.92E-04	2.44E-04	45.56%	1.44E-06	9.49E-09	3.29E+01	45.31	-1.85E-02	3.29E-02	2.59E-16	1.67E-09	1.67E-09	1.07E-09	1.37E-05	1.27E+04	500	4.82E-08	1.16E-22
1	34.97	5.70E+08	4.75E-07	2.00E-05	1.27%	60.809	1.29	25.839	3.13E-04	2.23E-04	41.56%	1.44E-06	7.57E-09	6.69E+01	64.90	-2.46E-02	3.56E-02	1.13E-16	2.78E-09	2.78E-09	1.01E-09	2.49E-05	2.48E+04	500	6.39E-08	1.74E-22
1	34.97	5.70E+08	4.75E-07	3.00E-05	1.27%	58.597	1.95	23.627	3.29E-04	2.07E-04	38.59%	1.62E-06	5.98E-09	6.09E+01	25.14	-4.04E-02	3.96E-02	2.93E-17	3.59E-09	3.59E-09	9.60E-10	3.47E-05	3.62E+04	500	4.16E-08	4.95E-23
1	34.97	5.70E+08	4.75E-07	4.00E-05	1.27%	57.679	1.58	22.709	3.42E-04	1.94E-04	36.22%	1.68E-06	6.61E-09	8.19E+01	59.54	-3.00E-02	3.87E-02	8.57E-17	4.22E-09	4.22E-09	9.24E-10	4.35E-05	4.70E+04	500	7.48E-08	2.24E-22
1	34.97	5.70E+08	4.75E-07	5.00E-05	1.27%	56.475	1.61	21.505	3.53E-04	1.84E-04	34.23%	1.73E-06	6.09E-09	8.70E+01	55.30	-3.17E-02	3.86E-02	5.95E-17	4.71E-09	4.71E-09	8.96E-10	5.13E-05	5.73E+04	500	7.57E-08	2.36E-22
1	34.97	5.70E+08	4.75E-07	6.00E-05	1.27%	55.414	1.62	20.444	3.62E-04	1.74E-04	32.50%	1.78E-06	5.59E-09	9.08E+01	50.71	-3.31E-02	3.82E-02	3.43E-17	5.10E-09	5.10E-09	8.72E-10	5.85E-05	6.71E+04	500	7.61E-08	2.35E-22
1	34.97	5.70E+08	4.75E-07	7.00E-05	1.27%	54.482	1.61	19.512	3.70E-04	1.66E-04	30.97%	1.82E-06	5.18E-09	9.41E+01	47.21	-3.40E-02	3.75E-02	1.70E-17	5.40E-09	5.40E-09	8.53E-10	6.51E-05	7.63E+04	500	7.72E-08	2.43E-22
1	34.97	5.70E+08	4.75E-07	8.00E-05	1.27%	53.636	1.60	18.666	3.77E-04	1.59E-04	29.61%	1.85E-06	4.83E-09	9.67E+01	43.45	-3.47E-02	3.67E-02	7.88E-18	5.64E-09	5.64E-09	8.36E-10	7.11E-05	8.50E+04	500	7.72E-08	2.50E-22
1	34.97	5.70E+08	4.75E-07	9.00E-05	1.27%	52.861	1.59	17.891	3.84E-04	1.52E-04	28.37%	1.89E-06	4.55E-09	9.84E+01	39.58	-3.54E-02	3.59E-02	3.26E-18	5.83E-09	5.83E-09	8.21E-10	7.66E-05	9.33E+04	500	7.72E-08	2.55E-22
1	34.97	5.70E+08	4.75E-07	1.00E-04	1.27%	52.141	1.58	17.171	3.90E-04	1.46E-04	27.24%	1.92E-06	4.31E-09	9.94E+01	35.71	-3.60E-02	3.50E-02	1.03E-18	5.97E-09	5.97E-09	8.08E-10	8.17E-05	1.01E+05	500	7.57E-08	2.57E-22
1	34.97	5.70E+08	4.75E-07	2.50E-04	1.27%	45.369	1.25	10.399	4.45E-04	9.07E-05	16.92%	2.19E-06	2.76E-09	9.29E+01	16.58	-3.66E-02	2.23E-02	0.00E+00	5.76E-09	5.76E-09	7.07E-10	1.27E-04	1.80E+05	500	5.99E-08	3.31E-22
1	34.97	5.70E+08	4.75E-07	5.00E-04	1.27%	40.579	0.65	5.609	4.83E-04	5.36E-05	10.00%	2.37E-06	1.89E-09	7.54E+01	29.86	-3.20E-02	1.02E-02	0.00E+00	4.02E-09	4.02E-09	6.51E-10	1.50E-04	2.30E+05	500	5.23E-08	7.13E-22
1	34.97	5.70E+08	4.75E-07	1.00E-03	1.27%	38.032	0.40	3.062	5.08E-04	2.85E-05	5.32%	2.50E-06	1.19E-09	7.75E+01	31.15	-1.69E-02	6.15E-03	0.00E+00	2.28E-09	2.28E-09	6.19E-10	1.60E-04	2.58E+05	250	4.62E-08	1.30E-21
1	34.97	5.70E+08	4.00E-07	1.00E-07	0.90%	66.886	2.19	31.916	2.54E-04	2.83E-04	52.70%	1.27E-06	2.47E-09	-3.62E-01	4.45	-1.11E-02	3.15E-02	7.26E-14	2.23E-11	2.24E-11	1.21E-09	1.58E-07	1.30E+02	500	3.35E-08	3.03E-23
1	34.97	5.70E+08	4.00E-07	1.00E-06	0.90%	66.107	1.30	31.137	2.61E-04	2.75E-04	51.34%	1.29E-06	9.91E-09	2.57E+00	35.51	-1.44E-02	3.17E-02	1.96E-14	2.12E-10	2.12E-10	1.18E-09	1.54E-06	1.30E+03	500	3.99E-08	8.01E-23
1	34.97	5.70E+08	4.00E-07	1.00E-05	0.90%	63.005	1.53	28.035	2.92E-04	2.44E-04	45.56%	1.44E-06	9.49E-09	3.33E+01	38.24	-2.19E-02	3.49E-02	2.45E-16	1.67E-09	1.67E-09	1.07E-09	1.37E-05	1.27E+04	500	3.64E-08	1.35E-22
1	34.97	5.70E+08	4.00E-07	2.00E-05	0.90%	60.631	1.53	25.661	3.13E-04	2.23E-04	41.55%	1.54E-06	7.32E-09	6.25E+01	47.09	-2.91E-02	3.70E-02	9.83E-17	2.78E-09	2.78E-09	1.01E-09	2.49E-05	2.48E+04	500	4.69E-08	1.95E-22
1	34.97	5.70E+08	4.00E-07	3.00E-05	0.90%	58.806	1.56	23.836	3.29E-04	2.07E-04	38.60%	1.62E-06	6.06E-09	7.87E+01	42.32	-3.47E-02	3.76E-02	3.07E-17	3.60E-09	3.60E-09	9.58E-10	3.47E-05	3.63E+04	500	5.07E-08	2.27E-22
1	34.97	5.70E+08	4.00E-07	4.00E-05	0.90%	57.432	1.74	22.462	3.42E-04	1.94E-04	36.22%	1.68E-06	6.00E-09	7.49E+01	40.10	-3.60E-02	3.91E-02	5.34E-17	4.22E-09	4.22E-09	9.24E-10	4.35E-05	4.70E+04	500	5.77E-08	2.30E-22
1	34.97	5.70E+08	4.00E-07	5.00E-05	0.90%	56.194	1.75	21.224	3.53E-04	1.83E-04	34.22%	1.73E-06	5.46E-09	7.87E+01	34.42	-3.84E-02	3.87E-02	2.58E-17	4.71E-09	4.71E-09	8.96E-10	5.13E-05	5.73E+04	500	5.70E-08	2.34E-22
1	34.97	5.70E+08	4.00E-07	6.00E-05	0.90%	55.126	1.73	20.156	3.62E-04	1.74E-04	32.50%	1.78E-06	5.00E-09	8.20E+01	29.99	-3.98E-02	3.79E-02	8.06E-18	5.10E-09	5.10E-09	8.73E-10	5.85E-05	6.70E+04	500	5.80E-08	2.49E-22
1	34.97	5.70E+08	4.00E-07	7.00E-05	0.90%	54.163	1.72	19.193	3.70E-04	1.66E-04	30.97%	1.82E-06	4.63E-09	8.41E+01	25.34	-4.12E-02	3.70E-02	1.29E-18	5.40E-09	5.40E-09	8.53E-10	6.51E-05	7.62E+04	500	5.74E-08	2.58E-22
1	34.97	5.70E+08	4.00E-07	8.00E-05	0.90%	53.290	1.70	18.320	3.77E-04	1.59E-04	29.61%	1.85E-06	4.34E-09	8.53E+01	21.65	-4.23E-02	3.60E-02	0.00E+00	5.64E-09	5.64E-09	8.36E-10	7.11E-05	8.50E+04	500	5.70E-08	2.68E-22
1	34.97	5.70E+08	4.00E-07	9.00E-05	0.90%	52.493	1.67	17.523	3.84E-04	1.52E-04	28.37%	1.89E-06	4.11E-09	8.60E+01	18.75	-4.32E-02	3.49E-02	0.00E+00	5.83E-09	5.83E-09	8.22E-10	7.66E-05	9.32E+04	500	5.64E-08	2.77E-22
1	34.97	5.70E+08	4.00E-07	1.00E-04	0.90%	51.766	1.64	16.796	3.90E-04	1.46E-04	27.24%	1.92E-06	3.92E-09	8.67E+01	16.81	-4.37E-02	3.38E-02	0.00E+00	5.97E-09	5.97E-09	8.09E-10	8.17E-05	1.01E+05	500	5.68E-08	2.93E-22
1	34.97	5.70E+08	4.00E-07	2.50E-04	0.90%	44.848	1.12	9.878	4.45E-04	9.07E-05	16.92%	2.19E-06	2.73E-09	7.87E+01	21.35	-4.47E-02	1.90E-02	0.00E+00	5.76E-09	5.76E-09	7.07E-10	1.27E-04	1.80E+05	500	5.34E-08	5.75E-22
1	34.97	5.70E+08	4.00E-07	5.00E-04	0.90%	39.962	0.41	4.992	4.83E-04	5.36E-05	10.00%	2.37E-06	2.04E-09	6.90E+01	34.69	-3.97E-02	6.74E-03	0.00E+00	4.02E-09	4.02E-09	6.52E-10	1.50E-04	2.30E+05	500	5.02E-08	3.14E-21
1	34.97	5.70E+08	4.00E-07	1.00E-03	0.90%	37.257	0.19	2.287	5.08E-04	2.85E-05	5.32%	2.50E-06	1.15E-09	-5.51E-01	5.45	-2.59E-02	3.64E-03	0.00E+00	2.28E-09	2.28E-09	6.19E-10	1.60E-04	2.58E+05	364	1.00E-08	4.59E-24
	Activity																									
0.1	34.97	2.50E+08	2.97E-07	1.00E-05	0.50%	52.572	1.48	17.602	3.90E-04	1.46E-04	27.24%	1.92E-06	5.42E-09	1.11E+01	7.61	-2.68E-02	3.59E-02	3.20E-18	5.97E-10	5.97E-10	8.08E-10	8.17E-06	1.01E+04	500	1.39E-08	3.67E-22
0.3	34.97	2.50E+08	2.97E-07	1.00E-05	0.50%	58.132	1.69	23.162	3.34E-04	2.02E-04	37.75%	1.64E-06	5.39E-09	2.33E+01	8.56	-4.00E-02	3.76E-02	3.04E-18	1.15E-09	1.15E-09	9.46E-10	1.13E-05	1.20E+04	500	1.31E-08	2.72E-22
0.5	34.97	2.50E+08	2.97E-07	1.00E-05	0.50%	60.130	2.27	25.160	3.13E-04	2.23E-04	41.55%	1.54E-06	5.91E-09	2.46E+01	7.33	-4.30E-02	3.94E-02	2.39E-17	1.39E-09	1.39E-09	1.01E-09	1.25E-05	1.24E+04	500	1.23E-08	2.40E-22
0.7	34.97	2.50E+08	2.97E-07	1.00E-05	0.50%	61.227	2.87	26.257	3.02E-04	2.34E-04	43.65%	1.49E-06	6.10E-09	2.49E+01	6.91	-4.47E-02	4.12E-02	7.33E-17	1.53E-09	1.53E-09	1.04E-09	1.31E-05	1.26E+04	500	1.17E-08	2.29E-22
0.9	34.97	2.50E+08	2.97E-07	1.00E-05	0.50%	61.922	3.47	26.952	2.95E-04	2.41E-04	45.02%	1.45E-06	6.11E-09	2.46E+01	6.43	-4.64E-02	4.32E-02	1.34E-16	1.63E-09	1.63E-09	1.06E-09	1.35E-05	1.27E+04	500	1.12E-08	2.26E-22
0.1	34.97	2.50E+08	2.50E-07	1.00E-05	0.35%	52.293	1.60	17.323	3.90E-04	1.46E-04	27.24%	1.92E-06	4.81E-09	1.01E+01	4.37	-3.28E-02	3.57E-02	8.80E-19	5.97E-10	5.97E-10	8.09E-10	8.17E-06	1.01E+04	500	8.27E-09	2.62E-22
0.3	34.97	2.50E+08	2.50E-07	1.00E-05	0.35%	57.802	1.97	22.832	3.34E-04	2.02E-04	37.75%	1.64E-06	4.71E-09	2.00E+01	3.84	-4.85E-02	3.76E-02	0.00E+00	1.15E-09	1.15E-09	9.46E-10	1.13E-05	1.20E+04	500	9.82E-09	3.13E-22
0.5	34.97	2.50E+08	2.50E-07	1.00E-05	0.35%	59.830	2.77	24.860	3.13E-04	2.23E-04	41.54%	1.54E-06	4.80E-09	2.11E+01	3.61	-5.17E-02	4.05E-02	3.83E-18	1.39E-09	1.39E-09	1.01E-09	1.25E-05	1.24E+04	500	9.52E-09	2.92E-22
0.7	34.97	2.50E+08	2.50E-07	1.00E-05	0.35%	60.952	3.55	25.982	3.02E-04	2.34E-04	43.65%	1.49E-06	4.71E-09	2.14E+01	3.99	-5.33E-02	4.38E-02	1.45E-17	1.53E-09	1.53E-09	1.04E-09	1.31E-05	1.26E+04	500	9.32E-09	3.01E-22
0.9	34.97	2.50E+08	2.50E-07	1.00E-05	0.35%	61.666	4.26	26.696	2.95E-04	2.41E-04	45.02%	1.45E-06	4.55E-09	2.15E+01	4.53	-5.49E-02	4.69E-02	4.23E-17	1.63E-09	1.63E-09	1.06E-09	1.35E-05	1.27E+04	500	9.15E-09	3.22E-22
0.1	34.97	5.70E+08	4.75E-07	1.00E-05	1.27%	53.329	0.39	18.359	3.90E-04	1.46E-04	27.23%	1.92E-06	2.34E-09	1.35E+01	30.98	-1.28E-02	2.84E-02	5.38E-19	5.97E-10	5.97E-10	8.05E-10	8.17E-06	1.01E+04	500	5.79E-08	5.21E-22
0.3	34.97	5.70E+08	4.75E-07	1.00E-05	1.27%	59.102	0.69	24.132	3.34E-04	2.03E-04	37.77%	1.64E-06	6.64E-09	2.84E+01	47.37	-1.68E-02	3.24E-02	3.28E-17	1.15E-09	1.15E-09	9.43E-10	1.13E-05	1.20E+04	500	5.66E-08	2.23E-22
0.5	34.97	5.70E+08	4.75E-07	1.00E-05	1.27%	61.108	0.78	26.138	3.13E-04	2.23E-04	#####	1.54E-06	7.22E-09	3.20E+01	49.44	-1.75E-02	3.26E-02	7.07E-17	1.39E-09	1.39E-09	1.00E-09	1.25E-05	1.24E+04	500	6.02E-08	1.71E-22
0.7	34.97	5.70E+08	4.75E-07	1.00E-05	1.27%	62.128	0.99	27.158	3.02E-04	2.34E-04	#####	1.49E-06	8.15E-09	3.51E+01	43.42	-1.91E-02	3.38E-02	1.14E-16	1.53E-09	1.53E-09	1.04E-09	1.31E-05	1.26E+04	500	4.77E-08	1.29E-22
0.9	34.97	5.70E+08	4.75E-07	1.00E-05	1.27%	62.866	1.16	27.896	2.95E-04	2.41E-04	#####	1.45E-06	9.18E-09	3.37E+01	46.38	-1.84E-02	3.27E-02	2.11E-16	1.63E-09	1.63E-09	1.07E-09	1.35E-05	1.27E+04	500	4.95E-08	1.18E-22
0.1	34.97	5.70E+08	4.00E-07	1.00E-05	0.90%	53.237	0.60	18.267	3.90E-04	1.46E-04	27.23%	1.92E-06	2.75E-09	1.79E+01	33.81	-1.48E-02	3.03E-02	1.92E-19	5.97E-10	5.97E-10	8.06E-10	8.17E-06	1.01E+04	500	4.27E-08	5.12E-22
0.3	34.97	5.70E+08	4.00E-07	1.00E-05	0.90%	58.999	0.85	24.029	3.34E-04	2.02E-04	37.77%	1.64E-06	6.37E-09	3.00E+01	41.42	-1.91E-02	3.38E-02	2.68E-17	1.15E-09	1.15E-09	9.43E-10	1.13E-05	1.20E+04	500	4.59E-08	2.01E-22
0.5	34.97	5.70E+08	4.00E-07	1.00E-05	0.90%	60.968	1.05	25.998	3.13E-04	2.23E-04	41.56%	1.54E-06	7.64E-09	3.43E+01	41.98	-2.07E-02	3.41E-02	6.51E-17	1.39E-09	1.39E-09	1.00E-09	1.25E-05	1.24E+04	500	4.31E-08	1.57E-22
0.7	34.97	5.70E+08	4.00E-07	1.00E-05	0.90%	62.058	1.22	27.088	3.02E-04	2.34E-04	43.66%	1.49E-06	8.46E-09	3.49E+01	41.08	-2.11E-02	3.43E-02	1.22E-16	1.53E-09	1.53E-09	1.04E-09	1.31E-05	1.26E+04	500	4.08E-08	1.51E-22
0.9	34.97	5.70E+08	4.00E-07	1.00E-05	0.90%	62.747	1.42	27.777	2.95E-04	2.41E-04	45.03%	1.45E-06	9.18E-09	3.39E+01	39.39	-2.16E-02	3.47E-02	1.99E-16	1.63E-09	1.63E-09	1.07E-09	1.35E-05	1.27E+04	500	3.78E-08	1.41E-22

Fascicle

act	alpha	E_col	colrad	k_ex	L_init	col_pr	alpha_s	std_al	delta al	L_end	Delta L	delta L (	l_sarc	std_l_sarc	labda_cer	labda_out	std_labda	std_labda	e_col	std_ecol	W_col	W_ex	W_tot	A_end	f_end	sigma	numi	ferr	verr
Input	Model Parameters						Output Parameters																				Convergence		
1,1,1,1,1,1,1	54.44	2.00E+08	2.50E-07	1.00E-05	5.36E-04	0.50%	71.191	2.80	16.751	3.28E-04	2.08E-04	38.78%	1.62E-06	1.21E-07	-2.49E+04	-3.43E+04	3.93E+03	2.78E+02	6.85E-02	4.82E-02	7.37E-09	8.46E-09	1.58E-08	6.34E-09	8.14E-05	1.28E+04	212	2.63E-11	9.37E-29
1,1,1,1,1,1,1	54.44	2.50E+08	2.50E-07	1.00E-05	5.36E-04	0.50%	70.814	2.62	16.374	3.33E-04	2.03E-04	37.90%	1.65E-06	1.18E-07	-2.91E+04	-4.08E+04	4.77E+03	2.87E+02	6.53E-02	4.58E-02	8.35E-09	8.08E-09	1.64E-08	6.28E-09	7.95E-05	1.27E+04	158	2.44E-11	1.04E-28
1,1,1,1,1,1,1	54.44	4.00E+08	2.50E-07	1.00E-05	5.36E-04	0.50%	69.932	2.22	15.492	3.44E-04	1.92E-04	35.85%	1.70E-06	1.11E-07	-3.93E+04	-5.77E+04	7.12E+03	3.07E+02	5.83E-02	4.03E-02	1.05E-08	7.23E-09	1.78E-08	6.14E-09	7.52E-05	1.23E+04	136	2.63E-11	9.64E-29
1,1,1,1,1,1,1	54.44	5.70E+08	2.50E-07	1.00E-05	5.36E-04	0.50%	69.199	1.91	14.759	3.53E-04	1.83E-04	34.15%	1.74E-06	1.05E-07	-4.84E+04	-7.39E+04	9.59E+03	3.07E+02	5.29E-02	3.60E-02	1.22E-08	6.56E-09	1.88E-08	6.02E-09	7.17E-05	1.19E+04	118	2.41E-11	2.65E-28
1,1,1,1,1,1,1	54.44	8.60E+08	2.50E-07	1.00E-05	5.36E-04	0.50%	68.291	1.57	13.851	3.64E-04	1.72E-04	32.06%	1.80E-06	9.96E-08	-6.04E+04	-9.69E+04	1.35E+04	3.19E+02	4.66E-02	3.10E-02	1.41E-08	5.78E-09	1.99E-08	5.88E-09	6.73E-05	1.14E+04	152	2.71E-11	1.00E-28
1,1,1,1,1,1,1	54.44	2.00E+08	4.00E-07	1.00E-05	5.36E-04	1.27%	69.426	2.00	14.986	3.50E-04	1.86E-04	34.68%	1.73E-06	1.07E-07	-4.55E+04	-6.87E+04	8.77E+03	3.07E+02	5.45E-02	3.73E-02	1.17E-08	6.76E-09	1.85E-08	6.06E-09	7.28E-05	1.20E+04	122	2.70E-11	1.05E-28
1,1,1,1,1,1,1	54.44	2.50E+08	4.00E-07	1.00E-05	5.36E-04	1.27%	68.948	1.81	14.508	3.56E-04	1.80E-04	33.57%	1.76E-06	1.04E-07	-5.16E+04	-7.99E+04	1.06E+04	3.07E+02	5.11E-02	3.46E-02	1.28E-08	6.34E-09	1.91E-08	5.98E-09	7.05E-05	1.18E+04	124	2.59E-11	1.63E-28
1,1,1,1,1,1,1	54.44	4.00E+08	4.00E-07	1.00E-05	5.36E-04	1.27%	67.893	1.43	13.453	3.69E-04	1.67E-04	31.15%	1.82E-06	9.72E-08	-6.58E+04	-1.08E+05	1.55E+04	3.31E+02	4.40E-02	2.90E-02	1.48E-08	5.46E-09	2.03E-08	5.82E-09	6.54E-05	1.12E+04	170	2.49E-11	1.12E-28
1,1,1,1,1,1,1	54.44	5.70E+08	4.00E-07	1.00E-05	5.36E-04	1.27%	67.070	1.18	12.630	3.79E-04	1.57E-04	29.26%	1.87E-06	9.27E-08	-7.78E+04	-1.34E+05	2.05E+04	4.51E+02	3.87E-02	2.51E-02	1.62E-08	4.81E-09	2.10E-08	5.69E-09	6.14E-05	1.08E+04	208	2.60E-11	1.15E-28
1,1,1,1,1,1,1	54.44	8.60E+08	4.00E-07	1.00E-05	5.36E-04	1.27%	66.104	0.94	11.664	3.91E-04	1.45E-04	27.05%	1.93E-06	8.81E-08	-9.31E+04	-1.70E+05	2.77E+04	6.88E+02	3.29E-02	2.11E-02	1.74E-08	4.11E-09	2.16E-08	5.54E-09	5.68E-05	1.02E+04	217	2.62E-11	1.40E-28
0.9,0.9,0.9,0.9,0.9,0.9,0.9	54.44	5.70E+08	4.00E-07	1.00E-05	5.36E-04	1.27%	66.789	1.10	12.349	3.83E-04	1.53E-04	28.61%	1.89E-06	9.11E-08	-7.29E+04	-1.28E+05	1.99E+04	4.49E+02	3.70E-02	2.39E-02	1.47E-08	4.60E-09	1.93E-08	5.65E-09	6.00E-05	1.06E+04	214	2.61E-11	9.19E-29
0.7,0.7,0.7,0.7,0.7,0.7,0.7	54.44	5.70E+08	4.00E-07	1.00E-05	5.36E-04	1.27%	66.119	0.94	11.679	3.91E-04	1.45E-04	27.07%	1.93E-06	8.75E-08	-6.20E+04	-1.13E+05	1.84E+04	4.51E+02	3.30E-02	2.11E-02	1.16E-08	4.12E-09	1.57E-08	5.55E-09	5.68E-05	1.02E+04	222	2.72E-11	1.18E-28
0.5,0.5,0.5,0.5,0.5,0.5,0.5	54.44	5.70E+08	4.00E-07	1.00E-05	5.36E-04	1.27%	65.226	0.74	10.786	4.02E-04	1.34E-04	25.02%	1.98E-06	8.31E-08	-4.95E+04	-9.49E+04	1.63E+04	4.56E+02	2.80E-02	1.78E-02	8.30E-09	3.52E-09	1.18E-08	5.41E-09	5.25E-05	9.70E+03	251	9.77E-11	1.43E-28
0.3,0.3,0.3,0.3,0.3,0.3,0.3	54.44	5.70E+08	4.00E-07	1.00E-05	5.36E-04	1.27%	63.894	0.51	9.454	4.18E-04	1.18E-04	21.97%	2.06E-06	7.68E-08	-3.43E+04	-7.10E+04	1.31E+04	4.33E+02	2.13E-02	1.34E-02	4.75E-09	2.71E-09	7.46E-09	5.22E-09	4.61E-05	8.83E+03	251	6.68E-10	1.33E-28
0.1,0.1,0.1,0.1,0.1,0.1,0.1	54.44	5.70E+08	4.00E-07	1.00E-05	5.36E-04	1.27%	61.189	0.21	6.749	4.52E-04	8.45E-05	15.77%	2.23E-06	6.31E-08	-1.41E+04	-3.37E+04	7.00E+03	2.71E+02	1.05E-02	6.69E-03	1.13E-09	1.40E-09	2.53E-09	4.86E-09	3.31E-05	6.81E+03	251	4.99E-08	8.92E-27
1,0.9,0.9,0.9,0.9,0.9,0.9	54.44	5.70E+08	4.00E-07	1.00E-05	5.36E-04	1.27%	66.831	1.12	12.391	3.82E-04	1.54E-04	28.70%	1.89E-06	9.12E-08	-7.36E+04	-1.29E+05	2.00E+04	4.42E+02	3.72E-02	2.41E-02	1.49E-08	4.63E-09	1.96E-08	5.66E-09	6.02E-05	1.07E+04	212	2.60E-11	1.17E-28
1,0.7,0.7,0.7,0.7,0.7,0.7	54.44	5.70E+08	4.00E-07	1.00E-05	5.36E-04	1.27%	66.278	0.97	11.838	3.89E-04	1.47E-04	27.42%	1.92E-06	8.78E-08	-6.45E+04	-1.16E+05	1.87E+04	4.19E+02	3.39E-02	2.18E-02	1.23E-08	4.23E-09	1.65E-08	5.57E-09	5.76E-05	1.03E+04	220	2.66E-11	1.17E-28
1,0.5,0.5,0.5,0.5,0.5,0.5	54.44	5.70E+08	4.00E-07	1.00E-05	5.36E-04	1.27%	65.581	0.82	11.141	3.98E-04	1.38E-04	25.79%	1.96E-06	8.39E-08	-5.42E+04	-1.02E+05	1.71E+04	3.85E+02	2.99E-02	1.91E-02	9.52E-09	3.75E-09	1.33E-08	5.47E-09	5.42E-05	9.91E+03	162	2.51E-11	6.12E-27
1,0.3,0.3,0.3,0.3,0.3,0.3	54.44	5.70E+08	4.00E-07	1.00E-05	5.36E-04	1.27%	64.642	0.63	10.202	4.10E-04	1.27E-04	23.60%	2.02E-06	7.98E-08	-4.24E+04	-8.39E+04	1.49E+04	3.29E+02	2.50E-02	1.59E-02	6.56E-09	3.15E-09	9.71E-09	5.33E-09	4.96E-05	9.32E+03	500	2.73E-11	1.11E-28
1,0.1,0.1,0.1,0.1,0.1,0.1	54.44	5.70E+08	4.00E-07	1.00E-05	5.36E-04	1.27%	63.208	0.41	8.768	4.28E-04	1.08E-04	20.18%	2.11E-06	8.09E-08	-2.80E+04	-6.00E+04	1.15E+04	2.33E+02	1.82E-02	1.18E-02	3.46E-09	2.32E-09	5.78E-09	5.13E-09	4.26E-05	8.31E+03	900	1.26E-08	1.48E-28
1,0,0,0,0,0,0	54.44	5.70E+08	4.00E-07	1.00E-05	5.36E-04	1.27%	62.060	0.28	7.620	4.44E-04	9.18E-05	17.12%	2.18E-06	1.26E-07	-1.92E+04	-4.40E+04	8.84E+03	1.82E+02	1.35E-02	1.03E-02	1.95E-09	1.70E-09	3.65E-09	4.97E-09	3.65E-05	7.34E+03	1100	2.43E-07	7.06E-24
1,1,1,1,1,1,1	54.44	5.70E+08	4.00E-07	1.00E-05	5.36E-04	1.27%	67.070	1.18	12.630	3.79E-04	1.57E-04	29.26%	1.87E-06	9.27E-08	-7.78E+04	-1.34E+05	2.05E+04	4.51E+02	3.87E-02	2.51E-02	1.62E-08	4.81E-09	2.10E-08	5.69E-09	6.14E-05	1.08E+04	208	2.60E-11	1.15E-28
1,1,1,1,1,1,1	54.44	5.70E+08	4.00E-07	2.00E-05	5.36E-04	1.27%	66.749	1.08	12.309	3.83E-04	1.53E-04	28.49%	1.89E-06	8.97E-08	-7.23E+04	-1.27E+05	1.97E+04	4.41E+02	3.67E-02	2.37E-02	1.45E-08	9.13E-09	2.36E-08	5.64E-09	1.20E-04	2.12E+04	194	2.71E-11	1.33E-28
1,1,1,1,1,1,1	54.44	5.70E+08	4.00E-07	3.00E-05	5.36E-04	1.27%	66.435	1.00	11.995	3.87E-04	1.49E-04	27.75%	1.91E-06	8.68E-08	-6.72E+04	-1.20E+05	1.90E+04	4.27E+02	3.48E-02	2.25E-02	1.30E-08	1.30E-08	2.60E-08	5.59E-09	1.75E-04	3.12E+04	174	2.50E-11	1.36E-28
1,1,1,1,1,1,1	54.44	5.70E+08	4.00E-07	4.00E-05	5.36E-04	1.27%	66.129	0.93	11.689	3.91E-04	1.45E-04	27.04%	1.93E-06	8.42E-08	-6.24E+04	-1.13E+05	1.83E+04	4.14E+02	3.30E-02	2.13E-02	1.17E-08	1.65E-08	2.81E-08	5.55E-09	2.27E-04	4.09E+04	166	2.45E-11	1.01E-28
1,1,1,1,1,1,1	54.44	5.70E+08	4.00E-07	5.00E-05	5.36E-04	1.27%	65.829	0.86	11.389	3.95E-04	1.41E-04	26.34%	1.95E-06	8.17E-08	-5.79E+04	-1.07E+05	1.76E+04	4.03E+02	3.13E-02	2.01E-02	1.05E-08	1.95E-08	3.00E-08	5.50E-09	2.76E-04	5.02E+04	158	2.58E-11	1.40E-28
1,1,1,1,1,1,1	54.44	5.70E+08	4.00E-07	6.00E-05	5.36E-04	1.27%	65.537	0.79	11.097	3.99E-04	1.38E-04	25.66%	1.97E-06	7.94E-08	-5.38E+04	-1.01E+05	1.69E+04	3.93E+02	2.97E-02	1.91E-02	9.37E-09	2.22E-08	3.16E-08	5.46E-09	3.23E-04	5.92E+04	152	2.56E-11	1.00E-28
1,1,1,1,1,1,1	54.44	5.70E+08	4.00E-07	7.00E-05	5.36E-04	1.27%	65.253	0.74	10.813	4.02E-04	1.34E-04	25.00%	1.98E-06	7.71E-08	-5.00E+04	-9.53E+04	1.62E+04	3.85E+02	2.81E-02	1.81E-02	8.40E-09	2.46E-08	3.30E-08	5.42E-09	3.67E-04	6.78E+04	146	2.67E-11	1.10E-28
1,1,1,1,1,1,1	54.44	5.70E+08	4.00E-07	8.00E-05	5.36E-04	1.27%	64.976	0.68	10.536	4.06E-04	1.31E-04	24.36%	2.00E-06	7.50E-08	-4.64E+04	-8.99E+04	1.56E+04	3.76E+02	2.66E-02	1.71E-02	7.53E-09	2.67E-08	3.43E-08	5.38E-09	4.09E-04	7.61E+04	142	2.51E-11	1.12E-28
1,1,1,1,1,1,1	54.44	5.70E+08	4.00E-07	9.00E-05	5.36E-04	1.27%	64.706	0.63	10.266	4.09E-04	1.27E-04	23.74%	2.02E-06	7.30E-08	-4.32E+04	-8.49E+04	1.49E+04	3.68E+02	2.52E-02	1.63E-02	6.75E-09	2.86E-08	3.53E-08	5.34E-09	4.49E-04	8.41E+04	136	2.56E-11	8.55E-29
1,1,1,1,1,1,1	54.44	5.70E+08	4.00E-07	1.00E-04	5.36E-04	1.27%	64.444	0.59	10.004	4.12E-04	1.24E-04	23.14%	2.03E-06	7.10E-08	-4.02E+04	-8.02E+04	1.43E+04	3.59E+02	2.39E-02	1.54E-02	6.06E-09	3.01E-08	3.62E-08	5.30E-09	4.86E-04	9.17E+04	130	2.67E-11	1.07E-28
1,1,1,1,1,1,1	54.44	5.70E+08	4.00E-07	2.50E-04	5.36E-04	1.27%	61.350	0.21	6.910	4.50E-04	8.61E-05	16.05%	2.22E-06	5.02E-08	-1.49E+04	-3.54E+04	7.31E+03	2.22E+02	1.11E-02	7.64E-03	1.29E-09	3.63E-08	3.76E-08	4.88E-09	8.43E-04	1.73E+05	127	2.36E-11	9.28E-29
1,1,1,1,1,1,1	54.44	5.70E+08	4.00E-07	5.00E-04	5.36E-04	1.27%	58.668	0.06	4.228	4.83E-04	5.29E-05	9.87%	2.38E-06	3.32E-08	-4.37E+03	-1.19E+04	2.67E+03	8.89E+01	3.85E-03	3.32E-03	1.63E-10	2.75E-08	2.76E-08	4.55E-09	1.04E-03	2.28E+05	172	2.49E-11	1.33E-28
1,1,1,1,1,1,1	54.44	5.70E+08	4.00E-07	1.00E-03	5.36E-04	1.27%	56.712	0.01	2.272	5.08E-04	2.85E-05	5.31%	2.50E-06	2.01E-08	-9.60E+02	-2.83E+03	6.67E+02	2.06E+01	9.25E-04	1.27E-03	1.12E-11	1.59E-08	1.59E-08	4.33E-09	1.12E-03	2.58E+05	219	2.57E-11	1.12E-28
1,1,1,1,1,1,1	54.44	2.50E+08	2.50E-07	1.00E-05	5.36E-04	0.50%	70.814	2.62	16.374	3.33E-04	2.03E-04	37.90%	1.65E-06	1.18E-07	-2.91E+04	-4.08E+04	4.77E+03	2.87E+02	6.53E-02	4.58E-02	8.35E-09	8.08E-09	1.64E-08	6.28E-09	7.95E-05	1.27E+04	158	2.44E-11	1.04E-28
1,1,1,1,1,1,1	54.44	2.50E+08	2.50E-07	2.00E-05	5.36E-04	0.50%	70.048	2.24	15.608	3.43E-04	1.93E-04	36.06%	1.69E-06	1.10E-07	-2.52E+04	-3.66E+04	4.49E+03	2.12E+02	5.92E-02	4.12E-02	6.81E-09	1.46E-08	2.14E-08	6.16E-09	1.51E-04	2.46E+04	144	2.46E-11	1.04E-28
1,1,1,1,1,1,1	54.44	2.50E+08	2.50E-07	3.00E-05	5.36E-04	0.50%	69.351	1.94	14.911	3.52E-04	1.84E-04	34.44%	1.74E-06	1.03E-07	-2.20E+04	-3.31E+04	4.24E+03	1.47E+02	5.39E-02	3.73E-02	5.62E-09	2.00E-08	2.56E-08	6.05E-09	2.17E-04	3.58E+04	138	2.48E-11	1.44E-28
1,1,1,1,1,1,1	54.44	2.50E+08	2.50E-07	4.00E-05	5.36E-04	0.005	68.712	1.69	14.272	3.60E-04	1.76E-04	32.91%	1.78E-06	9.76E-08	-1.93E+04	-3.00E+04	4.02E+03	1.03E+02	4.94E-02	3.39E-02	4.67E-09	2.44E-08	2.91E-08	5.94E-09	2.76E-04	4.65E+04	134	2.36E-11	1.29E-28
1,1,1,1,1,1,1	54.44	2.50E+08	2.50E-07	5.00E-05	5.36E-04	0.50%	68.123	1.47	13.683	3.67E-04	1.69E-04	31.54%	1.81E-06	9.26E-08	-1.70E+04	-2.73E+04	3.82E+03	7.26E+01	4.53E-02	3.09E-02	3.92E-09	2.80E-08	3.19E-08	5.85E-09	3.31E-04	5.66E+04	130	2.42E-11	1.29E-28
1,1,1,1,1,1,1	54.44	2.50E+08	2.50E-07	6.00E-05	5.36E-04	0.50%	67.578	1.30	13.138	3.74E-04	1.62E-04	30.28%	1.84E-06	8.81E-08	-1.50E+04	-2.49E+04	3.63E+03	5.08E+01	4.18E-02	2.84E-02	3.31E-09	3.10E-08	3.43E-08	5.77E-09	3.81E-04	6.61E+04	126	2.67E-11	1.07E-28
1,1,1,1,1,1,1	54.44	2.50E+08	2.50E-07	7.00E-05	5.36E-04	0.50%	67.071	1.14	12.631	3.80E-04	1.56E-04	29.11%	1.87E-06	8.40E-08	-1.34E+04	-2.29E+04	3.45E+03	3.75E+01	3.86E-02	2.61E-02	2.81E-09	3.34E-08	3.62E-08	5.69E-09	4.28E-04	7.52E+04	124	2.65E-11	1.32E-28
1,1,1,1,1,1,1	54.44	2.50E+08	2.50E-07	8.00E-05	5.36E-04	0.50%	66.598	1.02	12.158	3.86E-04	1.50E-04	28.02%	1.90E-06	8.04E-08	-1.20E+04	-2.10E+04	3.28E+03	3.30E+01	3.57E-02	2.42E-02	2.40E-09	3.54E-08	3.78E-08	5.62E-09	4.71E-04	8.38E+04	124	2.30E-11	1.26E-28
1,1,1,1,1,1,1	54.44	2.50E+08	2.50E-07	9.00E-05	5.36E-04	0.50%	66.156	0.91	11.716	3.91E-04	1.45E-04	27.01%	1.93E-06	7.70E-08	-1.08E+04	-1.94E+04	3.11E+03	3.24E+01	3.31E-02	2.25E-02	2.06E-09	3.70E-08	3.90E-08	5.55E-09	5.11E-04	9.20E+04	124	2.49E-11	1.19E-28
1,1,1,1,1,1,1	54.44	2.50E+08	2.50E-07	1.00E-04	5.36E-04	0.50%	65.742	0.82	11.302	3.96E-04	1.40E-04	26.07%	1.95E-06	7.39E-08	-9.69E+03	-1.79E+04	2.95E+03	3.48E+01	3.07E-02	2.10E-02	1.77E-09	3.83E-08	4.00E-08	5.49E-09	5.47E-04	9.97E+04	124	2.33E-11	1.21E-28
1,1,1,1,1,1,1	54.44	2.50E+08	2.50E-07	2.50E-04	5.36E-04	0.50%	61.627	0.23	7.187	4.47E-04	8.95E-05	16.70%	2.20E-06	4.67E-08	-2.81E+03	-6.58E+03	1.34E+03	4.94E+01	1.20E-02	9.52E-03	2.77E-10	3.93E-08	3.95E-08	4.91E-09	8.77E-04	1.78E+05	138	2.36E-11	1.19E-28
1,1,1,1,1,1,1	54.44	2.50E+08	2.50E-07	5.00E-04	5.36E-04	0.50%	58.696	0.06	4.256	4.83E-04	5.34E-05	9.96%	2.38E-06	2.95E-08	-7.54E+02	-2.05E+03	4.64E+02	3.37E+01	3.87E-03	4.38E-03	3.35E-11	2.80E-08	2.80E-08	4.55E-09	1.05E-03	2.30E+05	200	2.51E-11	1.26E-28
1,1,1,1,1,1,1	54.44	2.50E+08	2.50E-07	1.00E-03	5.36E-04	0.50%	56.706	0.01	2.266	5.08E-04	2.85E-05	5.32%	2.50E-06	1.78E-08	-1.62E+02	-4.80E+02	1.14E+02	1.31E+01	8.93E-04	1.86E-03	2.83E-12	1.59E-08	1.59E-08	4.33E-09	1.12E-03	2.58E+05	251	3.84E-10	1.21E-28

Stiffness

act	alpha_	E_col	colrad	k_ex	col_pro	L_end	Fex_tot	dlength	lstiff	Estiff	perc	sarclength	sarcstd
Input	Model Parameters						Stiffness Parameters						
	Collagen stiffness												
1	70.33	2.00E+08	3.04E-07	1.00E-05	1.27%	3.46E-04	3.27E-05	2.10E-05	1.56	8.74E+05	6.07%	1.81E-06	1.33E-03
1	70.33	2.50E+08	3.04E-07	1.00E-05	1.27%	3.54E-04	3.27E-05	1.99E-05	1.64	9.48E+05	5.62%	1.84E-06	1.05E-03
1	70.33	4.00E+08	3.04E-07	1.00E-05	1.27%	3.72E-04	3.27E-05	1.77E-05	1.85	1.13E+06	4.75%	1.92E-06	5.74E-04
1	70.33	5.70E+08	3.04E-07	1.00E-05	1.27%	3.87E-04	3.27E-05	1.61E-05	2.03	1.31E+06	4.16%	1.99E-06	3.58E-04
1	70.33	8.60E+08	3.04E-07	1.00E-05	1.27%	4.06E-04	3.27E-05	1.44E-05	2.27	1.54E+06	3.56%	2.07E-06	2.93E-04
1	70.33	2.00E+08	4.00E-07	1.00E-05	3.07%	3.66E-04	3.27E-05	1.83E-05	1.79	1.07E+06	5.01%	1.89E-06	7.01E-04
1	70.33	2.50E+08	4.00E-07	1.00E-05	3.07%	3.75E-04	3.27E-05	1.73E-05	1.89	1.17E+06	4.62%	1.93E-06	5.16E-04
1	70.33	4.00E+08	4.00E-07	1.00E-05	3.07%	3.95E-04	3.27E-05	1.53E-05	2.14	1.41E+06	3.87%	2.03E-06	3.05E-04
1	70.33	5.70E+08	4.00E-07	1.00E-05	3.07%	4.12E-04	3.27E-05	1.39E-05	2.36	1.64E+06	3.37%	2.10E-06	3.00E-04
1	70.33	8.60E+08	4.00E-07	1.00E-05	3.07%	4.32E-04	3.27E-05	1.23E-05	2.67	1.97E+06	2.84%	2.19E-06	3.26E-04
1	70.33	2.00E+08	1.90E-07	1.00E-05	0.50%	3.21E-04	3.27E-05	2.58E-05	1.27	6.51E+05	8.04%	1.70E-06	2.96E-03
1	70.33	2.50E+08	1.90E-07	1.00E-05	0.50%	3.26E-04	3.27E-05	2.47E-05	1.32	6.92E+05	7.58%	1.72E-06	2.51E-03
1	70.33	4.00E+08	1.90E-07	1.00E-05	0.50%	3.39E-04	3.27E-05	2.23E-05	1.47	8.02E+05	6.59%	1.77E-06	1.69E-03
1	70.33	5.70E+08	1.90E-07	1.00E-05	0.50%	3.50E-04	3.27E-05	2.05E-05	1.60	9.09E+05	5.85%	1.82E-06	1.19E-03
1	70.33	8.60E+08	1.90E-07	1.00E-05	0.50%	3.65E-04	3.27E-05	1.85E-05	1.77	1.06E+06	5.06%	1.89E-06	7.28E-04
1	70.33	2.00E+08	2.50E-07	1.00E-05	1.20%	3.34E-04	3.27E-05	2.31E-05	1.42	7.64E+05	6.90%	1.76E-06	1.92E-03
1	70.33	2.50E+08	2.50E-07	1.00E-05	1.20%	3.41E-04	3.27E-05	2.19E-05	1.49	8.24E+05	6.42%	1.78E-06	1.57E-03
1	70.33	4.00E+08	2.50E-07	1.00E-05	1.20%	3.57E-04	3.27E-05	1.95E-05	1.68	9.76E+05	5.47%	1.85E-06	9.56E-04
1	70.33	5.70E+08	2.50E-07	1.00E-05	1.20%	3.70E-04	3.27E-05	1.78E-05	1.84	1.12E+06	4.82%	1.91E-06	6.06E-04
1	70.33	8.60E+08	2.50E-07	1.00E-05	1.20%	3.88E-04	3.27E-05	1.60E-05	2.04	1.31E+06	4.14%	1.99E-06	3.51E-04
1	54.44	2.00E+08	4.00E-07	1.00E-05	1.27%	3.48E-04	3.27E-05	1.78E-05	1.84	7.67E+05	5.11%	1.80E-06	1.30E-04
1	54.44	2.50E+08	4.00E-07	1.00E-05	1.27%	3.55E-04	3.27E-05	1.66E-05	1.97	8.46E+05	4.68%	1.82E-06	1.06E-04
1	54.44	4.00E+08	4.00E-07	1.00E-05	1.27%	3.69E-04	3.27E-05	1.42E-05	2.30	1.05E+06	3.86%	1.88E-06	6.03E-05
1	54.44	5.70E+08	4.00E-07	1.00E-05	1.27%	3.80E-04	3.27E-05	1.26E-05	2.59	1.24E+06	3.33%	1.93E-06	3.37E-05
1	54.44	8.60E+08	4.00E-07	1.00E-05	1.27%	3.93E-04	3.27E-05	1.10E-05	2.97	1.51E+06	2.80%	1.99E-06	1.83E-05
1	54.44	2.00E+08	2.50E-07	1.00E-05	0.50%	3.25E-04	3.27E-05	2.31E-05	1.42	5.33E+05	7.12%	1.71E-06	1.90E-04
1	54.44	2.50E+08	2.50E-07	1.00E-05	0.50%	3.30E-04	3.27E-05	2.19E-05	1.50	5.75E+05	6.63%	1.73E-06	1.83E-04
1	54.44	4.00E+08	2.50E-07	1.00E-05	0.50%	3.41E-04	3.27E-05	1.92E-05	1.71	6.91E+05	5.62%	1.77E-06	1.54E-04
1	54.44	5.70E+08	2.50E-07	1.00E-05	0.50%	3.51E-04	3.27E-05	1.72E-05	1.90	8.04E+05	4.90%	1.81E-06	1.18E-04
1	54.44	8.60E+08	2.50E-07	1.00E-05	0.50%	3.63E-04	3.27E-05	1.51E-05	2.17	9.69E+05	4.15%	1.86E-06	7.63E-05
1	34.97	2.00E+08	4.75E-07	1.00E-05	1.27%	2.92E-04	3.27E-05	3.43E-05	0.96	2.60E+05	11.73%	1.60E+00	5.68E-03
1	34.97	2.50E+08	4.75E-07	1.00E-05	1.27%	2.92E-04	3.27E-05	3.43E-05	0.96	2.60E+05	11.74%	1.60E+00	6.16E-03
1	34.97	4.00E+08	4.75E-07	1.00E-05	1.27%	2.92E-04	3.27E-05	3.43E-05	0.96	2.59E+05	11.74%	1.60E+00	6.70E-03
1	34.97	5.70E+08	4.75E-07	1.00E-05	1.27%	2.92E-04	3.27E-05						
1	34.97	8.60E+08	4.75E-07	1.00E-05	1.27%	2.92E-04	3.27E-05	3.43E-05	0.95	2.59E+05	11.75%	1.60E+00	6.77E-03
1	34.97	2.00E+08	4.00E-07	1.00E-05	0.90%	2.92E-04	3.27E-05	3.42E-05	0.96	2.60E+05	11.72%	1.60E+00	2.99E-03
1	34.97	2.50E+08	4.00E-07	1.00E-05	0.90%	2.92E-04	3.27E-05						
1	34.97	4.00E+08	4.00E-07	1.00E-05	0.90%	2.92E-04	3.27E-05	3.42E-05	0.96	2.60E+05	11.72%	1.60E+00	5.65E-03
1	34.97	5.70E+08	4.00E-07	1.00E-05	0.90%	2.92E-04	3.27E-05	3.42E-05	0.96	2.60E+05	11.72%	1.60E+00	6.57E-03
1	34.97	8.60E+08	4.00E-07	1.00E-05	0.90%	2.92E-04	3.27E-05	3.42E-05	0.96	2.60E+05	11.72%	1.60E+00	7.06E-03
1	34.97	2.00E+08	2.97E-07	1.00E-05	0.50%	2.92E-04	3.27E-05	3.42E-05	0.96	2.60E+05	11.73%	1.60E+00	2.33E-03
1	34.97	2.50E+08	2.97E-07	1.00E-05	0.50%	2.92E-04	3.27E-05	3.42E-05	0.96	2.60E+05	11.73%	1.60E+00	2.96E-03
1	34.97	4.00E+08	2.97E-07	1.00E-05	0.50%	2.92E-04	3.27E-05	3.42E-05	0.96	2.60E+05	11.73%	1.60E+00	4.91E-03
1	34.97	5.70E+08	2.97E-07	1.00E-05	0.50%	2.92E-04	3.27E-05	3.43E-05	0.96	2.60E+05	11.73%	1.60E+00	5.94E-03
1	34.97	8.60E+08	2.97E-07	1.00E-05	0.50%	2.92E-04	3.27E-05	3.43E-05	0.96	2.59E+05	11.74%	1.60E+00	6.57E-03
1	34.97	2.00E+08	2.50E-07	1.00E-05	0.35%	2.92E-04	3.27E-05	3.42E-05	0.96	2.60E+05	11.73%	1.60E+00	1.12E-03
1	34.97	2.50E+08	2.50E-07	1.00E-05	0.35%	2.92E-04	3.27E-05						
1	34.97	4.00E+08	2.50E-07	1.00E-05	0.35%	2.92E-04	3.27E-05	3.42E-05	0.96	2.60E+05	11.72%	1.60E+00	1.86E-03
1	34.97	5.70E+08	2.50E-07	1.00E-05	0.35%	2.92E-04	3.27E-05	3.42E-05	0.96	2.60E+05	11.72%	1.60E+00	3.47E-03
1	34.97	8.60E+08	2.50E-07	1.00E-05	0.35%	2.92E-04	3.27E-05	3.42E-05	0.96	2.60E+05	11.72%	1.60E+00	5.12E-03
	External spring stiffness												
1	70.33	5.70E+08	3.04E-07	1.00E-05	1.27%	3.87E-04	5.46E-05	3.11E-05	1.75	1.13E+06	8.04%	2.06E-06	3.95E-04
1	70.33	5.70E+08	3.04E-07	2.00E-05	1.27%	3.92E-04	5.46E-05	2.60E-05	2.10	1.37E+06	6.64%	2.06E-06	3.95E-04
1	70.33	5.70E+08	3.04E-07	3.00E-05	1.27%	3.97E-04	5.46E-05	2.12E-05	2.57	1.70E+06	5.35%	2.06E-06	3.95E-04
1	70.33	5.70E+08	3.04E-07	4.00E-05	1.27%	4.01E-04	5.46E-05	1.67E-05	3.27	2.19E+06	4.16%	2.06E-06	3.95E-04
1	70.33	5.70E+08	3.04E-07	5.00E-05	1.27%	4.06E-04	5.46E-05	1.24E-05	4.41	2.99E+06	3.05%	2.06E-06	3.95E-04
1	70.33	2.50E+08	1.90E-07	1.00E-05	0.50%	3.26E-04	5.46E-05	4.83E-05	1.13	5.91E+05	14.8%	1.84E-06	2.51E-03
1	70.33	2.50E+08	1.90E-07	2.00E-05	0.50%	3.39E-04	5.46E-05	3.58E-05	1.53	8.33E+05	10.6%	1.84E-06	2.51E-03

1	70.33	2.50E+08	1.90E-07	3.00E-05	0.50%	3.49E-04	5.46E-05	2.51E-05	2.17	1.23E+06	7.19%	1.84E-06	2.51E-03
1	70.33	2.50E+08	1.90E-07	4.00E-05	0.50%	3.59E-04	5.46E-05	1.58E-05	3.44	2.01E+06	4.42%	1.84E-06	2.51E-03
1	70.33	2.50E+08	1.90E-07	5.00E-05	0.50%	3.67E-04	5.46E-05	7.60E-06	7.17	4.29E+06	2.1%	1.84E-06	2.51E-03
1	70.33	2.50E+08	2.50E-07	1.00E-05	1.20%	3.41E-04	5.46E-05	4.29E-05	1.27	7.01E+05	12.59%	1.89E-06	1.61E-03
1	70.33	2.50E+08	2.50E-07	2.00E-05	1.20%	3.51E-04	5.46E-05	3.29E-05	1.66	9.44E+05	9.38%	1.89E-06	1.61E-03
1	70.33	2.50E+08	2.50E-07	3.00E-05	1.20%	3.60E-04	5.46E-05	2.41E-05	2.27	1.33E+06	6.69%	1.89E-06	1.61E-03
1	70.33	2.50E+08	2.50E-07	4.00E-05	1.20%	3.68E-04	5.46E-05	1.62E-05	3.38	2.03E+06	4.39%	1.89E-06	1.61E-03
1	70.33	2.50E+08	2.50E-07	5.00E-05	1.20%	3.75E-04	5.46E-05	9.00E-06	6.06	3.72E+06	2.40%	1.89E-06	1.61E-03
1	70.33	5.70E+08	4.00E-07	1.00E-05	3.07%	4.12E-04	5.46E-05	2.64E-05	2.07	1.44E+06	6.41%	2.16E-06	2.94E-04
1	70.33	5.70E+08	4.00E-07	2.00E-05	3.07%	4.15E-04	5.46E-05	2.29E-05	2.38	1.67E+06	5.52%	2.16E-06	2.94E-04
1	70.33	5.70E+08	4.00E-07	3.00E-05	3.07%	4.19E-04	5.46E-05	1.96E-05	2.78	1.97E+06	4.68%	2.16E-06	2.94E-04
1	70.33	5.70E+08	4.00E-07	4.00E-05	3.07%		5.46E-05						
1	70.33	5.70E+08	4.00E-07	5.00E-05	3.07%		5.46E-05						
1	54.44	5.70E+08	4.00E-07	1.00E-05	1.27%	3.80E-04	5.46E-05	2.49E-05	2.19	1.05E+06	6.56%	1.99E-06	2.90E-05
1	54.44	5.70E+08	4.00E-07	2.00E-05	1.27%	3.84E-04	5.46E-05	2.06E-05	2.65	1.30E+06	5.37%	1.99E-06	2.90E-05
1	54.44	5.70E+08	4.00E-07	3.00E-05	1.27%	3.88E-04	5.46E-05	1.65E-05	3.31	1.65E+06	4.25%	1.99E-06	2.90E-05
1	54.44	5.70E+08	4.00E-07	4.00E-05	1.27%	3.92E-04	5.46E-05	1.25E-05	4.36	2.21E+06	3.19%	1.99E-06	2.90E-05
1	54.44	5.70E+08	4.00E-07	5.00E-05	1.27%	3.96E-04	5.46E-05	8.70E-06	6.27	3.23E+06	2.20%	1.99E-06	2.90E-05
1	54.44	2.50E+08	2.50E-07	1.00E-05	0.50%	3.30E-04	5.46E-05	4.33E-05	1.26	4.85E+05	13.12%	1.83E-06	1.71E-04
1	54.44	2.50E+08	2.50E-07	2.00E-05	0.50%	3.41E-04	5.46E-05	3.24E-05	1.68	6.79E+05	9.52%	1.83E-06	1.71E-04
1	54.44	2.50E+08	2.50E-07	3.00E-05	0.50%	3.50E-04	5.46E-05	2.29E-05	2.38	1.00E+06	6.54%	1.83E-06	1.71E-04
1	54.44	2.50E+08	2.50E-07	4.00E-05	0.50%	3.59E-04	5.46E-05	1.45E-05	3.78	1.65E+06	4.03%	1.83E-06	1.71E-04
1	54.44	2.50E+08	2.50E-07	5.00E-05	0.50%	3.66E-04	5.46E-05	6.82E-06	8.00	3.61E+06	1.86%	1.83E-06	1.71E-04
1	34.97	2.50E+08	2.97E-07	1.00E-05	0.50%	2.92E-04	5.46E-05	6.49E-05	0.84	2.28E+05	22.24%	1.753724	2.18E-03
1	34.97	2.50E+08	2.97E-07	2.00E-05	0.50%	3.13E-04	5.46E-05	4.35E-05	1.26	3.91E+05	13.86%	1.753676	1.64E-03
1	34.97	2.50E+08	2.97E-07	3.00E-05	0.50%	3.29E-04	5.46E-05	2.76E-05	1.98	6.77E+05	8.39%	1.753665	1.93E-03
1	34.97	2.50E+08	2.97E-07	4.00E-05	0.50%	3.42E-04	5.46E-05	1.49E-05	3.66	1.35E+06	4.36%	1.753661	2.08E-03
1	34.97	2.50E+08	2.97E-07	5.00E-05	0.50%	3.53E-04	5.46E-05	4.22E-06	12.92	5.08E+06	1.20%	1.753656	2.19E-03
1	34.97	5.70E+08	4.75E-07	1.00E-05	1.27%	2.92E-04	5.46E-05						
1	34.97	5.70E+08	4.75E-07	2.00E-05	1.27%	3.13E-04	5.46E-05	4.35E-05	1.26	3.91E+05	13.87%	1.753929	5.15E-03
1	34.97	5.70E+08	4.75E-07	3.00E-05	1.27%	3.29E-04	5.46E-05	2.76E-05	1.98	6.78E+05	8.38%	1.753806	4.33E-03
1	34.97	5.70E+08	4.75E-07	4.00E-05	1.27%	3.42E-04	5.46E-05	1.49E-05	3.66	1.36E+06	4.36%	1.753842	5.27E-03
1	34.97	5.70E+08	4.75E-07	5.00E-05	1.27%	3.53E-04	5.46E-05	4.20E-06	12.98	5.11E+06	1.19%	1.753836	5.20E-03
1	34.97	5.70E+08	4.00E-07	1.00E-05	0.90%	2.92E-04	5.46E-05	6.49E-05	0.84	2.28E+05	22.24%	1.753922	5.09E-03
1	34.97	5.70E+08	4.00E-07	2.00E-05	0.90%	3.13E-04	5.46E-05	4.35E-05	1.26	3.91E+05	13.87%	1.753882	4.43E-03
1	34.97	5.70E+08	4.00E-07	3.00E-05	0.90%	3.29E-04	5.46E-05	2.76E-05	1.98	6.79E+05	8.39%	1.753851	4.03E-03
1	34.97	5.70E+08	4.00E-07	4.00E-05	0.90%	3.42E-04	5.46E-05	1.49E-05	3.66	1.36E+06	4.36%	1.753806	4.61E-03
1	34.97	5.70E+08	4.00E-07	5.00E-05	0.90%	3.53E-04	5.46E-05	4.21E-06	12.97	5.11E+06	1.19%	1.753796	4.55E-03
1	54.44	5.70E+08	4.00E-07	1.00E-05	1.27%	3.80E-04	3.27E-05	1.26E-05	2.59	1.24E+06	3.33%	1.93E-06	3.37E-05
1	54.44	5.70E+08	4.00E-07	2.00E-05	1.27%	3.84E-04	3.27E-05	8.36E-06	3.92	1.92E+06	2.18%	1.93E-06	3.37E-05
1	54.44	5.70E+08	4.00E-07	3.00E-05	1.27%	3.88E-04	3.27E-05	4.24E-06	7.72	3.85E+06	1.09%	1.93E-06	3.37E-05
1	54.44	5.70E+08	4.00E-07	4.00E-05	1.27%	3.92E-04	3.27E-05	2.71E-07	120.95	6.13E+07	0.07%	1.93E-06	3.37E-05
1	54.44	5.70E+08	4.00E-07	5.00E-05	1.27%	3.96E-04	3.27E-05	-3.55E-06	-9.21	-4.75E+06	-0.90%	1.93E-06	3.37E-05
1	54.44	5.70E+08	4.00E-07	6.00E-05	1.27%	4.00E-04	3.27E-05	-7.25E-06	-4.52	-2.37E+06	-1.81%	1.93E-06	3.37E-05
1	54.44	5.70E+08	4.00E-07	7.00E-05	1.27%	4.03E-04	3.27E-05	-1.08E-05	-3.03	-1.61E+06	-2.68%	1.93E-06	3.37E-05
1	54.44	5.70E+08	4.00E-07	8.00E-05	1.27%	4.07E-04	3.27E-05	-1.43E-05	-2.30	-1.24E+06	-3.50%	1.93E-06	3.37E-05
1	54.44	5.70E+08	4.00E-07	9.00E-05	1.27%	4.10E-04	3.27E-05	-1.76E-05	-1.86	-1.02E+06	-4.29%	1.93E-06	3.37E-05
1	54.44	5.70E+08	4.00E-07	1.00E-04	1.27%	4.13E-04	3.27E-05	-2.08E-05	-1.57	-8.75E+05	-5.03%	1.93E-06	3.37E-05
1	54.44	2.50E+08	2.50E-07	2.00E-05	0.50%	3.41E-04	3.27E-05	1.10E-05	2.97	1.20E+06	3.23%	1.73E-06	1.83E-04
1	54.44	2.50E+08	2.50E-07	3.00E-05	0.50%	3.50E-04	3.27E-05	1.51E-06	21.68	9.12E+06	0.43%	1.73E-06	1.83E-04
1	54.44	2.50E+08	2.50E-07	4.00E-05	0.50%	3.59E-04	3.27E-05	-6.95E-06	-4.71	-2.06E+06	-1.94%	1.73E-06	1.83E-04
1	54.44	2.50E+08	2.50E-07	5.00E-05	0.50%	3.66E-04	3.27E-05	-1.46E-05	-2.24	-1.01E+06	-3.98%	1.73E-06	1.83E-04
1	54.44	2.50E+08	2.50E-07	6.00E-05	0.50%	3.73E-04	3.27E-05	-2.15E-05	-1.52	-7.07E+05	-5.77%	1.73E-06	1.83E-04
1	54.44	2.50E+08	2.50E-07	7.00E-05	0.50%	3.80E-04	3.27E-05	-2.79E-05	-1.17	-5.61E+05	-7.36%	1.73E-06	1.83E-04
1	54.44	2.50E+08	2.50E-07	8.00E-05	0.50%	3.86E-04	3.27E-05	-3.38E-05	-0.97	-4.75E+05	-8.78%	1.73E-06	1.83E-04
1	54.44	2.50E+08	2.50E-07	9.00E-05	0.50%	3.91E-04	3.27E-05	-3.93E-05	-0.83	-4.19E+05	-10.06%	1.73E-06	1.83E-04
1	54.44	2.50E+08	2.50E-07	1.00E-04	0.50%	3.96E-04	3.27E-05	-4.45E-05	-0.74	-3.79E+05	-11.22%	1.73E-06	1.83E-04

Activity

0.1	54.44	2.50E+08	4.00E-07	1.00E-05	1.27%	4.39E-04	3.27E-05	2.61E-04	0.13	7.81E+04	59%	3.45E-06	2.56E-04
0.3	54.44	2.50E+08	4.00E-07	1.00E-05	1.27%	3.99E-04	3.27E-05	4.67E-05	0.70	3.67E+05	12%	2.19E-06	1.13E-05
0.5	54.44	2.50E+08	4.00E-07	1.00E-05	1.27%	3.80E-04	3.27E-05	2.82E-05	1.16	5.58E+05	7%	2.01E-06	3.41E-05
0.7	54.44	2.50E+08	4.00E-07	1.00E-05	1.27%	3.68E-04	3.27E-05	2.16E-05	1.52	6.91E+05	5.86%	1.91E-06	6.46E-05
0.9	54.44	2.50E+08	4.00E-07	1.00E-05	1.27%	3.58E-04	3.27E-05	1.79E-05	1.83	7.99E+05	4.99%	1.85E-06	9.33E-05

0.1	54.44	2.50E+08	2.50E-07	1.00E-05	0.50%	4.22E-04	3.27E-05	3.78E-04	0.09	5.00E+04	90%	3.95E-06	8.98E-04
0.3	54.44	2.50E+08	2.50E-07	1.00E-05	0.50%	3.76E-04	3.27E-05	5.97E-05	0.55	2.59E+05	15.88%	2.14E-06	5.13E-05
0.5	54.44	2.50E+08	2.50E-07	1.00E-05	0.50%	3.55E-04	3.27E-05	3.68E-05	0.89	3.83E+05	10.35%	1.93E-06	1.12E-04
0.7	54.44	2.50E+08	2.50E-07	1.00E-05	0.50%	3.43E-04	3.27E-05	2.83E-05	1.16	4.71E+05	8.26%	1.82E-06	1.54E-04
0.9	54.44	2.50E+08	2.50E-07	1.00E-05	0.50%	3.34E-04	3.27E-05	2.36E-05	1.39	5.43E+05	7.06%	1.75E-06	1.77E-04

0.1	54.44	4.00E+08	4.00E-07	1.00E-05	1.27%	4.48E-04	3.27E-05	2.19E-04	0.15	9.66E+04	48.88%	3.29E-06	3.33E-04
0.3	54.44	4.00E+08	4.00E-07	1.00E-05	1.27%	4.12E-04	3.27E-05	4.07E-05	0.80	4.45E+05	9.88%	2.23E-06	4.28E-06
0.5	54.44	4.00E+08	4.00E-07	1.00E-05	1.27%	3.94E-04	3.27E-05	2.44E-05	1.34	6.86E+05	6.19%	2.06E-06	1.36E-05
0.7	54.44	4.00E+08	4.00E-07	1.00E-05	1.27%	3.82E-04	3.27E-05	1.85E-05	1.76	8.55E+05	4.86%	1.97E-06	3.05E-05
0.9	54.44	4.00E+08	4.00E-07	1.00E-05	1.27%	3.73E-04	3.27E-05	1.54E-05	2.13	9.91E+05	4.12%	1.91E-06	5.03E-05

0.1	54.44	4.00E+08	2.50E-07	1.00E-05	0.50%	4.30E-04	3.27E-05	3.13E-04	0.10	6.26E+04	72.72%	3.67E-06	3.79E-04
0.3	54.44	4.00E+08	2.50E-07	1.00E-05	0.50%	3.87E-04	3.27E-05	5.31E-05	0.62	3.06E+05	13.72%	2.17E-06	2.66E-05
0.5	54.44	4.00E+08	2.50E-07	1.00E-05	0.50%	3.67E-04	3.27E-05	3.24E-05	1.01	4.59E+05	8.82%	1.96E-06	6.82E-05
0.7	54.44	4.00E+08	2.50E-07	1.00E-05	0.50%	3.55E-04	3.27E-05	2.49E-05	1.32	5.65E+05	7.01%	1.86E-06	1.09E-04
0.9	54.44	4.00E+08	2.50E-07	1.00E-05	0.50%	3.45E-04	3.27E-05	2.07E-05	1.58	6.52E+05	5.99%	1.80E-06	1.41E-04

0.1	54.44	5.70E+08	4.00E-07	1.00E-05	1.27%	4.55E-04	3.27E-05	1.93E-04	0.17	1.13E+05	42.46%	3.19E-06	3.17E-04
0.3	54.44	5.70E+08	4.00E-07	1.00E-05	1.27%	4.21E-04	3.27E-05	3.66E-05	0.89	5.15E+05	8.69%	2.25E-06	5.08E-06
0.5	54.44	5.70E+08	4.00E-07	1.00E-05	1.27%	4.04E-04	3.27E-05	2.18E-05	1.50	8.02E+05	5.40%	2.10E-06	1.02E-05
0.7	54.44	5.70E+08	4.00E-07	1.00E-05	1.27%	3.92E-04	3.27E-05	1.65E-05	1.98	1.01E+06	4.21%	2.01E-06	1.62E-05
0.9	54.44	5.70E+08	4.00E-07	1.00E-05	1.27%	3.84E-04	3.27E-05	1.37E-05	2.40	1.17E+06	3.56%	1.95E-06	2.71E-05

0.1	54.44	5.70E+08	2.50E-07	1.00E-05	0.50%	4.37E-04	3.27E-05	2.73E-04	0.12	7.40E+04	62.37%	3.50E-06	2.68E-04
0.3	54.44	5.70E+08	2.50E-07	1.00E-05	0.50%	3.96E-04	3.27E-05	4.82E-05	0.68	3.51E+05	12.17%	2.19E-06	1.43E-05
0.5	54.44	5.70E+08	2.50E-07	1.00E-05	0.50%	3.77E-04	3.27E-05	2.92E-05	1.12	5.31E+05	7.75%	2.00E-06	4.14E-05
0.7	54.44	5.70E+08	2.50E-07	1.00E-05	0.50%	3.64E-04	3.27E-05	2.23E-05	1.47	6.57E+05	6.13%	1.90E-06	7.49E-05
0.9	54.44	5.70E+08	2.50E-07	1.00E-05	0.50%	3.55E-04	3.27E-05	1.86E-05	1.76	7.59E+05	5.23%	1.84E-06	1.05E-04

Fascicle

0.1,0.1,0.1,0.1,0.1,0.1,0.1,0.1	54.44	5.70E+08	4.00E-07	1.00E-05	1.27%	4.52E-04	2.29E-04	2.16E-04	1.06	1.46E+05	32.40%	3.29E+00	1.08E-01
0.3,0.3,0.3,0.3,0.3,0.3,0.3,0.3	54.44	5.70E+08	4.00E-07	1.00E-05	1.27%	4.18E-04	2.29E-04	3.71E-05	6.17	5.38E+05	8.15%	2.24E+00	5.35E-02
0.5,0.5,0.5,0.5,0.5,0.5,0.5,0.5	54.44	5.70E+08	4.00E-07	1.00E-05	1.27%	4.02E-04	2.29E-04	2.15E-05	10.67	8.34E+05	5.07%	2.09E+00	6.96E-02
0.7,0.7,0.7,0.7,0.7,0.7,0.7,0.7	54.44	5.70E+08	4.00E-07	1.00E-05	1.27%	3.91E-04	2.29E-04	1.60E-05	14.32	1.05E+06	3.93%	2.01E+00	7.78E-02
0.9,0.9,0.9,0.9,0.9,0.9,0.9,0.9	54.44	5.70E+08	4.00E-07	1.00E-05	1.27%	3.83E-04	2.29E-04	1.31E-05	17.53	1.23E+06	3.30%	1.95E+00	8.35E-02

unstable

D

Calculations

D.1. Model

The system is considered as a constrained non-linear static system. The volume constraint will be implemented by means of lagrange multipliers.

The equations representing the system are the following:

$$\vec{f}(\vec{q}) + \vec{\Omega}^T(\vec{q})\vec{\lambda} = \vec{f}^e \tag{D.1}$$

$$\vec{C}(\vec{q}) = \vec{0} \tag{D.2}$$

Where $\vec{C}(\vec{q})$ represents the constraint equations, $\vec{\lambda}$ represents the Lagrange multipliers and $\vec{\Omega}$ is the Jacobian matrix of the constraint equations with respect to the generalized coordinates $\vec{q}$. $\vec{f}e$ is a known external force vector.

$$\vec{\Omega}(\vec{q}) = \begin{bmatrix} \frac{\partial C_1}{\partial q_1} & \frac{\partial C_1}{\partial q_2} & \dots & \frac{\partial C_1}{\partial q_n} \\ \frac{\partial C_2}{\partial q_1} & \frac{\partial C_2}{\partial q_2} & \dots & \frac{\partial C_2}{\partial q_n} \\ \vdots & \vdots & \vdots & \vdots \\ \frac{\partial C_m}{\partial q_1} & \frac{\partial C_m}{\partial q_2} & \dots & \frac{\partial C_m}{\partial q_n} \end{bmatrix} \tag{D.3}$$

The system is then linearized by means of the Taylor expansion series as in [2].

$$\vec{f}(\vec{q}) + \vec{K}\Delta\vec{q} + \vec{\Omega}^T(\vec{q})\vec{\lambda} + \vec{\Omega}^T(\vec{q})\Delta\vec{\lambda} + \vec{K}^b(\vec{q},\vec{\lambda})\Delta\vec{q} + \dots = \vec{f}e \tag{D.4}$$

$$\vec{C}(\vec{q}) + \vec{\Omega}(\vec{q})\Delta\vec{q} + \dots = \vec{0} \tag{D.5}$$

With,

$$\vec{K}^b(\vec{q},\vec{\lambda}) = \frac{\partial(\vec{\Omega}^T\vec{\lambda})}{\partial\vec{q}} \tag{D.6}$$

By neglecting the higher order terms we find the following set of linearized equations:

$$\begin{bmatrix} \vec{K} + \vec{K}^b & \vec{\Omega}^T \\ \vec{\Omega} & \vec{0} \end{bmatrix} \begin{bmatrix} \Delta\vec{q} \\ \Delta\vec{\lambda} \end{bmatrix} = \begin{bmatrix} \vec{f}^e - \vec{f} + \vec{\Omega}^T\vec{\lambda} \\ -\vec{C}(\vec{q}) \end{bmatrix}; \tag{D.7}$$

A solution can now be found using the Newton-Raphson iteration scheme. From this point on we will consider $\vec{q}$ to be $\vec{q} = \begin{bmatrix} \vec{q} \\ \vec{\lambda} \end{bmatrix}$.

$$\Delta\vec{q}^{(1)} = (\vec{K} + \vec{K}^b)^{-1}(\vec{q}^{(1)})[\vec{f}^e - \vec{f}(\vec{q}^{(1)}) + \vec{\Omega}^T\vec{\lambda}^{(1)}] \tag{D.8}$$

$$\vec{q}^{(2)} = \vec{q}^{(1)} + \Delta\vec{q}^{(1)} \tag{D.9}$$

$$\vec{q}^{(k+1)} = \vec{q}^{(k)} + (\vec{K} + \vec{K}^b)^{-1}(\vec{q}^{(k)})[\vec{f}^e - \vec{f}(\vec{q}^{(k)}) + \vec{\Omega}^T\vec{\lambda}^{(k)}] \tag{D.10}$$

Three different convergence criterions are used as described in [1]:

$$|\vec{f}^{e} - \vec{f}| < \varepsilon_1 \tag{D.11}$$

$$|\vec{C}(\vec{q})| < \varepsilon_2 \tag{D.12}$$

$$|\vec{\lambda}^{(k)} - \vec{\lambda}^{(k-1)}| < \varepsilon_3 \tag{D.13}$$

The volume constraint is built up in the following way: To formulate the volume constraint, first the volume will be calculated in terms of the nodal positions. To calculate the volume of each segment, each hexagon can be divided into two trapezoidal prisms, which each can be subdivided into five tetrahedrons. The sum of these tetrahedrons will be the total volume of the segment. The volume of a tetrahedron V_T from its vertices can be found in the following way:

Using this method, the volume of the fiber can always be found, even when the fiber is deformed.

$$\vec{C}_i(\vec{q}) = \vec{V}_i(\vec{q}) - \vec{V}_{0,i} \tag{D.14}$$

$$\vec{V}_i(\vec{q}) = \sum_{n=1}^{k} \vec{V}_{T_n,i} \tag{D.15}$$

$$V_{T_n,i} = \left| \frac{1}{6} \cdot \det \begin{bmatrix} x_{B,i} & x_{D,i} & x_{C,i+1} & x_{E,i+1} \\ y_{B,i} & y_{D,i} & y_{C,i+1} & y_{E,i+1} \\ z_{B,i} & z_{D,i} & z_{C,i+1} & z_{E,i+1} \\ 1 & 1 & 1 & 1 \end{bmatrix} \right|; \tag{D.16}$$

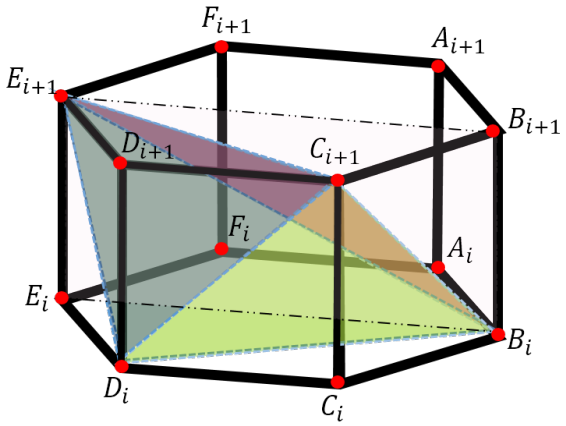

Figure D.1: Side view of modelling structures with different braiding angles

The constraint matrix, Ω can be found when taking the the partial derivative toward the generalized coordinates of the system.

Contraction force

The contraction force of is induced by modelling the longitudinal elements as pretensioned springs of which the initial length ℓ_0 will be adapted according to the force exerted by the force-length relationship for that sarcomere length. First we need to find the representative sarcomere length. This is done by calculating the strain of the longitudinal element relative to the initial length, which we will refer to as ℓ_{ic} and then implementing this strain to the sarcomere resting length.

$$\varepsilon_\ell = \frac{\ell - \ell_{ic}}{\ell_{ic}} \tag{D.17}$$

$$\ell_{sarc} = \ell_{rest}(1 + \varepsilon_\ell) \tag{D.18}$$

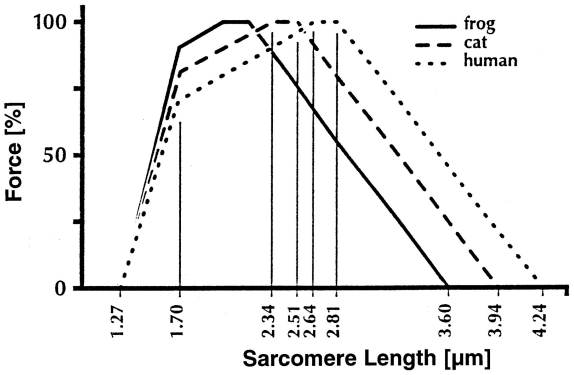

(a) Force-Length relationship for frog, cat and human [14]

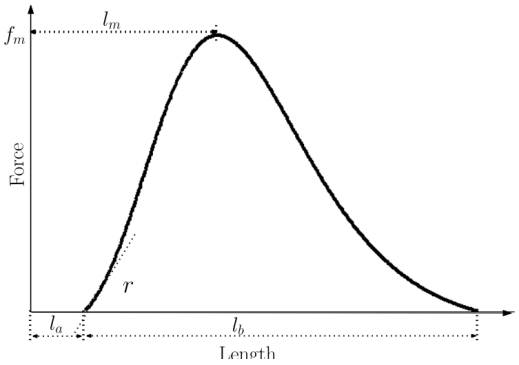

(b) Asymmetric Gaussian function [8]

Figure D.2: Single fibre and fascicle model

The length-tension relationship is implemented as an asymmetric Gaussian function. The Gaussian is parametrized according to the method described in [8]. Where a parameter mapping method is described that results in a parameter set with clear physical meanings:

$$\begin{aligned} \ell_a &= \text{minimum length} \\ \ell_a + \ell_b &= \text{maximum length} \\ \ell_m &= \text{optimal length} \\ f_m &= \text{optimal force} \\ r &= \text{slope of the curve at } l_a \end{aligned}$$

These parameters will me mapped to a number of constants $c_0..c_4$ which will be used to calculate the force.

$$f(\ell_{sarc}) = -c_0 + c_1 e^{-(\frac{\ell_{sarc}-c_2}{c_3+c_4 l})^2} \tag{D.19}$$

$$\ell_0 = \ell - \frac{f}{k_f} \tag{D.20}$$

Where k_f is a proportionally predefined stiffness parameter.

The following parameters were derived from [14] (Figure D.2a) for a human force-length relationship.

- minimum length: 1.27μm
- maximum length: 4.24μm
- optimal length: 2.64μm

The optimal force for the model will be calculated based on two model parameters, the fibre diameter D_{fib} and the maximum isometric tension for a sarcomere σ_{max} which will be further discussed in the next section. First the area for a regular hexagon is calculated using the the fibre diameter. This is then divided by the number of sarcomere elements to allocate a representative area to each longitudinal contracting element. Using the maximum isometric tension and scaling this by the activation parameter one can now calculate the maximum force per longitudinal contracting element f_{max}.

$$A_{fib} = \frac{3\sqrt{3}}{8} D_{fib}^2 \tag{D.21}$$

$$A_{sarc} = \frac{A_{fib}}{6} \tag{D.22}$$

$$f_{max} = \sigma_{max} A_{sarc} a \tag{D.23}$$

First we need to find the representative sarcomere length. This is done by calculating the strain of the longitudinal element relative to the initial length, which we will refer to as ℓ_{seg} and then implementing this strain to the sarcomere resting length.

D.1.1. Stiffness Matrix Calculation

(Source: Arend L. Schwab, personal communication, 4/2016).

The stiffness matrix is numerically calculated. Three types of elements are included in the stiffness matrix, the crossed collagen elements, the external spring elements and the pretensioned spring sarcomere elements. All are represented by 3D truss elements. A local stiffness matrix is calculated per element and included in the whole stiffness matrix. Consider a 3D truss element.

Assuming linear elasticity we have $\sigma = S\varepsilon$. Where σ is the stress, S is the stiffness modulus ($S = \frac{EA}{\ell_0}$) and ε is the strain in the member.

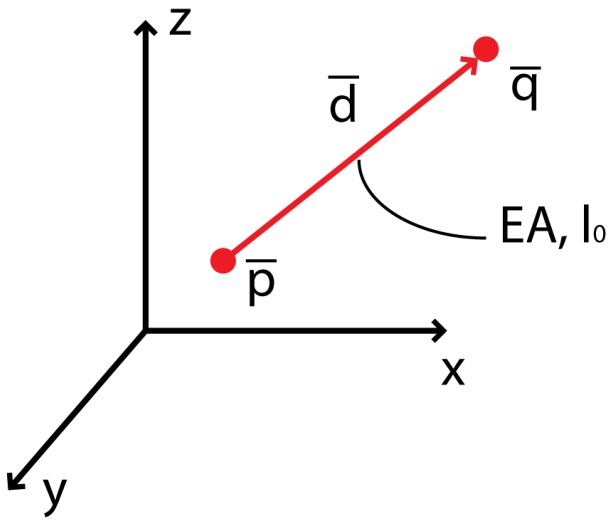

Figure D.3: 3D representation of a truss element

Consider a truss between two points, $\vec{p}$ and $\vec{q}$ (Figure D.3). The vector of the truss itself is represented by $\vec{d}$. A set of generalized coordinates is defined as x_i.

$$\vec{p}(x_i) = \begin{bmatrix} x_p \\ y_p \\ z_p \end{bmatrix} \qquad \vec{q}(x_i) = \begin{bmatrix} x_q \\ y_q \\ z_q \end{bmatrix}$$

$$\vec{d}(x_i) = \vec{q}(x_i) - \vec{p}(x_i)$$

$$x_i = \begin{bmatrix} x_p & y_p & z_p & x_q & y_q & z_q \end{bmatrix}$$

The elongation $e(x_i)$ is found by calculating the difference between the current $\ell(x_i)$ and initial length ℓ_0 of the member. The unit vector $\vec{r}(x_i)$ is calculated to find the numeric Jacobian of the elongation $D_{,i}$.

$$\ell(x_i) = |\vec{d}(x_i)|$$

$$e(x_i) = \ell(x_i) - \ell_0$$

$$\vec{r}(x_i) = \frac{\vec{d}(x_i)}{\ell(x_i)}$$

$$D_{,i} = \frac{\partial e(x_i)}{\partial x_i}$$

$$D_{,i} = \begin{bmatrix} -\vec{r}^t & \vec{r} \end{bmatrix}$$

The normal force N is represented by the product of the element stiffness and its elongation. The nodal forces f_i are found by taking the product of the transposed Jacobian and the normal force.

$$N = Se(x_i)$$

$$f_i = D_{,i}^T N$$

Now the stiffness matrix can be calculated by an approximation of the derivative of the nodal forces.

$$
\begin{aligned}
\Delta f_i &= \frac{\partial D_{,i}^T}{\partial x_j} N \Delta x_j + D_{,i}^T \frac{\partial N}{\partial x_j} \Delta x_j \\
\Delta f_i &= D_{,ij}^T N \Delta x_j + D_{,i}^T S D_{,j} \Delta x_j \\
\Delta f_i &= K_{g_{ij}} \Delta x_j + K_{s_{ij}} \Delta x_j \\
K_{s_{ij}} &= D_{,i}^T S D_{,j} \\
&= S \cdot \begin{bmatrix} A & -A \\ -A & A \end{bmatrix}, \qquad A = \vec{r} \cdot \vec{r}^t \\
K_{g_{ij}} &= D_{,ij}^T N \\
&= N \cdot \begin{bmatrix} B & -B \\ -B & B \end{bmatrix}, \qquad B = (I - A)/\ell(x_i) \\
K_{ij} &= K_{s_{ij}} + K_{g_{ij}}
\end{aligned}
$$

The element stiffness matrix can now be added to the total stiffness matrix.

Imposing single stiffness direction in collagen fibre
For the collagen fibre elements the assumption of a single stiffness direction is done. This means the elements will only have a stiffness when in tension and not in compression. This is included in the stiffness matrix by calculating the collagen strain in the elements for each iteration. When the strain ε_{col} is negative the ℓ_0 of the concerning spring will be changed to the same value as the current spring length by means of an if/else statement. For a positive strain ℓ_0 remains the same.

$$
\varepsilon_{col} = \frac{\ell_{col}(x_i) - \ell_{col_0}}{\ell_{col_0}}
$$

if $\varepsilon_{col} < 0$
$\ell_0 = \ell_{col}$
else
$\ell_0 = \ell_{col_0}$

D.1.2. Output Parameter Calculation

All model output that in relation to the separate elements in the model will need to be averaged to get a clear model output. To do this, only the middle segment of the fiber will be analyzed to exclude any bias due to boundary conditions. All angle configurations have the same fiber length, but not the same amount of segments. Therefore, in the 34.97˚ configuration, the bottom 5 segments and the top 5 segments will be excluded. In the 54.44˚ configuration the bottom and top 10 segments will be excluded and in the 70.33˚ configuration the top and bottom 20 segments will be excluded. By doing this, the segment of the fiber that will be analyzed will be the same for all configurations (Figure D.4).

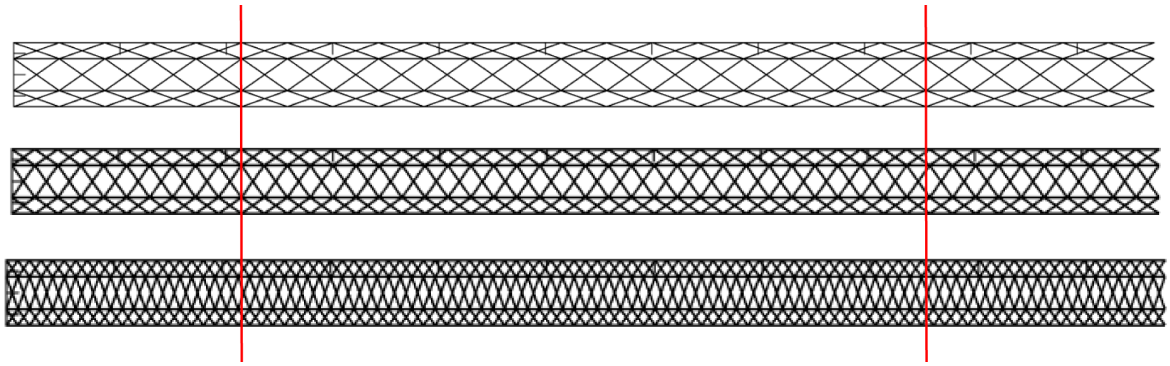

Figure D.4: Visual overview of the part of the fibre that is used for averaging analysis in the three configurations

This method is used to calculate the average pressure λ_{avg}, sarcomere length $\ell_{sarc_{avg}}$, collagen strain $\varepsilon_{col_{avg}}$ and , final braiding angle $\alpha_{end_{avg}}$.
The pressures are given per segments and therefore we only need to average over the amount of segments n to find an average value. To find the average sarcomere length we need to average over each segment (n) as well as each sarcomere within a segment (q). To find the average collagen strain, we first calculate the strain for each collagen element. Then we average over the amount of segments (n) and the amount of sarcomere elements within a segment (m). The final braiding angle is calculated by taking the inverse cosine of the dot product between the collagen element vector ($\vec{d}_{col}$) and the adjacent sarcomere element vector ($\vec{d}_{sarc}$) divided by their lengths. This will be done for all elements and to find the average a summation will be done over the number of segments (n) and the number of collagen elements (m).

$$\lambda_{avg} = \sum_{i=1}^{n} \lambda_i \tag{D.24}$$

$$sarc_{avg} = \sum_{i=1}^{n} \sum_{p=1}^{q} l_{sarc_{i,p}} \tag{D.25}$$

$$\varepsilon_{col} = \frac{\ell_{col} - \ell_{col_0}}{\ell_{col_0}} \tag{D.26}$$

$$\varepsilon_{col_{avg}} = \sum_{i=1}^{n} \sum_{j=1}^{m} \varepsilon_{col_{i,j}} \tag{D.27}$$

$$\alpha_{end_{avg}} = \sum_{i=1}^{n} \sum_{j=1}^{m} \alpha_{end_{i,j}} \tag{D.28}$$

$$\alpha_{end} = cos^{-1} \frac{\vec{d}_{sarc} \cdot \vec{d}_{col}}{|\vec{d}_{sarc}| \cdot |\vec{d}_{col}|} \tag{D.29}$$

E

Other Results

In this appendix some extra results are presented that were not in the paper and (might) have been referred to by the paper.

E.1. Collagen Modulus

In Figure E.1 the same plot as in the paper, displaying the angle change vs. the collagen modulus is displayed. Here the standard deviations are added. What can be noticed is that the 70.33° configuration has a very large standard deviation. Furthermore the slope in the 34.97° configuration falls within the standard deviation and is therefore likely the result of model inaccuracy.

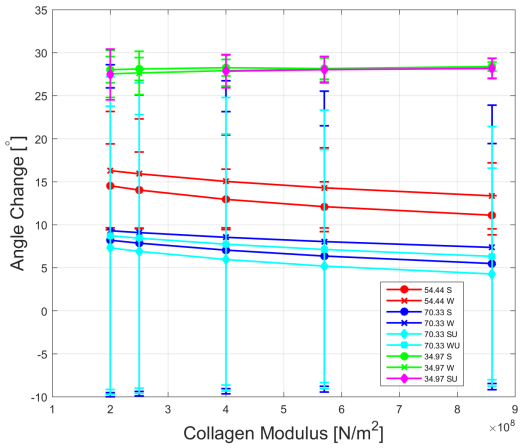

Figure E.1: Collagen modulus vs. Angle Change with error bars

E.1.1. Work

Separate plots were made for the internal work. In Figure E.3 the potential energy inside the collagen E.2a, the potential energy inside the external springs E.2b and the total potential energy E.2c are displayed for different collagen moduli in compensated and uncompensated configuration for all angles.

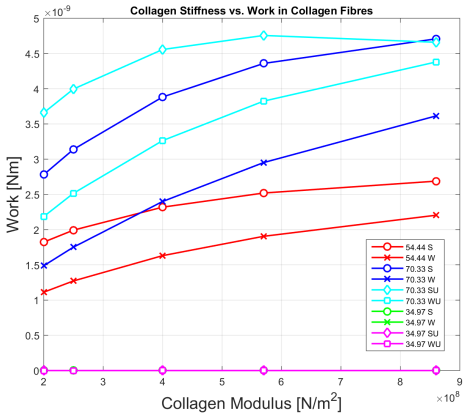

(a) Work inside collagen lattice

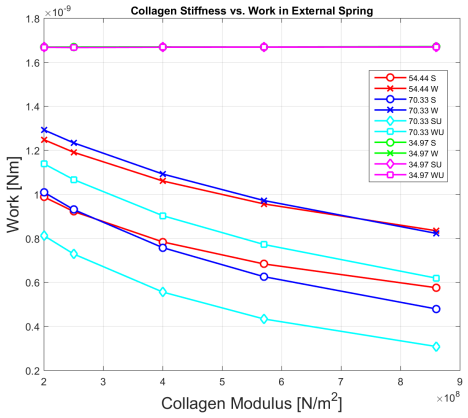

(b) Work inside external springs

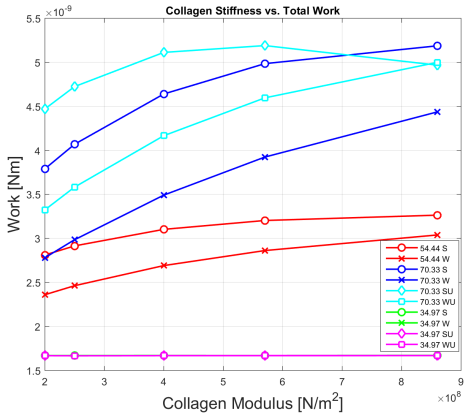

(c) Total amount of work in the passive elements

Figure E.2: Three plots displaying the amount of potential energy in different elements within the fiber for various configurations.

E.1.2. Stiffness

Several stiffness plots were made, however because the initial lengths could not be compared, they were not reported. In Figure E.3a longitudinal stiffness modulus is plotted against collagen modulus. It can be seen that the highest angle configuration has the highest stiffness, however the length from which the stiffness was measured was also longer. This means the starting point for the measurement is higher up the force-length relationship curve which could result in a higher stiffness measurement, but not a fair comparison. In Figure E.3b therefore the longitudinal stiffness was plotted against the relative length change the fiber had at the start of the measurement compared to its original configuration.

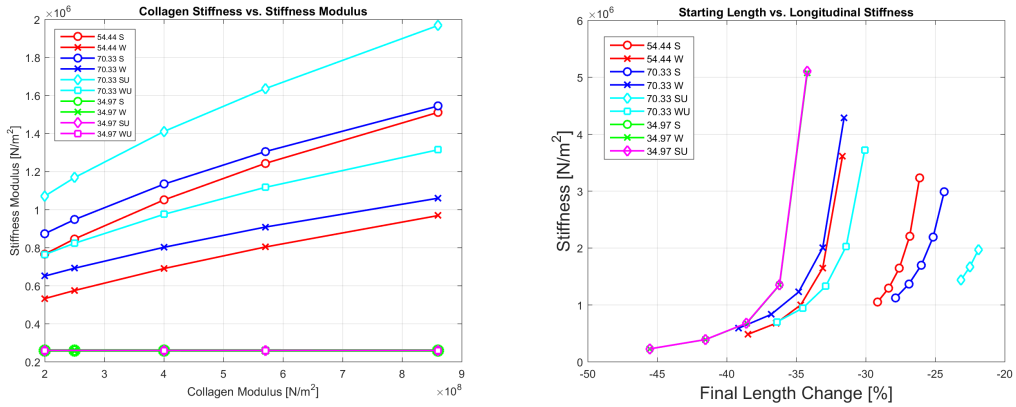

(a) Longitudinal Stiffness modulus vs. Collagen stiffness modulus

(b) Final Length change vs. Longitudinal Stiffness

Figure E.3: Longitudinal stiffness modulus vs. length change for various configurations (a) and longitudinal stiffness modulus vs. initial length change

E.2. Force-length Relationship

Because in the force-length plot in the paper it seemed likely that the 34.97° configuration followed the exact same path as the input force-length relationship, this hypothesis was tested by putting both normalized force and length curves into one figure (E.4).

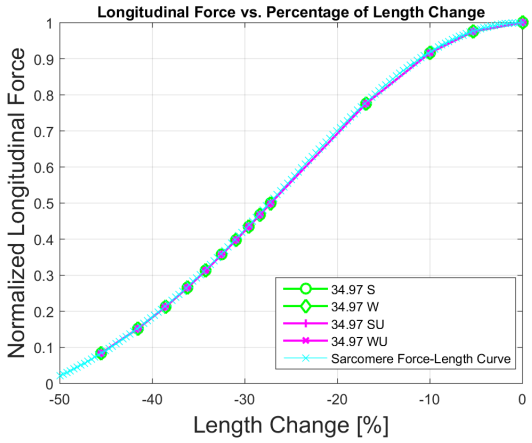

Figure E.4: Normalized Force-Length results for 34.97° compared to force-length input curve

E.3. Fascicle

The paper only shows displacement results for a fiber. Therefore here the additional plots for a fascicle are displayed. In E.5 a top view of the fascicle before contraction (black) and after contraction (magenta) is given. It can be noticed that the fascicle tends to move to one side to allow for space for the central fiber to expand. In E.6 a side view is given before and after contraction. Here it can also be noticed that the model tends to 'bend' towards one direction.

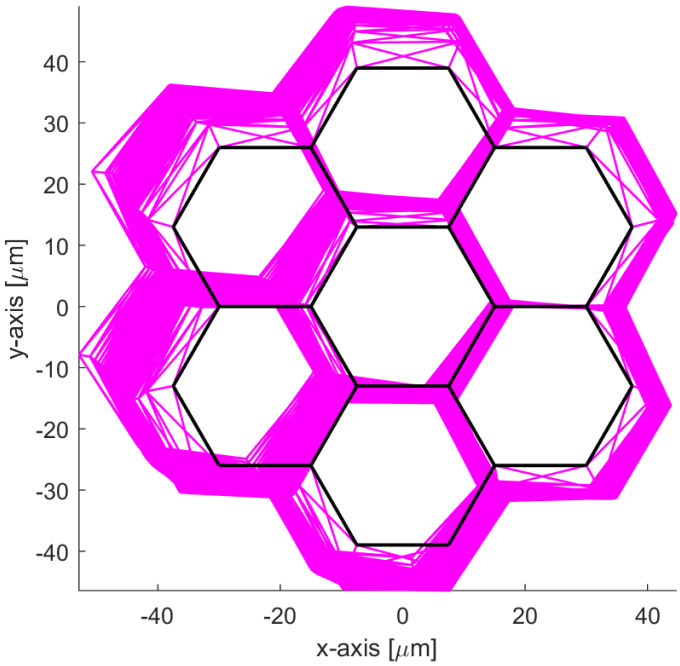

Figure E.5: Top view of a fascicle model simulation with the original shape (black) and the shape after simulation (magenta).

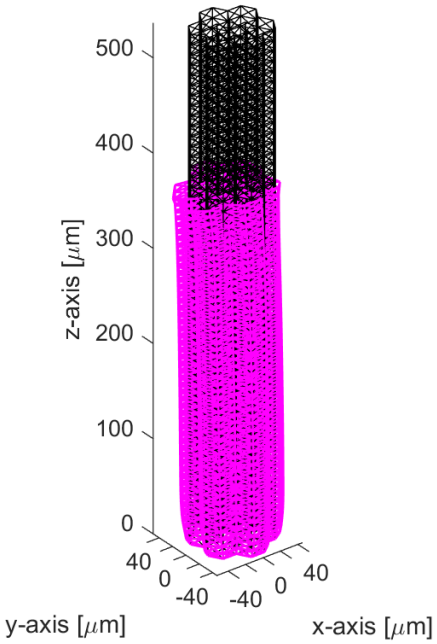

Figure E.6: Side view of a fascicle model before (black) and after (magenta) simulation.

F

Convergence Analysis and Running Time

F.1. Convergence

To prevent (near) singularity in the model it was necessary to scale all parameters to μ levels. This was implemented by converting all meters to μm and all N to μN. If this was not carried out Matlab would issue a warning for near singularity. To account for any scaling errors, scaled output parameters were compared to unscaled output parameters. The results were equal.

The three convergence criteria that were used for the model were ε_1, ε_2 and ε_3. Where ε_1 describes the difference between the external and internal force. The value chosen for convergence was the maximum force $\sigma_{max}A_{sarc}$ that can be produced by a sarcomere. For the current models that value is 27.28μN and this was multiplied by 1e-6 to find ε_1. To analyze convergence a plot of the errors for every iteration was made on a logarithmic scale (Figure F.1).

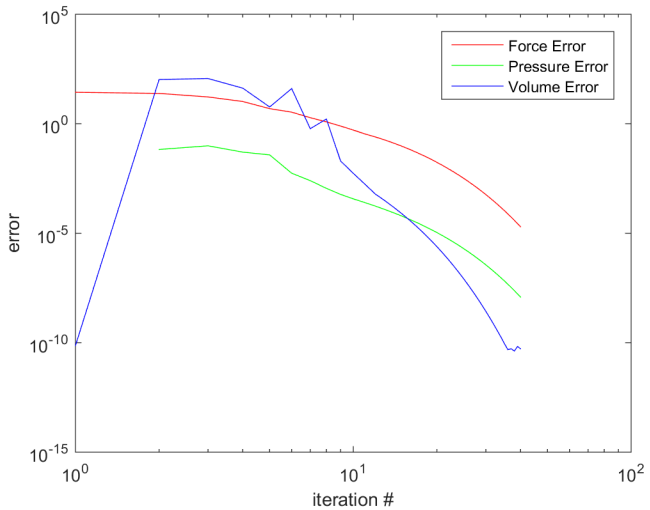

Figure F.1: The different errors per iteration on a logarithmic scale. This simulation: α_{init}=54.44°, E_{col}=570, r_{col}=0.4

The model with the smallest initial angle of 34.97° was not converging towards the selected ε_1 value. This was due to the fact that in this configuration the contraction ended due to reaching the left end of the force-length relationship, see figure F.2a. This hypothesis was tested by doing a similar simulation with a force-length relationship that was shifted to the right so that the left end of the ascending limb would lie around 0. In this configuration the model did converge and therefore it could be concluded that

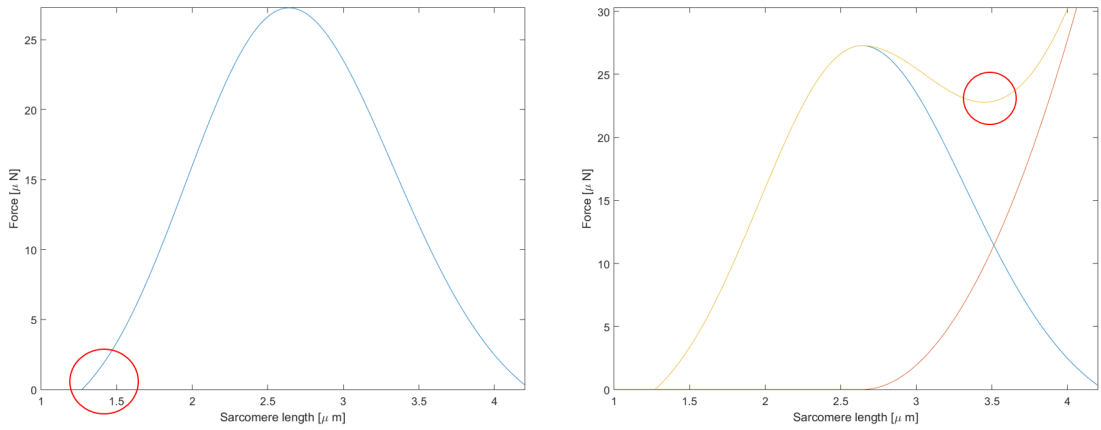

(a)
Typical sarcomere length result for 34.97°

(b)
Typical sarcomere length result for 54.44°

Figure F.2: Overview of the different sarcomere lengths per iteration gives an indication of the model convergence, note that the values on the axes are not the same

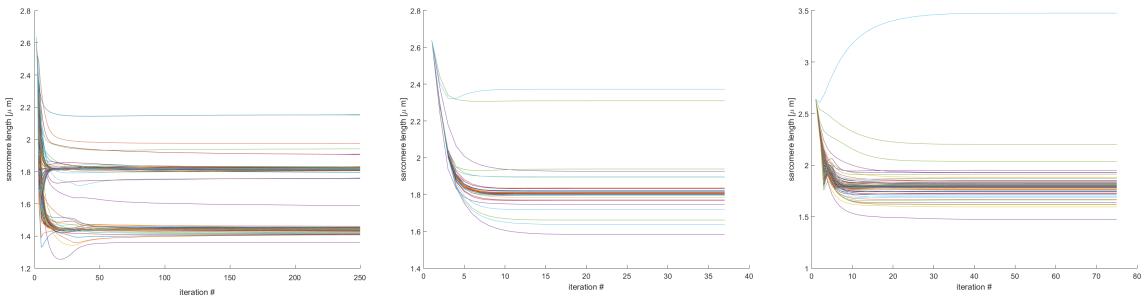

(a)
Typical sarcomere length result for 34.97°

(b)
Typical sarcomere length result for 54.44°

(c)
Typical sarcomere length result for 70.33°

Figure F.3: Overview of the different sarcomere lengths per iteration gives an indication of the model convergence, note that the values on the axes are not the same.

this was the cause of the poor convergence. Therefore for this configuration ε_1 was increased to 1e-8. In figure F.3 the sarcomere lengths of all sarcomeres in the configuration are plotted against the number of iterations. From these figures it becomes clear that all configurations do converge within about 50 iterations and show only slight alterations beyond this point. Therefore the margin of a minimum of 250 iterations if no convergence was reached is sufficient.

Another interesting thing that is happening in F.3 is for the 70.33° angle where one of the lines points to sarcomeres extending. When evaluating the simulation the case is that two of the sarcomere elements in the bottom segments extend, potentially to allow for more space in the other segments. These sarcomeres (despite being activated) therefore follow the descending limb, which was initially unaccounted for in the force-length relationship because physiologically a passive force component would keep sarcomeres from lengthening extensively. Therefore a passive force-length curve was added for this configuration. The sarcomere length indicated by the red circle in F.2b indicates the length that the sarcomeres ultimately reach. To check for this being the result of potential calculation errors a simulation was with the sarcomeres as linear pretensioned springs, forcing all sarcomeres to contract. From this end-configuration another simulation was done with the force-length relationship and the effect remained, thereby excluding the possibility of it being the result of calculation errors.

F.2. Simulation times

The simulation times can be described in two parts; generating the Jacobian matrices and actually running the simulation. The time needed to generate the matrices ($\Omega(q)$ [n x $\vec{x}$], $K^b(q)$ [$\vec{x}$ x $\vec{q}$] and $C(q)$ [n x 1] was quite extensive, however this only needed to be done once for every amount of segments used since the result was completely symbolic (where $\vec{x}$ is the vector of generalized coordinates without λ and $\vec{q}$ the size of the generalized coordinates including λ). Generating the Jacobian matrices takes the longest for the fascicles since this has the largest number of segments.

Jacobian Generation:
1 segment: ≈ 3 sec
25 segments: ≈ 2.5 min
50 segments: ≈ 8 min
100 segments: ≈ 35 min
Fascicle 50 segments: ≈ 4h

The other part is the model simulation time. This is dependent on both the number of segments in the model as well as the number of iterations needed for convergence (in appendix D under numit, the number of iterations needed for every simulation is stated). The matrix division is the most computationally expensive calculation in the every iteration. The fastest model is the 54.44˚ configuration. While the smallest angle configuration actually has the least segments, this configuration requires more iterations due to poor convergence. Below is an overview of the model simulation times where s/it stands for seconds per iteration.

Model Simulation Times

1 segment: ≈ 10 sec	(≈ 0.2 s/it)
25 segments: ≈ 15 min	(≈ 1.7 s/it)
50 segments: ≈ 3 min	(≈ 3.8 s/it)
100 segments: ≈ 10 min	(≈ 7.0 s/it)
Fascicle 50 segments: ≈ 30 min	(≈ 12 s/it)

This is an overview for having the fiber or fascicle contract maximally until an equilibrium is reached. Another simulation that is carried out is the stiffness simulation. Here the external springs are removed and replaced by external forces. This alters the convergence time to usually being slightly more extensive than in a normal simulation.

Finally the model is sensitive to step size, and in some configurations therefore becomes unstable. Since the step size in the model is implicitly determined by the force-length relationship it was quite difficult to alter this. For most configurations this could be solved by using the results from a configuration with similar parameters, altering the parameters and letting it converge from there. This was explicably more time-consuming than a regular simulation.
The longest running times were achieved in calculating the stiffness of the fascicles. These calculations could take up to 7 hours a piece.

G

Discretization Comparison

An attempt was made to compare the different discretizations of the system. Similar initial angles with differing discretizations were compared. The setup is displayed in figure G.1. With this setup in combination with a positive pressure inside the fibre will lead to buckling of the sarcomere elements in the second setup. The most reliable comparison will therefore be provided by comparing the 34.97° angle because this configuration leads to a (neglible) negative pressure inside the fibre like was concluded before.

(a) Original discretization (b) Comparison discretization

Figure G.1: Two different discretizations that were used in the comparison. The red dots indicate the nodes, the blue lines represent the collagen fibres and the green arrows depict the sarcomere contraction direction.

From figure (G.2) it can be concluded that a reasonable resemblance is reached, however relatively large differences are present in the collagen strain, this becomes visisble in figure G.2b where the blue lines are slightly more expanded. This is probably due to the fact that different volume elements were used for the model, this is likely resulting in some buckling of the middle nodes. The general length change, the average pressure and the endpoint force are relatively similar however.

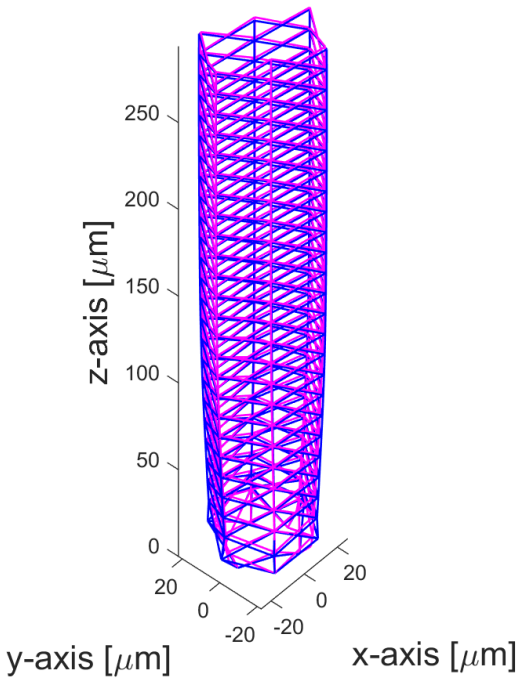

(a) 3D view of comparison

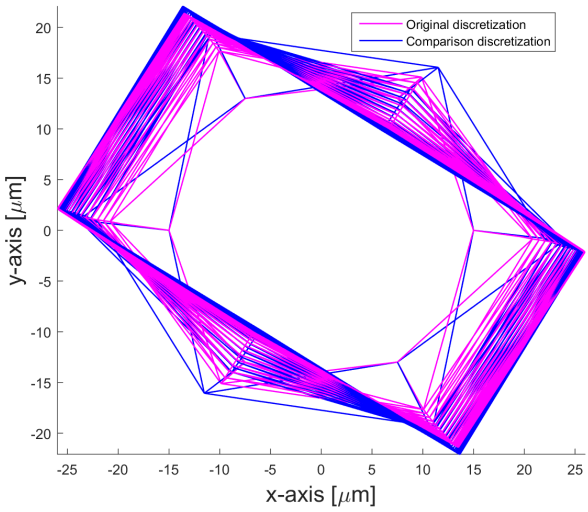

(b) Top view of comparison

Figure G.2: Visualizaion of Discretization Comparison, where magenta depicts the original configuration and blue the comparison discretization

H

Stiffness Data Comparison

To find out whether the stiffness values found are realistic, a comparison was done with values from literature. A study by Kubo [4] was chosen. In this study, the stiffness of the human medial gastrocnemius was measured by inducing a fast twitch. The data are on whole muscle scale, but because the authors also measured fascicle length the data can be extrapolated.
To compare the scales, stiffness will be expressed as a Young's Modulus, in which case the force difference is normalized for the cross-sectional area of the fibre and the length difference is normalized for the fibre length.
In the article by Kubo[4] two figures were of importance to do this, the change in fascicle length (δLf) in mm versus the percentage of the maximum voluntary contraction and the active muscle stiffness (k_{act}) in N/mm versus the percentage of maximum voluntary contraction. To calculate the Young's modulus, we need the initial fascicle length (Lf_{init}) and the physiological cross-sectional ($PCSA$) are which were both indicated in the article. With these parameters first the force is calculated by multiplying the length difference (δLf) with the active stiffness (k_{act}). With the found force, the stiffness modulus can now be calculated for the activation levels.

$$F = k_{act} \cdot \delta Lf \tag{H.1}$$

$$E = \frac{F \cdot Lf_{init}}{PSCA \cdot \delta Lf} \tag{H.2}$$

We can do this for every activation level and this leads to the following figure H.1:

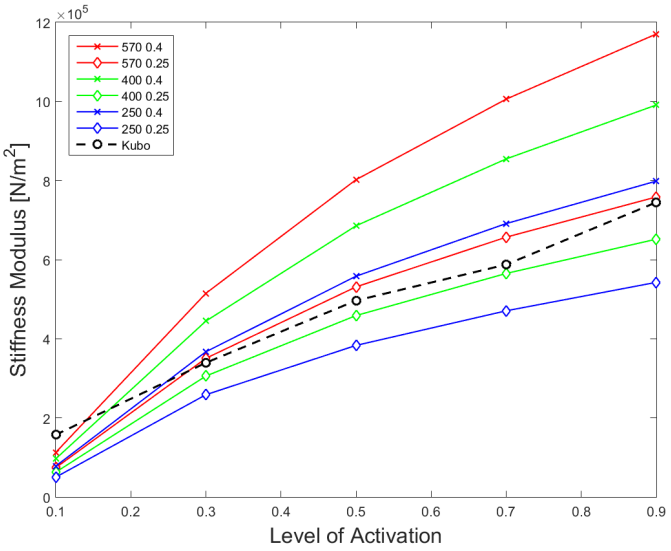

Figure H.1: Different model stiffness output variables compared to experimental data by [4] indicated in black. In the legend collagen modulus (in μN/m^2) and collagen radius (in μm are indicated) for a 54.44° model configuration.

Angle Orientation Comparison

In [13] the angle reorientation properties of the endomysium were analysed and in [10] the same was done for the perimysium. They indicated an initial angle of 59° and 55° respectively at sarcomere lengths of 2.05μm, and 1.9-2.1μm. This was done for bovine stemomandibularis (neck) muscle. These measurements were done for a specific muscle by the same author, therefore it is not unlikely that a large variety of these parameters exists for other muscle types.
Since the 54.44° configuration is closest to the ones described by Purslow, this one is chosen for comparison. When translating the strain levels found in the model to those found in the endomysium model by Purslow, final orientation angles from the model can be compared to Figure 6 from the article by Purslow. In I.1 red and blue lines are drawn over the original figure. They indicate the strong(E_{col}=570MPa,r_{col}=0.4μm) and weak (E_{col}=250MPa,r_{col}=0.25μm) setups respectively of the 54.44° configuration. The model seems to resemble the figure well, only the angle change is slightly lower in our model. This can be explained by the initial angle which for our model is 54.44° and in the article 59°, therefore one can expect a slightly shifted graph.

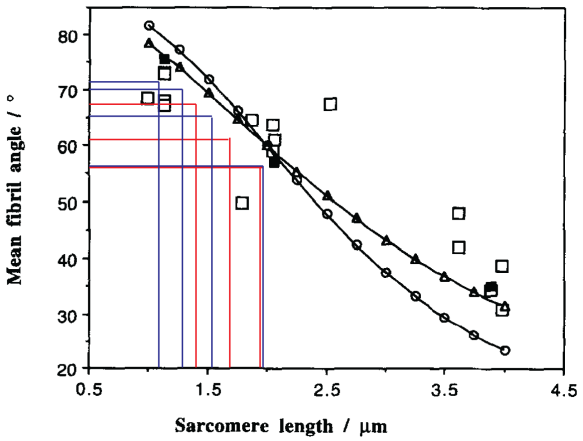

Fig. 6. Numerically-weighted mean fibril orientation of endomysium vs. muscle sarcomere length. Data points shown are from both image analysed (open squares) and manually analysed (filled squares) orientation distributions. The two lines shown are the predicted mean orientation vs. sarcomere length from (open circles) the isoareal model and (open triangles) the constant shape model.

Figure I.1: Figure 6 from Purslow(1994)[13] describing the numerically-weighted mean fibril orientation for different orientation distributions. The red and blue lines drawn in over the figure depict our model output with red the strong configuration, E_{col}=570MPa,r_{col}=0.4μm and blue the weak one,E_{col}=250MPa,r_{col}=0.25μm

J

Table of symbols and definitions

symbol	definition	unit
$\vec{f}$	internal model force vector	N
$\vec{f^e}$	external force vector	N
$C(\vec{q})$	constraint vector	
$\vec{q}$	vector of generalized coordinates	
$\vec{K}$	stiffness matrix	N/m
$\vec{K^b}$	stiffness matrix	N/m
$\vec{\Omega}$	volume constraint Jacobian matrix	m^2
$\vec{\lambda}$	vector of Lagrange multipliers representing compartmental pressure	N/m^2
ε_1	convergence criterion for force	N
ε_2	convergence criterion for volume	m^3
ε_3	convergence criterion for pressure	N/m^2
D_{fib}	starting fibre diameter	m
ℓ_{seg}	segment length	m
α	collagen braiding angle	°
E_{col}	collagen modulus of elasticity	MPa
k_{ex}	external spring stiffness	N/m
L_{init}	initial fibre length	m
a	level of activation between 0 and 1	
r_{col}	collagen fibre radius	m
p_{col}	volume percentage of collagen fibre	%
ℓ_{rest}	sarcomere resting length	m
σ_{max}	maximum isometric tension	kPa
α_{init}	initial braiding angle	°
ℓ_{ex}	initial external spring length	m
δ	resulting displacements	m
L_{end}	fibre length after simulation	m
W_{tot}	total work inside muscle fiber after contraction	J
λ	segmental pressure	N/m^2
α_{end}	average final fibre area	m^2
E_{stiff}	muscle fibre modulus of elasticity	MPa
F_{end}	total endpoint force after simulation	N
$\ell_{sarc_{end}}$	sarcomere length after simulation	m
ε_{col}	collagen strain	
$\Delta\alpha$	change in braiding angle	°
A_{col}	collagen area	m^2

σ_{end}	endpoint tension after simulation	Pa
ΔL	total length difference	m
$\Delta L\%$	relative length difference	%
n	number of segments	
fib_{act}	activity of the different fibres within a fascicle	
V_T	volume of a tetrahedron within a segment	m^3
$V_i(\vec{q})$	current volume vector	m^3
$\vec{V_0}, i$	initial volume vector	m^3
ℓ_0	initial longitudinal spring length for regulating force in force-length relationship	m
ℓ_{ic}	length of longitudinal element in initial condition	m
ℓ	longitudinal element length	m
ε_l	longitudinal element strain	
k_f	stiffness parameter for imposing force-length relationship	N/m
f	force from force-length relationship imposed on longitudinal element	N
ℓ_a	minimum sarcomere length	μm
ℓ_b	sarcomere length range	μm
ℓ_m	optimal sarcomere length	μm
f_m	optimal sarcomere force	N
r	slope of force-length relation curve at l_a	
c_0	constant in asymmetric Gaussian function	
c_1	constant in asymmetric Gaussian function	
c_2	constant in asymmetric Gaussian function	
c_3	constant in asymmetric Gaussian function	
c_4	constant in asymmetric Gaussian function	
A_{fib}	initial fibre section area	m^2
A_{sarc}	sarcomere dedicated area of CSA	m^2
f_{max}	maximum force for a single sarcomere	N
ℓ_{col}	length of a cross-fibre element	m
ℓ_{col_0}	initial length of a cross-fibre element	m
ℓ_{sarc}	sarcomere length	m
$\vec{d}_{sarc}$	sarcomere element vector	m
$\vec{d}_{col}$	collagen element vector	m

Table J.1: Table of Symbols and definitions

Bibliography

[1] Rafael Avilés, Goizalde Ajuria, Vicente Gómez-Garay, and Santiago Navalpotro. Comparison among nonlinear optimization methods for the static equilibrium analysis of multibody systems with rigid and elastic elements. *Mechanism and Machine Theory*, 35(8):1151–1168, 2000. ISSN 0094114X. doi: 10.1016/S0094-114X(99)00053-1.

[2] Olivier Bauchau. *Flexible Multibody Dynamics*, volume 176. Springer, 2011. ISBN 9789400703346. doi: 10.1007/978-94-007-0335-3. URL http://www.springer.com/engineering/mechanical+engineering/book/978-94-007-0334-6$\backslash$nhttp://www.springerlink.com/index/10.1007/978-94-007-0335-3.

[3] A. Kelly. *Concise Encyclopedia of Composite Materials*. Elsevier Science, 2012. ISBN 0080912656. URL https://books.google.com/books?id=Ia6GAAAAQBAJ{&}pgis=1.

[4] Keitaro Kubo, Daisuke Miyazaki, Toshihiro Ikebukuro, Hideaki Yata, Masaji Okada, and Naoya Tsunoda. Active muscle and tendon stiffness of plantar flexors in sprinters. *Journal of sports sciences*, 00(00):1–7, 2016. ISSN 1466-447X (Electronic). doi: 10.1080/02640414.2016.1186814. URL http://dx.doi.org/10.1080/02640414.2016.1186814.

[5] Richard L Lieber. *Skeletal Muscle Structure, Function, and Plasticity: The Physiological Basis of Rehabilitation*. 2010. ISBN 0781775930. URL http://books.google.nl/books/about/Skeletal{_}Muscle{_}Structure{_}Function{_}and{_}P.html?id=Ak1SPgAACAAJ{&}pgis=1.

[6] Richard L Lieber, Suzanne Steinman, Ilona A Barash, and Hank Chambers. Structural and functional changes in spastic skeletal muscle. *Muscle & nerve*, 29(5):615–27, may 2004. ISSN 0148-639X. doi: 10.1002/mus.20059. URL http://www.ncbi.nlm.nih.gov/pubmed/15116365.

[7] Elaine N Marieb and Katja Hoehn. *Human Anatomy & Physiology*. 2013. ISBN 9780321743268.

[8] Goran Abdulrahman Mohammed and Ming Hou. Optimization of Active Muscle Force-Length Models Using Least Squares Curve Fitting. *IEEE Transactions on Biomedical Engineering*, 63(3):630–635, 2016. ISSN 15582531. doi: 10.1109/TBME.2015.2467169.

[9] E. Passerieux, R. Rossignol, A. Chopard, A. Carnino, J.F. Marini, T. Letellier, and J.P. Delage. Structural organization of the perimysium in bovine skeletal muscle: Junctional plates and associated intracellular subdomains. *Journal of Structural Biology*, 154(2):206–216, may 2006. ISSN 10478477. doi: 10.1016/j.jsb.2006.01.002. URL http://www.sciencedirect.com/science/article/pii/S1047847706000165.

[10] P P Purslow. Strain-induced reorientation of an intramuscular connective tissue network: Implications for passive muscle elasticity. *Journal of Biomechanics*, 22(1):21–31, jan 1989. ISSN 00219290. doi: 10.1016/0021-9290(89)90181-4. URL http://www.sciencedirect.com/science/article/pii/0021929089901814.

[11] P P Purslow. The structure and functional significance of variations in the connective tissue within muscle. *Comparative Biochemistry and Physiology Part A: Molecular & Integrative Physiology*, 133(4):947–966, dec 2002. ISSN 10956433. doi: 10.1016/S1095-6433(02)00141-1. URL http://www.sciencedirect.com/science/article/pii/S1095643302001411.

[12] P P Purslow. Muscle fascia and force transmission. *Journal of bodywork and movement therapies*, 14(4):411–7, oct 2010. ISSN 1532-9283. doi: 10.1016/j.jbmt.2010.01.005. URL http://www.sciencedirect.com/science/article/pii/S1360859210000069.

[13] P.P. Purslow and John A. Trotter. The morphology and mechanical properties of endomysium in series-fibred muscles: variations with muscle length. *Journal of Muscle Research and Cell Motility*, 15(3), jun 1994. ISSN 0142-4319. doi: 10.1007/BF00123482. URL http://link.springer.com/10.1007/BF00123482.

[14] D.E. Rassier, B.R. MacIntosh, and W. Herzog. Length dependence of active force production in skeletal muscle. (127):626–634, 1999.

[15] Bahar Sharafi and Silvia S Blemker. A mathematical model of force transmission from intrafascicularly terminating muscle fibers. *Journal of biomechanics*, 44(11):2031–9, jul

2011. ISSN 1873-2380. doi: 10.1016/j.jbiomech.2011.04.038. URL http://www.sciencedirect.com/science/article/pii/S0021929011003708.

[16] J A Trotter and P P Purslow. Functional morphology of the endomysium in series fibered muscles. *Journal of morphology*, 212(2):109–22, may 1992. ISSN 0362-2525. doi: 10.1002/jmor.1052120203. URL http://www.ncbi.nlm.nih.gov/pubmed/1608046.

[17] Andrea Turrina, Miguel Antonio Martínez-González, and Carla Stecco. The muscular force transmission system: role of the intramuscular connective tissue. *Journal of bodywork and movement therapies*, 17(1):95–102, jan 2013. ISSN 1532-9283. doi: 10.1016/j.jbmt.2012.06.001. URL http://www.mendeley.com/research/muscular-force-transmission-system-role-intramuscular-connective-tissue/.